THE EFFECT OF PIPE SPACING
ON MARINE PIPELINE SCOUR

A Thesis

by

JOSEPH HENRY WESTERHORSTMANN

Submitted to the Office of Graduate Studies of
Texas A&M University
in partial fulfillment of the requirements for the degree of

MASTER OF SCIENCE

December 1988

Major Subject: Ocean Engineering
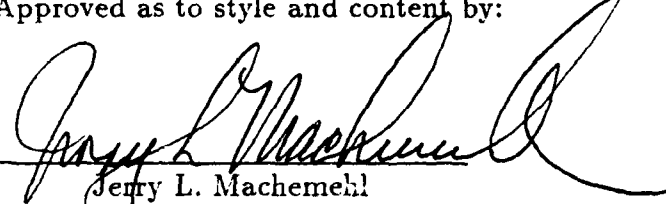
DTIC
ELECTE
FEB 0 7 1989
H

89   2   6   114

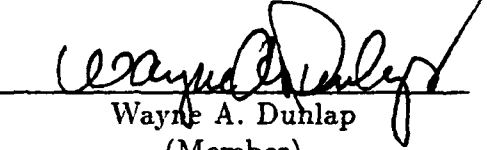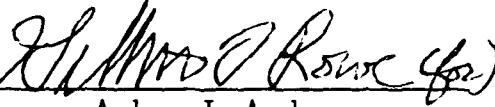# THE EFFECT OF PIPE SPACING

ON MARINE PIPELINE SCOUR

A Thesis

by

JOSEPH HENRY WESTERHORSTMANN
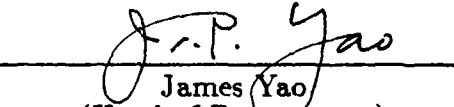
Approved as to style and content by:

_____
Jerry L. Machemehl
(Chair of Committee)

_____
Robert E. Randall
(Member)

_____
Wayne A. Dunlap
(Member)

_____
Aubrey L. Anderson
(Member)

_____
James Yao
(Head of Department)

December 1988

ABSTRACT

The Effect of Pipe Spacing On Marine Pipeline Scour

(December 1988)

Joseph Henry Westerhorstmann, B.S., University of Florida

Chair of Advisory Committee: Dr. Jerry L. Machemehl

Scour is a major threat to deep water pipelines. A study was performed to determine the relationship between pipe geometry and scour depth, and examine scour hole dimensions under multiple pipes. Model tests were conducted in a two-dimensional wave-current flume facility in which pipes were exposed to unidirectional flow and unidirectional flow with oscillatory motion. The model testing investigated pipes in contact with a sand bed and the effect of pipe spacing on scour. Scour hole profiles were measured and plotted to show the scour hole shape under multiple pipe systems. For two pipe systems, spacing between pipes of 1/2 pipe diameter resulted in less scour depth than full diameter spacing. Unidirectional flow with oscillatory motion resulted in less scour than unidirectional flow.

ACKNOWLEDGMENTS

The author is deeply indebted to Dr. J. L. Machemehl for his positive encouragement and support throughout the duration of this study. Also, a note of thanks to Dr. R. E. Randall for his help and advice during the model testing and preparation of this report. A note of thanks is due to the U. S. Navy Civil Engineer Corps and Naval Facilities Engineering Command for providing the author the opportunity to pursue post graduate studies. A special note of thanks to Captain D. R. Wells, his most valuable support made it possible for the author to become a part of the Navys' Ocean Facilities Program. And finally, to my wife Melinda, who stood by me throughout endless toil. Without her love, patience and understanding, this would not have been possible.

TABLE OF CONTENTS

TABLE OF CONTENTS (Continued)

LIST OF TABLES

LIST OF FIGURES

LIST OF FIGURES (Continued)

CHAPTER I

INTRODUCTION

Purpose

The most economical method of transporting oil onshore from offshore production facilities is through submarine pipelines. Submarine pipelines are also used for the disposal of industrial and sanitary wastes. The stability of these subsea pipelines is threatened by loss of bed support resulting from scour. This thesis reviews pipeline scour and presents results of model testing on single and multiple pipes in contact with a sand bed.

Few theoretical models exist which accurately describe or predict scour depth beneath pipelines. The most widely accepted models predicting scour depth are based on experimental research.

The objectives of this research are :

(1) To determine the relationship between pipe geometry and scour depth, and

(2) To examine scour hole dimensions under multiple pipes subject to undirectional flow and unidirectional flow with oscillatory motion.

The citations on the following pages follow the style of the *Journal of Waterway, Port, Coastal and Ocean Engineering Division, ASCE.*

Pipe spacing and scour depth were studied to determine the difference in scour depth between a single pipe and multiple pipes subjected to similar conditions. Single and multiple pipe systems were exposed to both currents and currents with wave action (oscillatory motion).

Problem

Pipelines are being placed in deeper waters over greater distances. Pipelines on the ocean floor cause disruptions of the flow pattern and changes in the local fluid velocity which create bed scour. Damage usually occurs during severe storms, when large ocean waves increase bottom currents. Because of larger horizontal drag and inertial forces as the storm intensifies, scour may uncover and expose a buried pipeline. The exposed pipe may be damaged since pipelines generally are not designed for conditions where spanning and vibrations due to vortex shedding occur (Herbich et al. 1984).

In shallow depths, pipelines are usually buried, placed in trenches or undergo self burial (Hulsbergen 1984). A severe storm generates combined current and wave action on the seabed, producing higher than normal fluid velocities. The combined current and wave action effect on the seabed results in additional sediment transport, exposing buried pipelines. Once exposed, the pipe lays on the surface of the seabed, and is further subjected to scouring currents.

Local and area scour threaten pipeline stability which may damage the pipe. Scour holes endanger stability when large free spans create unacceptable stresses due to static deformations, (Bruschi et al. 1986). During the development of the scour hole under the pipeline, the stresses inside the wall of the pipe increase due to the sagging of the pipe. The suspended part of the pipe deflects like a uniformly loaded beam with fixed or simply supported ends, Fig. 1. The pipe will rupture if the static bending stresses exceed the ultimate strength of the pipe.

Flow around the pipe creates a series of complex vortices which cause the suspended section of the pipe to vibrate. This results in the development of a deeper scour hole. Pipe vibrations cause pipe failure due to fatique. Scour is a direct consequence of vortex shedding. As the scour hole deepens, the frequency of vibrations may increase until the pipe ruptures. Vibrations may be caused by the external fluid velocity on the pipe or the internal fluid transport, or a combination of the two. A ruptured pipeline will discharge its product (such as oil) into the environment. High repair costs, income loss from down time and shorter lifetime are experienced.

Simply supported beam.

Fixed end beam.

Pipe in contact with sand bed.

Small scour hole, no deflection.

Scour hole grows, pipe begins to deflect.

Pipe deflects into scour hole.
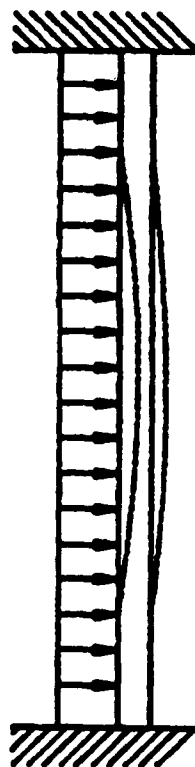
Fig. 1. Comparison between fixed or simply supported beam and pipeline scour.

CHAPTER II

LITERATURE REVIEW

Definition of Scour

The mechanism of scour is characterized by a fine balance between the local flow condition, sediment transportation and sediment deposition. Based on research conducted by Fredsoe et al. (1988), vortex shedding in the pipeline wake is the the major cause of scour. Turbulence diffused from the leeward side of the pipe wall allows sediment to remain in suspension, allowing for easy transport by currents. Scour will occur if the rate of sediment transport upstream of the pipe is less than the transport downstream.

Scour depth is a function of sediment characteristics, pipe geometry, flow and wave properties. Among all the variables involved in the phenomenon of equilibrium scour depth, scour depth (Sd) is the dependent variable and can be expressed as a function of the following independent variables:

Mean fluid velocity ($\bar{U}$),

Critical velocity of sediment motion (V_c),

Water depth (y),

Pipeline diameter (D),

Wave height (H),

Wave length (L),

Wave period (T),

Dynamic viscosity of water (μ),

Fluid density (ρ),

Effective sediment size (d_s),

Sediment density (ρ_s),

Relative density of sediment in water ($\Delta = \left(\frac{\rho_s - \rho}{\rho}\right)$), and

Gravitational acceleration (g).

Note that kinematic viscosity ($\nu = \mu/\rho$) replaces dynamic viscosity over density of water.

Ibrahim and Nalluri (1986) developed the following dimensionless relationships between variables:

$$Sd/D = f\left[\, (\bar{U}D/\nu),\ (\bar{U}y/\nu),\ (\bar{U}/\sqrt{gD}),\ (H/gT^2),\ (\bar{U}T/D), \right. \tag{1}$$
$$\left. (HL^2/y^3),\ (\bar{U}/\sqrt{gy}),\ (H/D),\ (L/D),\ (\bar{U}/V_c),\ (\bar{U}/\sqrt{g\Delta d_s})\right]$$

The most significant relationships from Eq. 1 which influence scour are the following dimensionless parameters:

$(\bar{U}D/\nu)$ and $(\bar{U}y/\nu)$ are pipe and flow Reynolds Numbers, measuring turbulence,

(H/gT^2) is wave steepness, which is the disturbing capability of the wave,

(HL^2/y^3) is the wave Ursell Number which defines the relative magnitude of wave motion and water depth.

$(\bar{U}/\sqrt{gD})$, $(\bar{U}/\sqrt{gy})$ and $(\bar{U}/\sqrt{g\Delta d_s})$ are the pipe, flow, and sediment Froude Numbers, the prime force behind the movement of the seabed, and

$(\bar{U}T/D)$ is the Keulegan–Carpenter number, describing the dominant type of flow, (i.e., current or wave).

Incipient Motion

The action of flow on the bed which initiates sediment motion is measured by the critical bed shear stress (τ_c). Critical bed shear stress is expressed as the dimensionless shear stress or Shields parameter (θ), defined as:

$$\theta = \frac{\tau_c}{\rho g(\Delta - 1)d_s} \tag{2}$$

where:

$$\tau_c = V_c^2 \rho \tag{3}$$

The critical bed shear stress τ_c is related to the bed friction by:

$$\tau_c = c\rho U_{100}^2 \tag{4}$$

where:

$c =$ frictional drag coefficient of sand bed, and

$U_{100} =$ fluid velocity at 100 cms above the bed.

Most of the data on critical shear stress comes from observations made in flume experiments. These experiments show sediment motion as highly unsteady and nonuniformly distributed over the bed area. In near critical conditions, grain motion occurs in turbulent bursts over small areas, increasing as near shear stress conditions increase.

When shear stress is near the critical value, gusts of sediment motion become random in space and time. This was observed by Shields (1936), who described the initiation of motion as statistical in nature. Einstein (1942) was first to develop transport relations based on probabilistic concepts. Due to the statistical nature of incipient motion, it is difficult to define a true condition for initiation of motion.

Critical shear stress data is based on arbitrary definitions of critical conditions. Vanoni (1966) refers to the following three intensities of motion near the critical or threshold condition:

(1) Weak movement— few or several of the smallest sand particles are in motion in isolated spots in sufficiently small quantities such that those moving in one square centimeter of the bed can be counted.

(2) Medium movement— grains of mean diameter are in motion in numbers too large to be counted. The movement is no longer local in character. It is not sufficiently strong to affect the bed configuration and does not result in appreciable sediment discharge.

(3) General movement— sand grains up to and including the largest are in motion and movement is occurring in all parts of the bed at all times.

The definition of critical conditions varies widely among scientists and engineers. This explains, in part, the variation in research results on sediment motion. However, the weak movement described above agrees with most studies. It also agrees with Shields critical condition (Shields 1936).

As the velocity of fluid flow over a bed of sediments is increased, the fluid exerts a force or stress on the particles. Eventually this force becomes sufficient for particle movement and results in transporting sediment from the bed. This is known as the threshold of sediment movement, or the critical stage of erosion. The fluid velocity which results in threshold movement is the critical velocity of sediment movement, V_c.

Threshold curves form the basis for predicting initial sediment motion. Curves based on a combination of sediment grain diameter, density, velocity, stress or friction are entered for values of sediment movement.

Shields diagram, shown in Fig. 2, is a relationship between the boundary Reynolds number, (R_*) and Shields parameter, (θ). The Shields parameter θ is defined by Eq. 2.

The boundary Reynolds number is defined as:

$$R_* = \frac{U_* d_s}{\nu} \tag{5}$$

where:

11
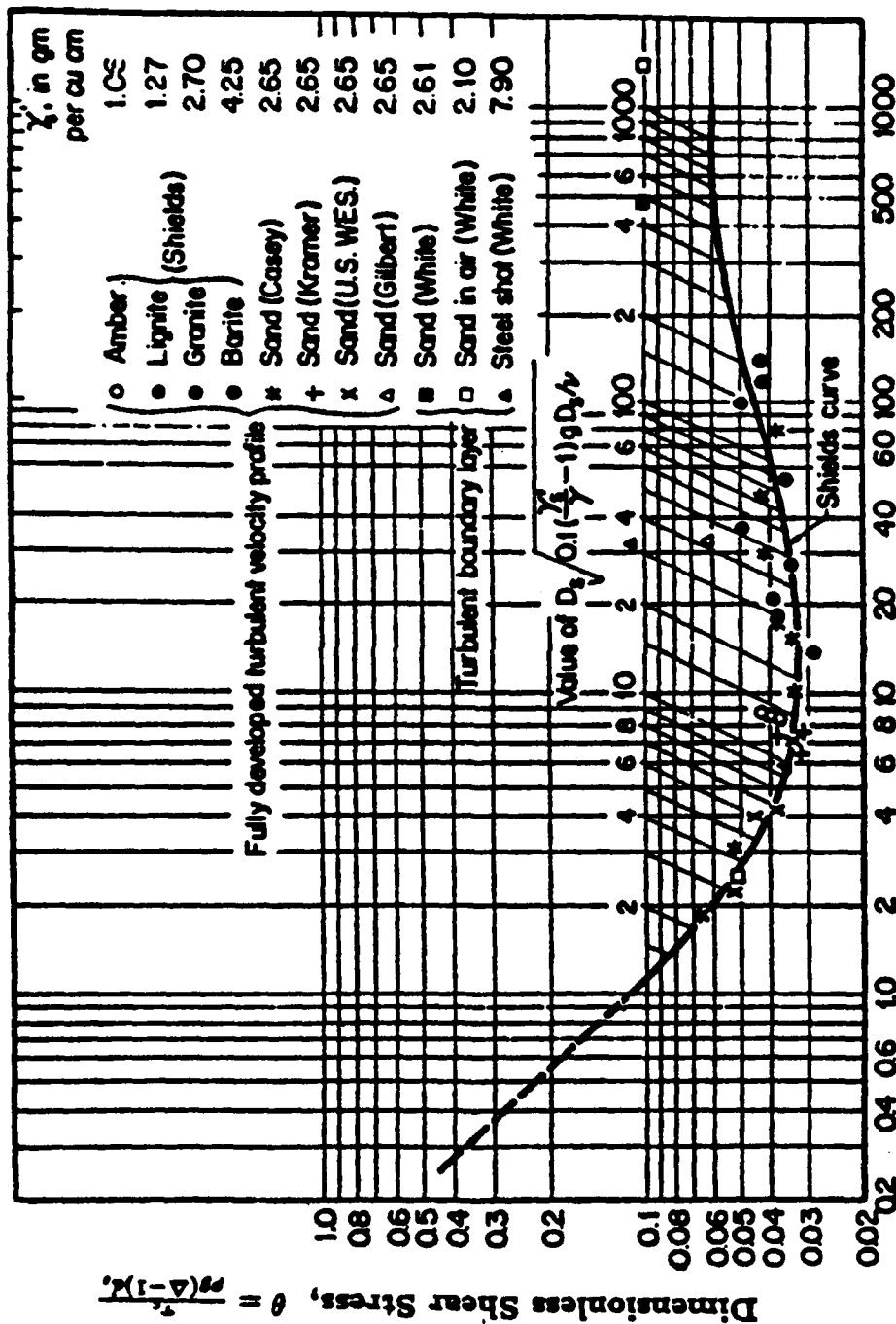
Fig. 2. Shields diagram (from Simons and Şentürk 1977).

d_s = effective sediment diameter,

ν = kinematic viscosity of water, and

U_* = turbulent shear velocity.

Turbulent shear velocity U_* is defined as:

$$U_* = \sqrt{\tau_o/\rho} \qquad (6)$$

where:

τ_o = bed shear stress, and

ρ = density of water.

Bed shear stress τ_o is defined as:

$$\tau_o = \frac{F_d}{C_1 d_s^2} \qquad (7)$$

where:

d_s = effective sediment size,

C_1 = form coefficient defining the effective surface area of the particle, and

F_d = drag force on the particle.

The effective surface is defined as the projection of the particle on a plane perpendicular to the direction of fluid motion.

Drag force on a particle is defined as:

$$F_D = \frac{1}{2}C_D\rho A U_d^2 \tag{8}$$

where:

C_D = drag coefficient,

A = projected area of particle on a plane perpendicular to the fluid flow direction,

U_d = local velocity at distance d above bed, and

ρ = density of water.

Shields determined this relationship by measuring bed load transport for values of θ. Values for θ were measured at greater than twice the critical value. He then extrapolated θ to the point of the vanishing bed. This procedure was used to avoid random orientation of grains and variations in flow conditions which result in grain movement when θ is smaller, Simons and Şentürk (1977).

Shields diagram expresses the threshold of sediment movement as a function of the following:

Sediment density (ρ_s),

Effective grain size (d_s),

Bed shear stress (τ_o),

Critical bed shear stress (τ_c),

Kinematic fluid viscosity (ν), and

Fluid density (ρ).

The determination of incipient motion is important in the study of pipeline scour. Incipient motion of sediment leads to scour. Shields published his diagram for critical shear stress utilizing boundary layer theory and fluid mechanics. Considerable dissatisfaction with this shear stress criterion is presented in the literature, Liu (1958), Vanoni et al. (1966) and Yang (1973).

Yang (1973) summarizes this dissatisfaction with the following:

(1) By assuming the existence of a universal velocity distribution law, shear velocity or shear stress is a measure of the intensity of turbulent fluctuations. Knowledge of turbulence is limited mainly to model tests.

(2) Shields derived his criterion on incipient motion by using the concept of laminar sublayer. According to that theory, the laminar sublayer should not have any effect on the velocity distribution when the shear Reynolds number is greater than 70. Shields diagram indicates that the dimensionless critical shear stress still varies with shear velocity Reynolds number greater than 70.

(3) Shields extends his curve to a straight line when the shear velocity Reynolds number is less than 3. This means that when the sediment particle is very small, the critical tractive force is independent of the sediment size. It has been shown that the critical tractive force is proportional to the sediment size.

(4) The critical shear stress cannot be determined directly from Shields diagram. It must be determined through trial and error.

(5) Shields simplifies the problem by neglecting the lift force and considers tangential force. Lift force must be considered for high shear velocity Reynolds number.

(6) Sediment transport cannot be uniquely determined by shear stress. Using critical shear stress as the criterion for incipient motion for the study of sediment transport is questionable.

Based on the preceding, it is doubtful that the Shields diagram is the best criterion for incipient motion.

Fig. 3 shows curves on critical velocity plotted against mean sediment size for quartz sediment in water ($\rho_s = 2.65 g/cm^3$) as presented by Vanoni (1966). The curves shown are for the upper and lower limit of the mean critical velocity
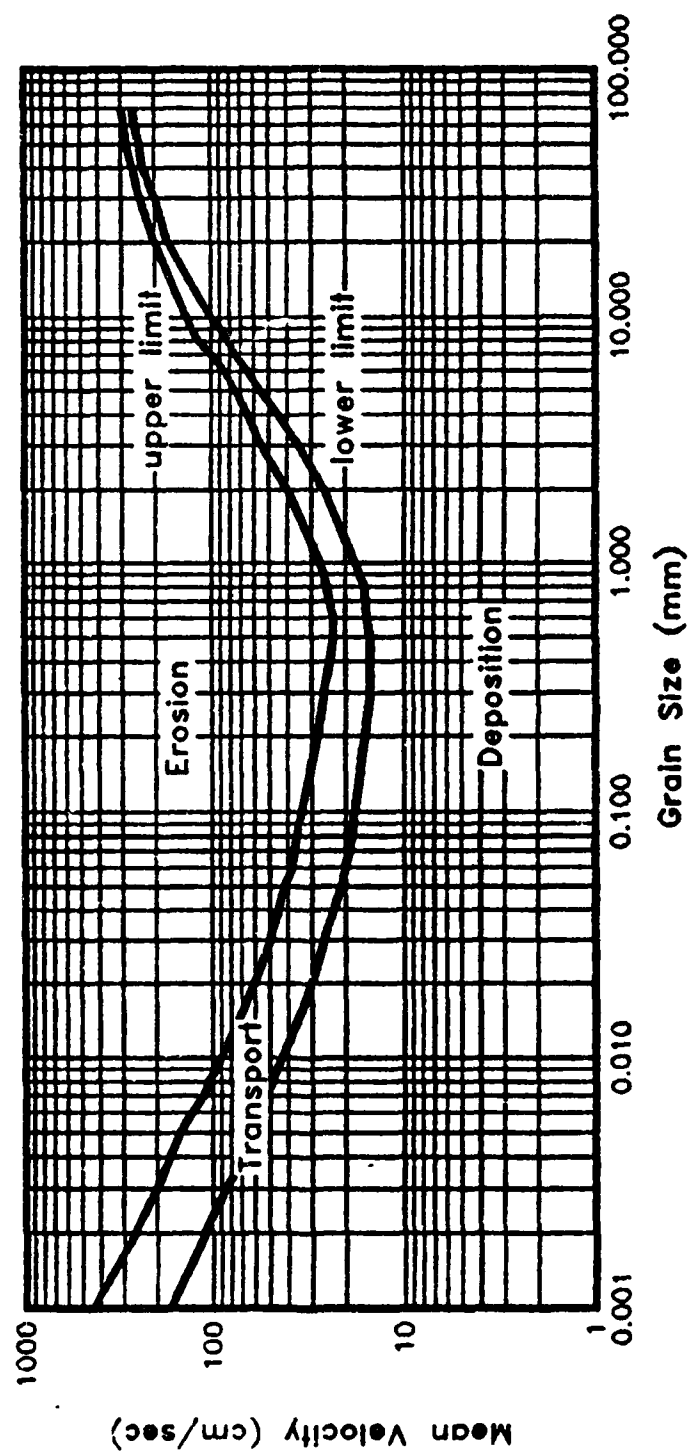
Fig. 3. Critical water velocities for quartz sediment as a function of mean grain sise (from Vanoni et al. 1966).

taken from several sources. The curves are for depths of at least one meter. The relationship was developed by fitting the curves with observed data. The bottom velocities are obtained by extrapolating velocity measurements to the plane of the bed.

Scour Depth and Profile

Kjeldsen (1973) proposed the following formula for scour depth:

$$Sd = 0.972(U^2/g)^{0.2}\ D^{0.8} \tag{9}$$

where:

$Sd =$ maximum equilibrium scour depth,

$U =$ mean local fluid velocity,

$g =$ gravity, and

$D =$ pipe diameter.

Bijker and Leeuwestein (1983) proposed the following modification to Kjeldsen's equation, which incorporates mean grain size:

$$Sd = 0.929(U^2/2g)^{0.26}\ D^{0.78}\ (d_{50})^{-0.04} \tag{10}$$

where: $d_{50} =$ mean particle diameter.

Mean particle diameter is the grain diameter of the sediment particle such that half the sediment particles (by weight) have larger diameters and half have smaller diameters.

Mao (1986) developed the scour hole profile from potential flow theory as:

$$h(x) = \begin{cases} \epsilon + \frac{D}{2} + \frac{Sd}{2}(1 + cos(2\pi\frac{x}{w})) & \text{for } |x| < \frac{w}{2} \\ \epsilon + \frac{D}{2} & \text{for } |x| > \frac{w}{2} \end{cases} \qquad (11)$$

where:

$h(x)$ = Vertical distance from pipe center to bottom of scour hole,

w = Width of trench, and

ϵ = Distance between pipe and bed.

Experimental Results

The most recent significant model test on pipe scour is based on the inter-action between a fixed pipeline and an erodible bed. Mao (1986) studied the influence of a fixed pipe on an erodible sand bed under various wave and current conditions. The experimental set-up was typical for model tests on pipes. Tests were run on both a 5 cm pipe and a 10 cm pipe placed on a quartz sand bed.

The model test resulted in the following conclusions:

(1)   The scour process consists of a jet period and a wake period,

(2)   The flow stagnation point is on the upper part of the pipe,

(3)   The scour rate is very high at an early stage, later on it decreases,

(4)   In equilibrium, bed velocities are similar to mean current velocity,

(5)   The bigger the initial gap, the shallower the scour depth,

(6)   The scour depth is a weak function of Shields parameter, θ,

(7)   The final scour depth Sd is usually less than the diameter of the pipe, and

(8)   The final scour depth is influenced by the wake behind the pipe.

Fredsoe et al. (1988) studied the interaction between a vibrating pipe and erodible bed. The experimental set-up was similar to the preceding model test, with the following difference: a spring supported rigid cylinder was used as the model pipe, which was then vibrated.

The influence of pipe vibration on scour and the influence of scour on pipe vibration results in the following conclusions:

(1)   Pipe vibration induces additional erosion, which gives rise to relatively larger scour depths and scour widths. This effect was found to be most pronounced for smaller gaps between the pipe and the bed.

(2)   Vibrations are dominated by vortex shedding due to this extra erosion. Additional erosion occurs even if the pipe is placed very close to the original undisturbed bed.

Ibrahim and Nalluri (1986) studied pipeline scour due to currents and currents with waves. Tests were performed on three different grades of bed sand of sizes

d_s = 0.425 mm, 0.80 mm, and 1.50 mm. Pipe sizes were 2.50 cm, 5.00 cm, and 7.50 cm. The pipes were fully exposed to flow, *i.e.* resting on a sand bed. They also studied pipelines that were one-half and three-quarters buried. The action between pipeline, seabed and flow due to the combined wave and current was more intense compared to that due to unidirectional current.

Ibrahim and Nalluri (1986) developed dimensionless plots between the relative scour depth, Sd/D and the following dimensionless parameters:

(1) $(\bar{U}/\sqrt{gD})$ — pipe Froude Number, (Nfp), Fig. 4,

(2) $(\bar{U}/\sqrt{g\Delta d_s})$ — sediment Froude Number, $(Ns))$, Fig. 5,

(3) (HL^2/y^3) — wave Ursell Number, Fig. 6, and

(4) (H/gT^2) — wave steepness, Fig. 7.

Figs. 4-7 attempt to identify the influence of several groupings in Eq. 1 on relative scour depth, Sd/D. These plots become useful in comparing the data obtained in this research to that of Ibrahim and Nalluri (1986).
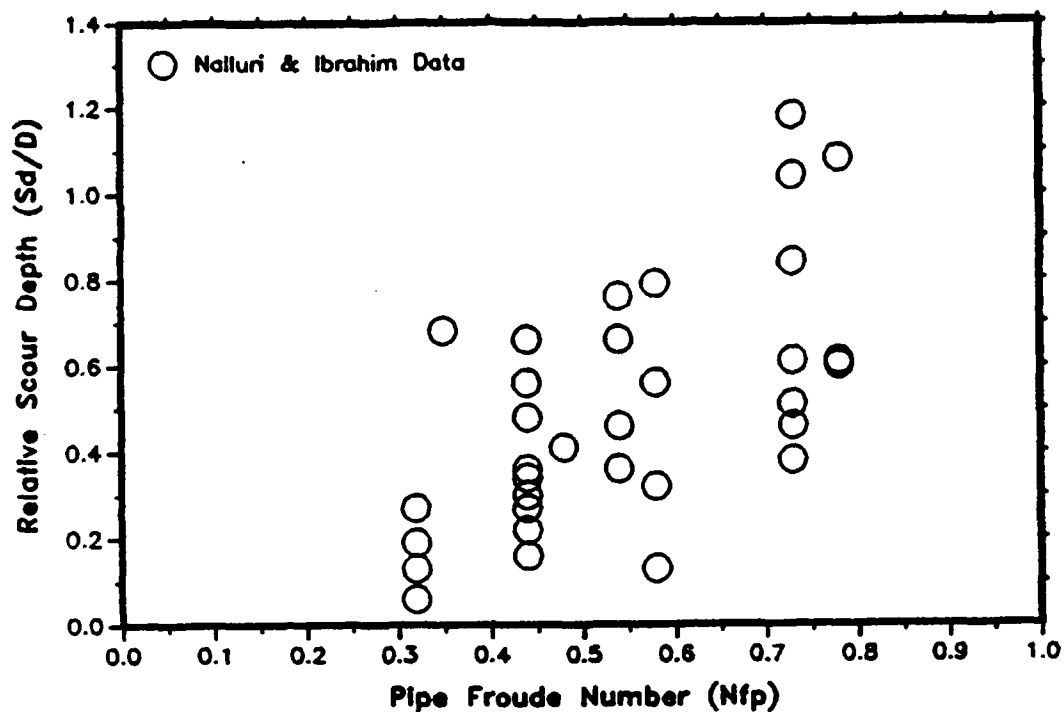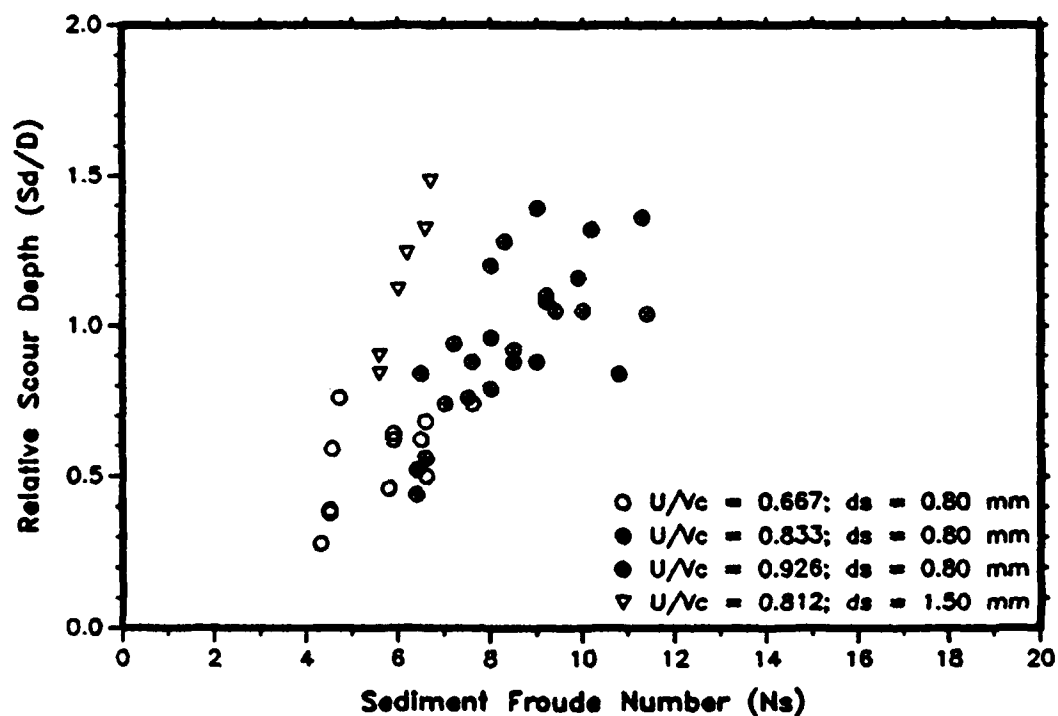
Fig. 4. Influence of pipe Froude Number $(\bar{U}/\sqrt{gD})$ **on scour.**
(Ibrahim and Nalluri 1986)

Fig. 5. Influence of sediment Froude Number $(\bar{U}/\sqrt{g\Delta d_s})$ **on scour.**
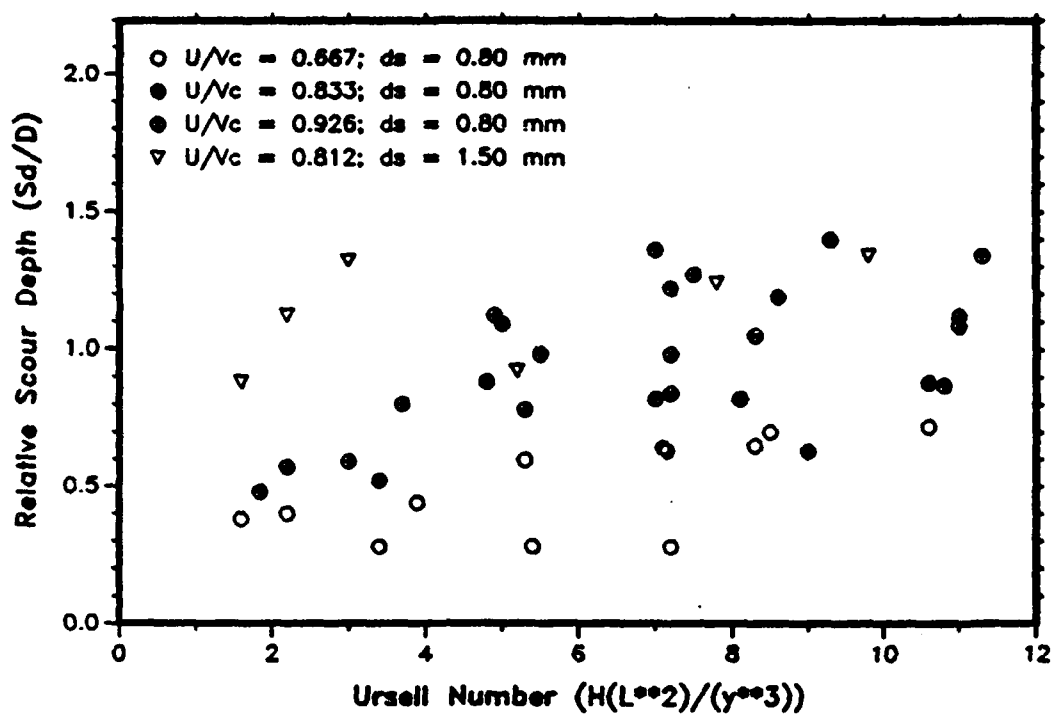(Ibrahim and Nalluri 1986)

Fig. 6. Influence of wave Ursell Number (HL^2/y^3) on scour.
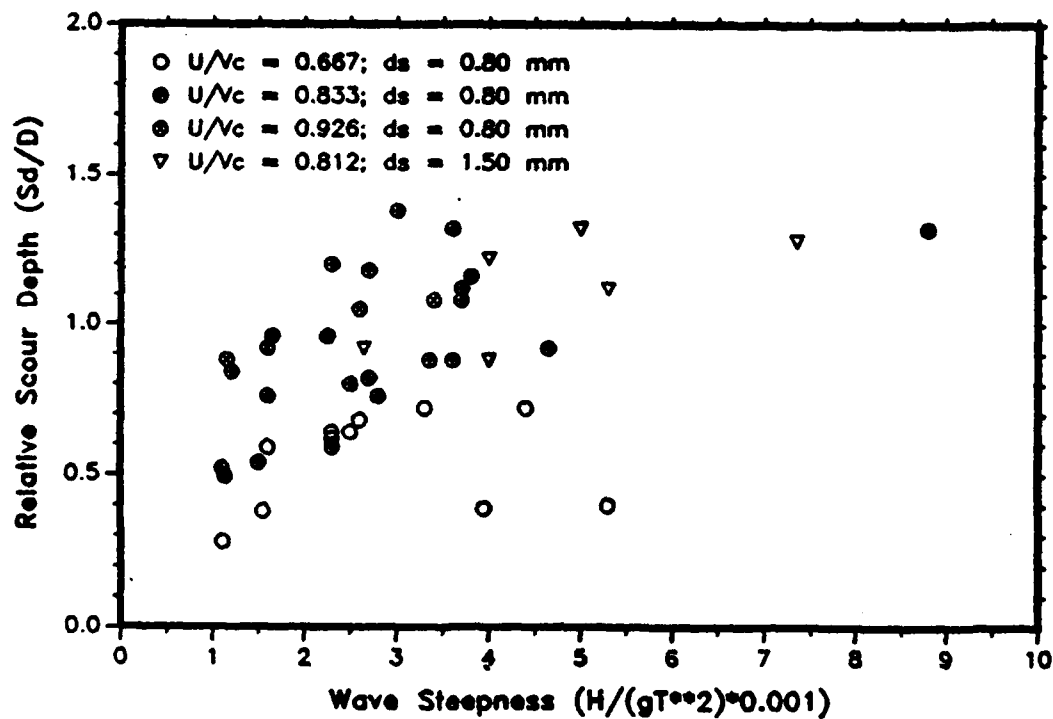(Ibrahim and Nalluri 1986)

Fig. 7. Influence of wave steepness (H/gT^2) on scour.
(Ibrahim and Nalluri 1986)

Despite the scatter of data points in Fig. 4 and 5, a trend reveals a relationship between Sd/D and flow velocity. The flow velocity is part of the Froude Number, which represents an inertia–gravity force ratio. The relative scour depth Sd/D increases with increasing Froude Number. This is expected — larger fluid velocity creates deeper scour.

Fig. 6 is the influence of the wave Ursell Number (HL^2/y^3) on scour. The Ursell Number represents relative magnitude between H/L and y/L, where:

H = wave height,

L = wave length, and

y = water depth.

The region where $U_r < 1$ corresponds to deeper water and a region where Stokes wave theory is applicable. This group tends to reveal a non-interdependency of data. According to Ibrahim and Nalluri (1986), the wave Ursell Number defines the magnitude of energy generated by the wave and transmitted to the bed. The data in Fig. 6 fall in a region where $U_r > 1$, signifying shallow water.

Fig. 7, the wave steepness, describes the disturbing capability of the wave on the sediment. For shallow depths, the data indicates an increase in Sd/D for steeper waves.

CHAPTER III

PIPELINE SCOUR

Types of Pipeline Scour

Two categories of scour are global and local. Global scour is an area erosion of the bed in the vicinity of the disturbance. Generally, it is an elliptical shape with the major axis in the direction of the dominant flow. Local scour develops at the seabed immediately adjacent to the pipeline. Local pipeline scour results in a scour hole below the pipeline (Dahlberg 1983).

When examining local scour, the two-dimensional case is considered. The primary cross-sectional area is a transverse cut through the pipe and seabed. Span analysis examines the cross-sectional area along the pipe axial length. Flow parameters which influence scour are steady flow (current), oscillatory motion (wave), or a combination of current with superimposed wave velocity. The net effect is a pulsating mass transfer in one direction. The combined oscillatory motion and current velocities yield the mean flow in one direction. The scour due to a steady current is greater than the combined wave–current affect.

Leeuwestein (1984) describes three types of local scour based on relative position to the pipe as tunnel, luff and lee erosion, Fig. 8. Lee erosion occurs while the sediment remains in suspension in the wake. During lee erosion the sediments are transported up by jet flow into the wake and then carried away by currents. Total scour depth is larger for current–induced scour than for wave–induced scour. Bijker and Leeuwestein (1983) found that wave induced scour is about 30% the depth of current–induced scour. The reason for smaller wave–induced scour is that the orbital nature of the flow results in some sediment remaining in the scour hole.

Lee erosion extends further downstream, resulting in a wide trench around the pipe, Fig. 8. Luff erosion generally appears just upstream of pipelines in the absence of tunnel erosion, usually near partially buried pipelines. Luff erosion is not of major concern because it generally does not result in free spans. The primary influence on scour beneath a pipe is lee erosion. Tunnel erosion occurs in the early stages of the scour process, then lee erosion takes over during the growth phase of the scour hole. Tunnel erosion is the scour which occurs directly beneath the pipe. Tunnel erosion leads to lee erosion which results in free spans.
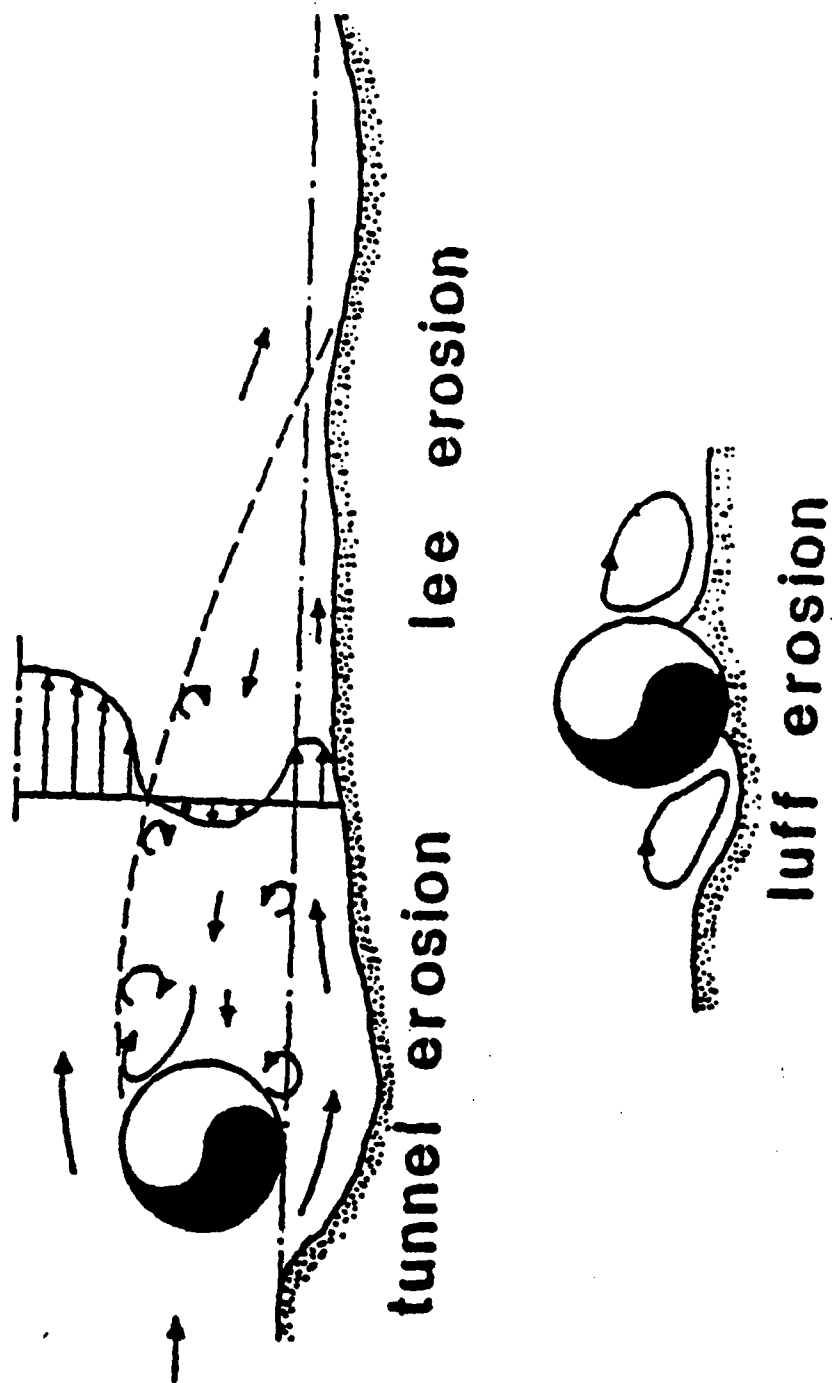
lee erosion

tunnel erosion

luff erosion

Fig. 8. Types of pipeline scour (from Leeuwestein 1984).

Contributing Factors

Maximum equilibrium scour depth is a function of several factors. The major cause of erosion is the vortex shedding in the wake. Vortex shedding is turbulence diffused from the leeward side of the pipe wall, allowing sediment to remain in suspension. Sediment is transported up by jet flow into the wake of the vortex and then carried off by currents. Vortex shedding drives lee erosion.

The Keulegan–Carpenter number (KC) is the parameter which describes the type of flow, being either *steady flow (current)*, *oscillatory motion (wave)*, or a combination of the two. The KC number is a non–dimensional measure of the flow, described earlier as:

$$KC = UT/D \tag{12}$$

where:

U = local fluid velocity near pipe,

T = wave period, and

D = pipe diameter.

A low KC number (*i.e.* < 50) means that oscillatory flow dominates. As KC increases, current flow dominates.

According to Fredsoe et al.(1988), KC represents the effect of the lee–wake on the scour and constitutes the most important parameter which governs equilibrium scour.

Mechanics of Scour

Sediment transport conditions do not necessarily exist upstream of the pipe. The presence of the pipe is responsible for generating enhanced flow conditions that trigger the scouring process. A pipeline near an erodible bed is subjected to constantly changing scour conditions. Pipe movement above the scour hole, from sag and vortex shedding induced vibrations, also contributes to the variability of flow regimes.

Sediment mechanics, incipient motion and pipeline/soil interaction are primary factors that influence scour. Sediment motion is determined by the bed shear stress, which is defined as the tangential force exerted along the seabed by the passing flow of water. Scour is effected by the leeward wake created by vortex shedding of the pipe. Hydrodynamic forces on the pipeline may influence the scour beneath a pipeline, but they are not the principle driving force. Lift forces or pipe vibrations on the pipeline raise the pipe sufficiently for jet flow through a gap between the pipe and bed. This is known as the nucleation phase or the jet period. During this phase a small hole is created under the pipe.

Incipient motion occurs when the jet velocity between the pipe and bed exceeds the critical velocity needed to begin sediment movement, and tunnel erosion is initiated, Fig. 9. Vortex shedding creates a turbulent wake leeward of the pipe, which keeps the sediment suspended for sufficient time for current to carry the sediment downstream. The growth phase or wake period of the scour hole occurs while the vortex shedding creates a turbulent wake leeward of the pipe.

The sediment in suspension is balanced against gravitational forces that tend to pull it back into the bed. Lee erosion takes place while the sediment is carried off in the wake of vortex shedding. Vortex shedding may be further enhanced by pipe vibrations.

Equilibrium scour depth is reached when the velocity near the bed surface is about equal to the current velocity. Sediment removal from the scour hole continues as long as the critical velocity of sediment movement exists. Critical velocity dominates as long as the the current velocity is greater than the threshold value of sediment movement. The growing scour hole alters the flow until a new dynamic equilibrium is reached between the erosion and deposition. The increase in the scour hole size causes a decrease in the jet–like effect until it returns to normal mean fluid velocity. This happens when the depth of the scour hole is approximately one pipe diameter deep. At this point the scour process ceases.
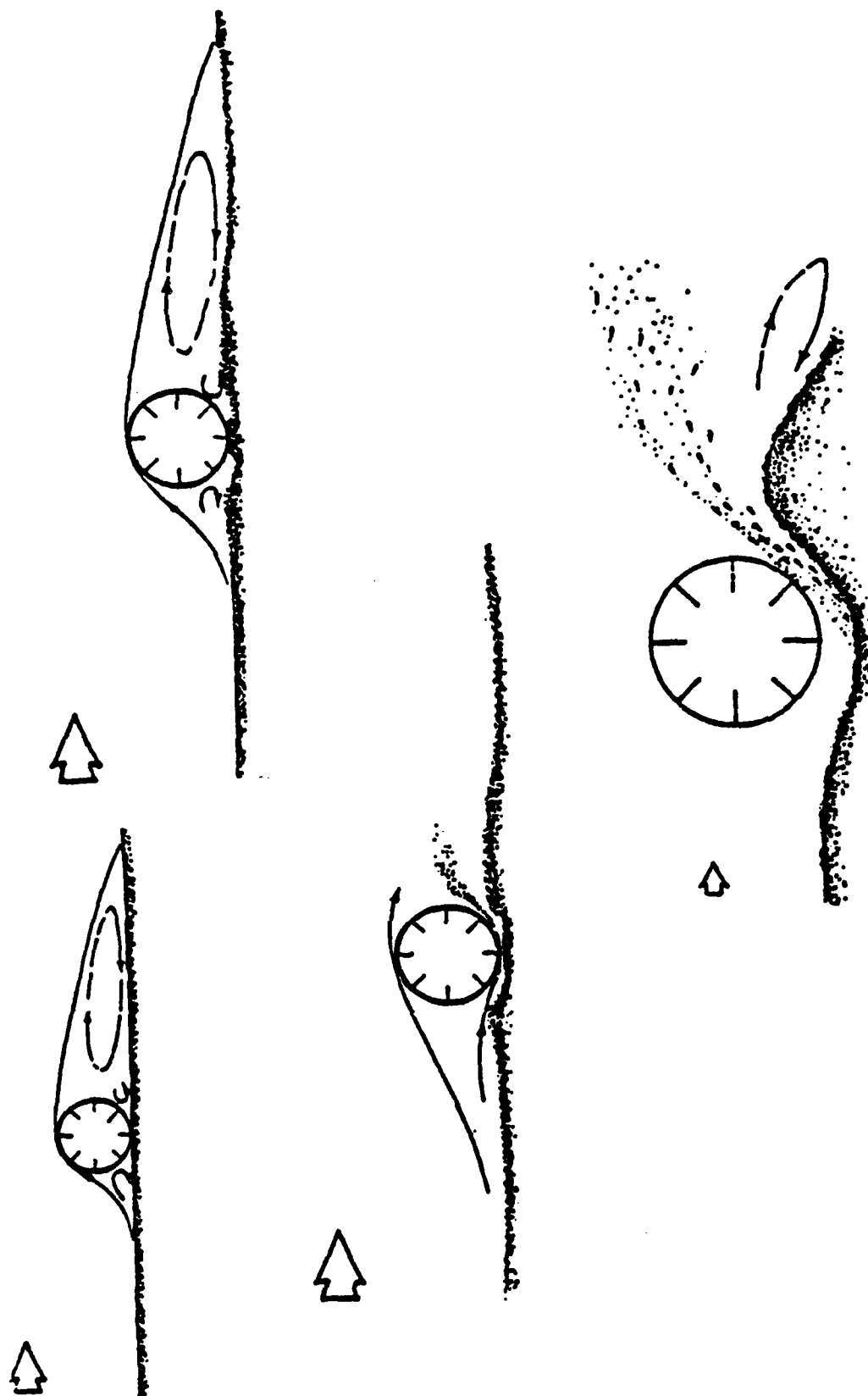
Fig. 9. Initiation of scour (from Mao 1986).

The presence of the pipeline causes vortex shedding. Vortex shedding complicates evaluation of boundary conditions for scour initiation. Boundary conditions are determined by the type of soil. Boundary layer parameters are the bed shear stress (τ_o) and bed friction coefficient (c), both parameters of the sediment. Shear stress (τ) due to current flow or oscillatory motion is determined as a function of bed roughness and effective grain size. Critical shear stress (τ_c) which contributes to initial movement, is a function of the immersed weight of a grain of sediment, mean grain size and critical velocity.

Time scale effect on the formulation of scour rate is related to the dominant type of flow through the Shields parameter (θ). The scour rate is high at first, then it decreases with time. The larger the Shields parameter (θ), the higher the scour rate in the early stages. The presence of superimposed waves greatly increases the rate at which sediment is transported, which accelerates the formation rate of the scour hole. However, the equilibrium scour depth is less in the combination flow condition than in steady flow.

The shape of the scour hole will vary in symmetry, and is also a function of the dominating type of flow. This is best described by the Keulegan–Carpenter (KC) number. The width of the hole is a function of the sediment characteristics, and the symmetry is a function of the type of flow. In a unidirectional flow, the leeward side of the pipe will have less of a slope than the upstream side. In a two–directional oscillatory flow, the profile is symmetrical. Both the symmetry and dominating flow are closely related to the Keulegan–Carpenter (KC) number.

Scale Effects

One of the difficulties in conducting model tests is insuring that scale factors are accurate. Scale effects are based on scaling laws for local scour and are related to the similarity of sediment size, grain shape, and grain Froude number. The limiting grain size for permissible reduction of sediment in a model is about 0.05 mm. Pipe sizes are a function of the test flume dimensions. Typical offshore oil pipelines are one meter in diameter. In this case a model pipe of ten centimeters represents a 1:10 scale.

Test conditions which govern the applicability of experiments are the Reynolds (R_e) number and Keulegan–Carpenter (KC) number. The R_e number is a measure of the turbulence and the KC number describes the type of flow. A high R_e puts the flow in the turbulent range, representing typical field conditions. A KC number greater than 50 describes a steady flow, whereas a lower value takes into account the oscillatory flow contribution from the wave velocity. For wave–current experiments the following R_e and KC ranges are recommended:

(1) Reynolds number:

$$R_e = \frac{UD}{\nu} > 10^5$$

(2) Keulegan–Carpenter number:

$$KC = \frac{UT}{D} < 50$$

CHAPTER IV

COMPUTER PROGRAM

Program Development

The program SCOUR.FOR is a FORTRAN coded program which calculates the maximum scour depth and scour profile based on equations defined earlier:

(1) Equilibrium scour depth, (see Fig. 10):

$$Sd = K_s (U^2/g)^{0.2} \ D^{0.8}$$

where: K_s is a sediment factor taking into account effective sediment size (d_s) and density (ρ_s).

(2) Scour profile, Eq. 7, (see Fig. 11):

$$h(x) = \begin{cases} \epsilon + \frac{D}{2} + \frac{Sd}{2}(1 + cos(2\pi \frac{x}{w})) & \text{for } |x| < \frac{w}{2} \\ \epsilon + \frac{D}{2} & \text{for } |x| > \frac{w}{2} \end{cases}$$
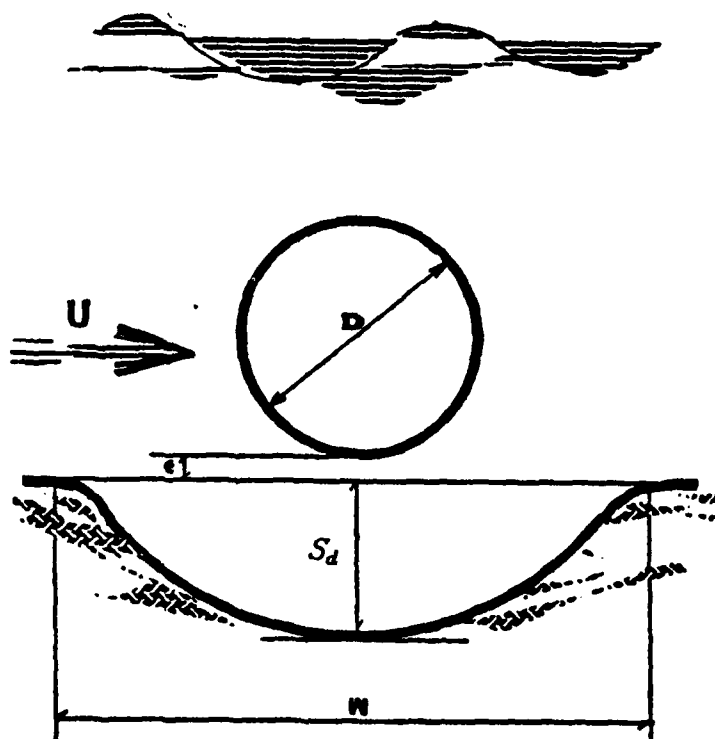
Fig. 10. Definition sketch of scour under a pipe.
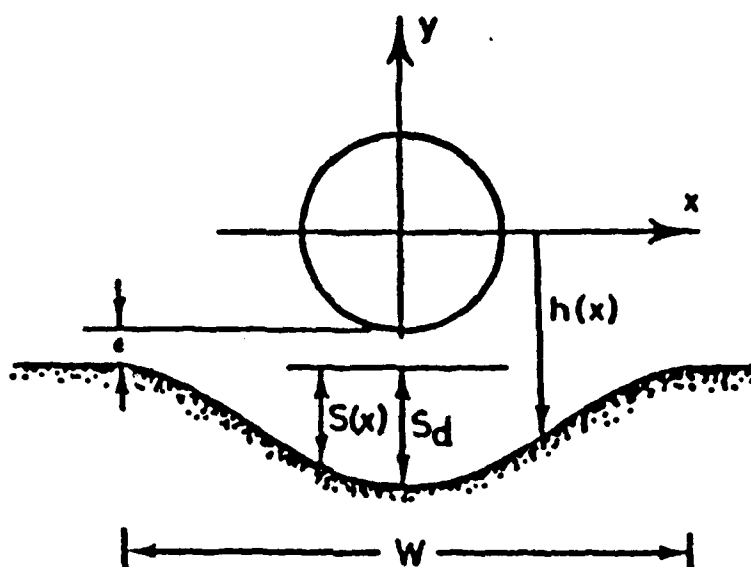
Fig. 11. Scour hole profile, from Mao (1986).

SCOUR.FOR inputs Stokes III wave theory as a subroutine, WAVE123. Stokes V wave theory is the recommended guideline adopted by the American Petroleum Institute (API) for use in offshore design problems. The theory has wide applications in the coastal and offshore industry. For purposes of this program, Stokes III will suffice.

The WAVE123 subroutine, modified for the SCOUR.FOR program, computes the maximum wave velocity at a depth of interest near the pipe. The wave velocity is combined with current, yielding the mean local fluid velocity (U) acting on the pipe. The input wave height and period are for extreme events, resulting in the highest bottom velocities. Extreme events are storm or hurricane conditions.

The program is governed by the following assumptions:

(1)   The maximum wave velocity at the depth of interest is algebraically summed with the current velocity, yielding mean fluid velocity acting on the pipe.

(2)   Although wave velocity is oscillatory, the net effect is a pulsating mass transfer in one direction.

(3)   A normal angle of attack on the pipe has the greatest effect on scour depth, resulting in maximum scour depth.

(4)   The computer program is based on a unidirectional flow from the combined effect of current and wave velocities. The velocities are algebraically added. The shape factor is determined by the width of the scour hole in terms of pipe diameters.

(5)   The program is designed for depths in the 100 meter range under extreme storm conditions.

Program Flexibility

The SCOUR.FOR program flow chart, Fig. 12, is a visual representation of the solution sequence. The flow chart depicts the flow of control, identifying interrelationships and decision requirements of the program sequence. The flow chart is adjustable to other computer languages and systems capable of executing basic numerical computations.

The program accommodates any type of pipe orientation to the bed. The gap distance value ϵ must be input if the pipe does not rest on the seabed. When the pipe is in contact with the seabed, $\epsilon = 0$. The scour profile coordinate system is measured from the center of the pipe if $\epsilon > 0$, otherwise the coordinate system is adjusted to the seabed for $\epsilon = 0$.
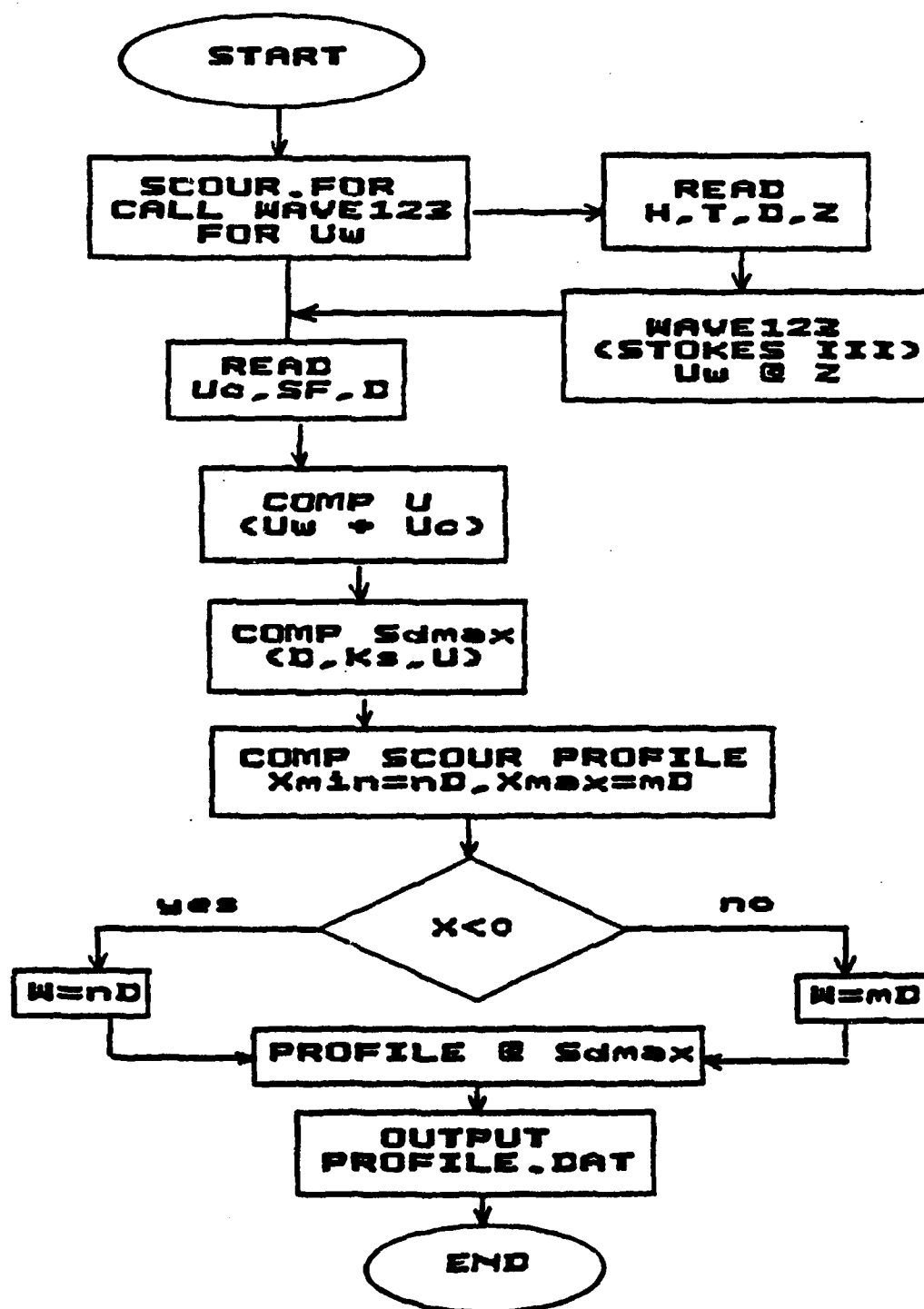
Fig. 12. SCOUR.FOR flow chart.

The effect of sediment characteristics is controlled by the sand factor (S_f) and the sediment factor (K_s). The sediment factor will influence the equilibrium scour depth and is a function of the type of sediment. It is adjustable in the program listing.

The inputed sand factor (S_f) relates the pipe diameter to the scour hole width (w), and is a function of Shields parameter (θ). The symmetry of the scour hole is controlled in the program list and is a function of the dominant type of flow, being either oscillatory or unidirectional. The Keulegan–Carpenter (KC) number governs the type of flow. The SCOUR.FOR FORTRAN program CODE list is included in Appendix I.

Execution

SCOUR.FOR reads pipe diameter (D), sand factor (K_s) and current velocity (U_c), in metric units, from the input file MAIN.DAT. The program subroutine WAVE123 input is wave height (H), period (T), water depth (d) and depth of interest near the pipe (Z).

SCOUR.FOR program output creates an output file PROFILE.DAT, which is easily plotted using any standard graphics package.

The program was designed on a Digital 8000 VAX/VMS mainframe computing system with FORTRAN compiler located at Texas A&M University. The SCOUR.FOR and WAVE123 FORTRAN codes are loaded into the mainframe and executed with the following commands:

(1) FOR SCOUR,WAVE123

(2) LINK SCOUR,WAVE123

(3) RUN SCOUR

The program is best demonstrated by varying the MAIN.DAT input data (current velocity (U_c), pipe diameter (D) and sand factor (S_f)), while keeping the WAVE123 data constant (except for depth of interest (y) when changing (D)), and comparing the plotted results. The sample output, Fig. 13, was created from the SCOUR.FOR output file, PROFILE.DAT, using the VAX/VMS graphics system PICSURE package.

PIPE DIAMETER = 50 cm

Water Depth = 100 meters
Storm Wave Height = 20 meters
Current & Wave Velocity = 2.2 m/s
Wave Period = 15 sec

U

U

Quartzite sand bed

Maximum Scour Depth = 22.3 cm

Scour Profile (cm)

Scour Depth (cm)
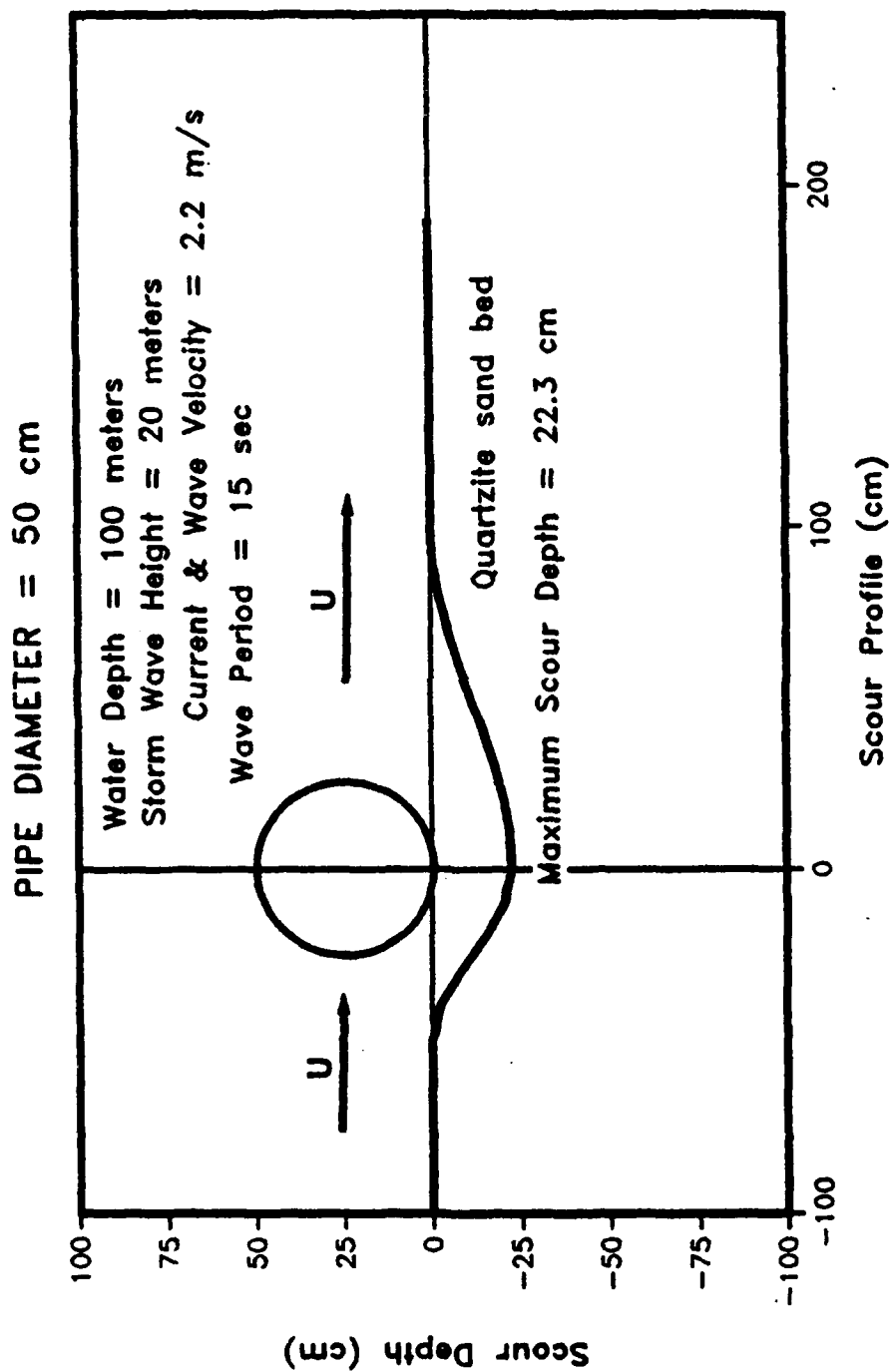
Fig 18. Graphic representation of SCOUR.FOR output.

CHAPTER V

EXPERIMENTAL APPARATUS AND EQUIPMENT

Model testing was conducted in a two-dimensional wave and flume facility as shown in Fig. 14. The wave-flume is 45.72 m long, 0.46 m wide, and 1.22 m deep. One side of the flume consists of a plexiglas side wall for observing tests. Fig. 15 is the schematic layout of the test facility.

A 6.0 m long ramp section consisted of a 3.0 m long gradual rise (1:15) followed by a level 3.0 m long section, Fig. 16. The ramp preceded the sand test section and provided for a smooth transition from the flume bottom to sand bed. It also contributed to the development of the boundary layer.

A test section located approximately 20.0 m from the wave generator consisted of a 6.0 m long by 0.20 m deep sand bed. This test section was 12 m long, including the ramp and sand bed section, shown in Fig. 16. Pipes were placed on the bed at about 3.0 m downstream of the ramp. This allowed for development of a boundary layer and equilibrium condition in the sand bed section before the current reached the pipes.
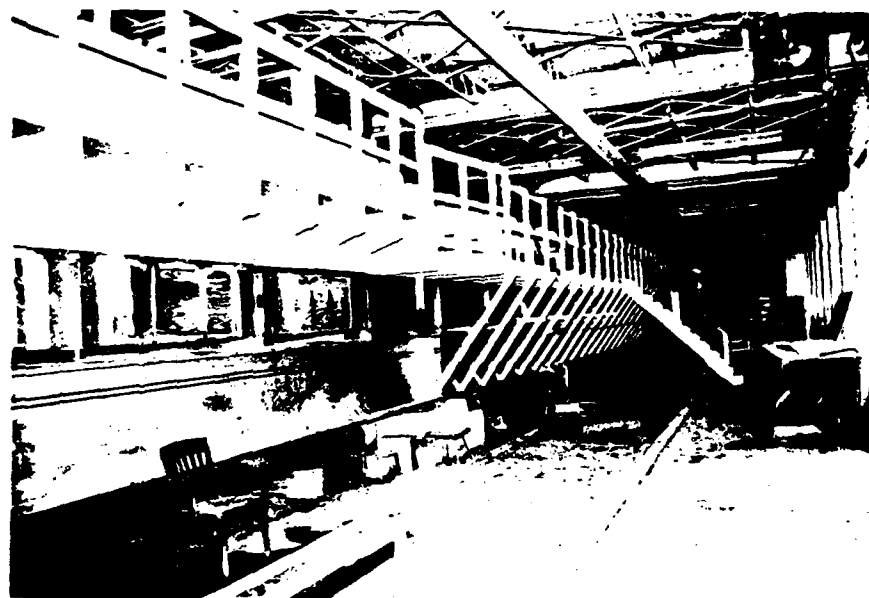
Fig 14. Test facility.

WAVE/CURRENT FLUME
TEST FACILITY — SCHEMATIC

NO SCALE

ADJUSTABLE
WEIR

WAVE
ABSORBER

TEST AREA

FILTER

WAVE
GENERATOR

FLOW
CONTROL VALVE

FLOW
CONTROL VALVE
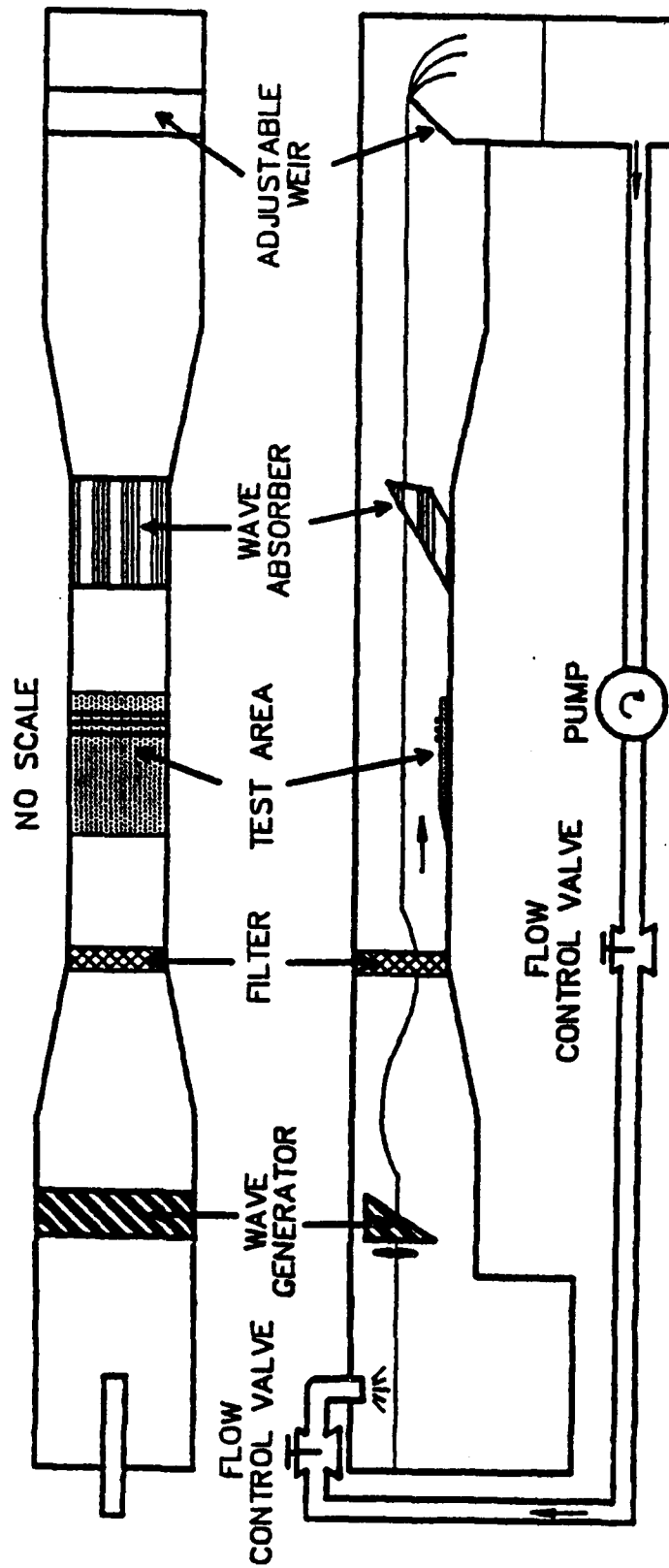
PUMP

Fig 15. Schematic layout of test facility.

wave gauge

pipes

velocity profile

∇ SWL

0.60 m

0.20 m

sand bed (d_{50} = 0.08 mm)

3.0 m   3.0 m   3.0 m   3.0 m
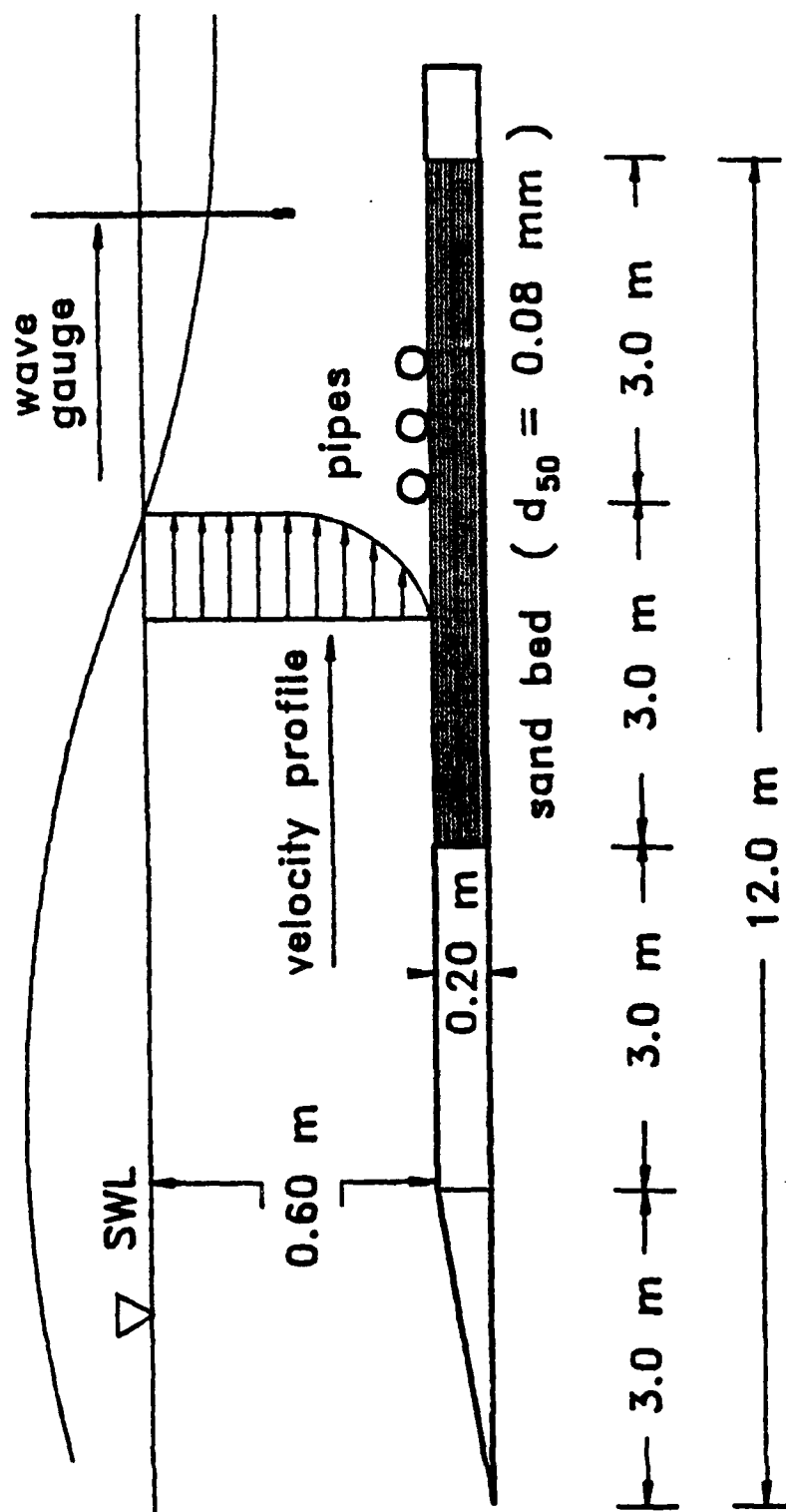
12.0 m

Fig 16. Schematic layout of test section.

Currents were produced by a pumping system capable of developing a flow velocity of 1.20 m/sec. The flow rate is controlled by two flow control valves. Water depth is controlled by an adjustable weir located at the end of the tank. Currents were controlled by adjusting the flow control valves and weir.

The wave generator produces a wave by the plunging motion of a wedge, where the height of the wave is determined by the depth of the plunger and the depth of water. Wave period and wave length were adjusted by a rheostat which controls the plunger speed. The wave generator was preset for test conditions. A wire mesh wave filter which dissipated the small surface ripples from the generated waves was located 2.0 m from the plunger.

A wave absorber was placed at the end of the tank to reduce wave reflection. The wave absorber design permits passage of large volumes of water. This allows for significant currents and waves with undisturbed current flow and reduced wave reflection.

Three sizes of pipes are utilized: 3.0, 6.0, and 9.0 cm. The pipes were secured in the tank through compression springs and dowels placed inside each pipe. Each pipe was placed in the tank under flow conditions, and set in place with the flow direction normal to the longitudinal axis of the pipe. Proper pipe spacing was achieved through the use of spacers. The pipe spacing is the clear width between outer pipe diameters.

Current velocity was measured with a propeller current meter. Velocity measurements were taken at 5.0 cm from the bottom up to the water surface. Velocity profiles were developed by measuring the current at 5, 10, 20, 30, 40, 50, and 60 cm from the bottom.

A Seasim resistance type autocompensating wave gauge and Hewlett Packard Model 17403A strip chart recorder were used to measure and record the wave characteristics. The wave gauge consists of a 40.0 cm long stainless steel probe with anodized aluminum calibration rod and clamp attachment. The maximum recommended cable and circuit resistance is 1.0 ohm and frequency range in autocompensation mode is 0.2 to above 10.0 Hz.

Scour profiles were measured with a point gauge profiler. The profiler was manually operated with a precision of 5.0 mm.

CHAPTER VI

EXPERIMENTAL PROCEDURES

Seventy-two test runs were conducted for this study. Pipe sizes of 3.0, 6.0, and 9.0 cm were placed on a sand bed test section. Fig. 17 is the result of a sieve analysis of the sand; it shows that $d_{50} = 0.08$ mm. Table I shows the test pipe configurations, flow conditions and test numbers. Each pipe configuration was subjected to four flow conditions:

(1) Current only:

$$U = 0.37 \ m/sec$$

(2) Current with wave:

$$U = 0.37 \ m/sec$$

wave characteristics:

$$H = 6.0 \ cm, \quad L = 1.0 \ m, \quad T = 1.2 \ sec$$
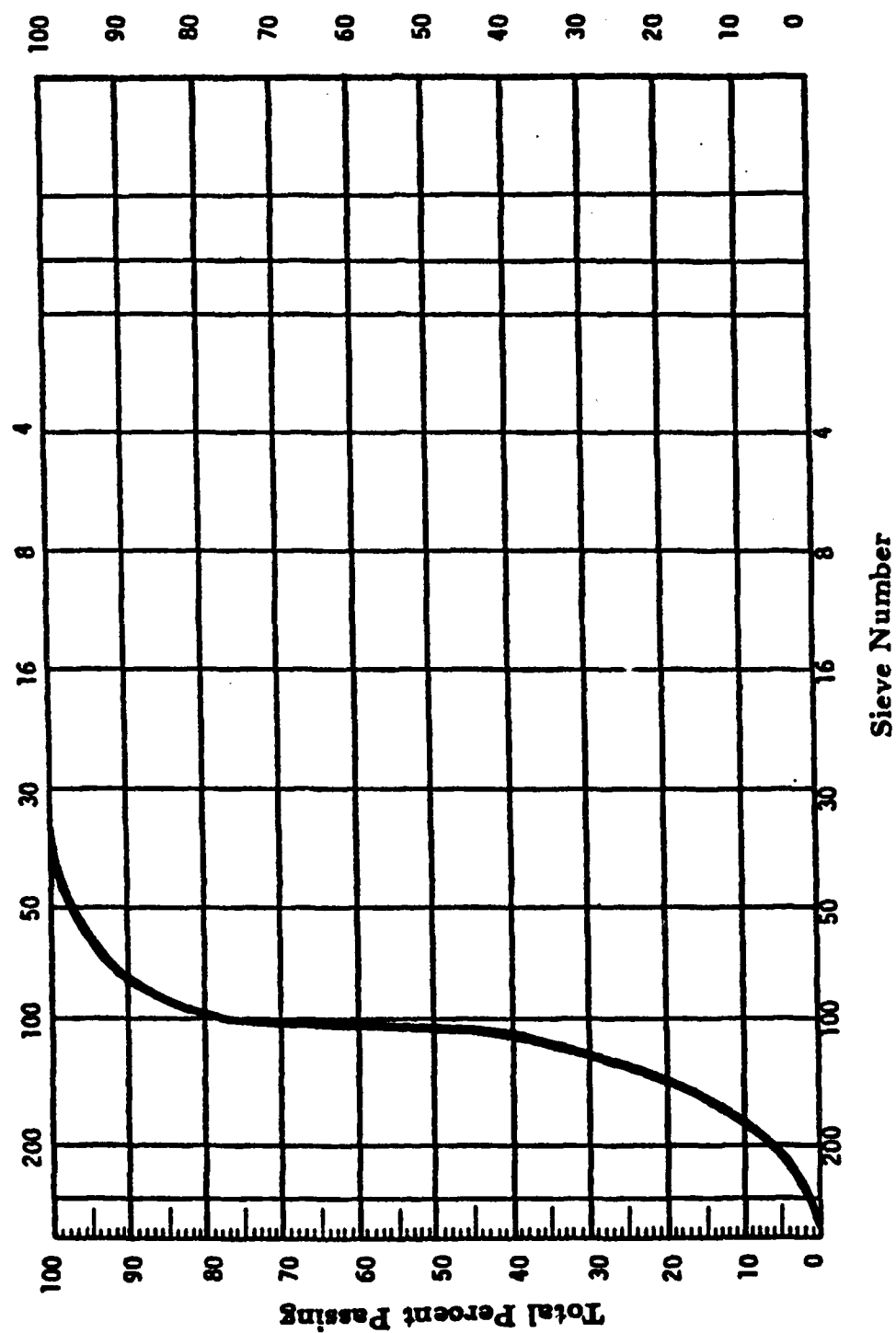
Fig 17. Sieve analysis.

Table I. Test Numbers and Test Conditions.

TEST NUMBERS

TEST CONFIGURATION	U = 0.37 m/s			U = 0.26 m/s		
	PIPE DIAMETER – D – (cm)					
	3	6	9	3	6	9
— ◯	1	15	29	43	53	63
≈ ◯	2	16	30	44	54	64
— ◯ D/2 ◯	3	17	31	45	55	65
≈ ◯ D/2 ◯	4	18	32	46	56	66
— ◯ D ◯	5	19	33	47	57	67
≈ ◯ D ◯	6	20	34	48	58	68
— ◯ D/2 ◯ D/2 ◯	7	21	35	49	59	69
≈ ◯ D/2 ◯ D/2 ◯	8	22	36	50	60	70
— ◯ D ◯ D ◯	9	23	37	51	61	71
≈ ◯ D ◯ D ◯	10	24	38	52	62	72
— ◯ D/2 ◯ (stacked)	11	25	39	NOTES :		
≈ ◯ D/2 ◯ (stacked)	12	26	40	— ◯ current only		
— ◯ D ◯ (stacked)	13	27	41	≈ ◯ current & wave		
≈ ◯ D ◯ (stacked)	14	28	42	height = 6 cm length = 1.0 m period = 1.2 sec		

(3) Current only:

$$U = 0.26 \; m/sec$$

(4) Current with wave:

$$U = 0.26 \; m/sec$$

wave characteristics:

$$H = 6.0 \; cm, \quad L = 1.0 \; m, \quad T = 1.2 \; sec$$

where: U = mean local velocity 5.0 cm above bed.

The pipe spacing is the clear width between outer pipe diameters. The flow control valve, adjustable weir and wave maker were calibrated and preset for the test conditions.

The critical velocity of incipient motion, V_c, was determined experimentally:

$$V_c = 0.40 \; m/sec$$

This was done by gradually filling the tank to the test depth of 0.60 m, which developed the equilibrium bed. The current velocity was slowly increased until weak movement was observed. A few sand particles just began to move in isolated areas of the bed. The current velocity was measured with the current meter 5.0 cm above the bed. This procedure was repeated several times.

Comparison between the experimentally determined V_c and the values in Fig. 3 reveal a close correspondence. The experimental value of $V_c = 0.40\ m/sec$ is slightly higher then that shown in Fig. 3. This may be due to:

(1) the precision of the current meter, and

(2) measuring the velocity at 5.0 cm above the bed.

Measurements less than 5.0 cm from the bed result in the current meter disturbing the bed. The V_c profile is shown along with the velocity profiles of each test condition in Fig. 18. V_c is determined under current only conditions. A hypothetical tangent line from 5.0 cm above the bed on the velocity profile curve on Fig. 18 to the plane of the bed (x–axis) gives theoretical values for velocity. These values are in the boundary layer. Incipient motion occurs at velocities in the boundary layer. For purposes of this study, the values used are measurable quantities taken at 5.0 cm above the bed.

At $U = V_c$ one may observe a slight movement in the bed. Close observation revealed a few grains of sand rolling along the bed in the direction of the current. At $U < V_c$ no sand moves. When the test wave was run with V_c, the measured velocity at 5.0 cm was the same as the measured velocity for current only. But with the wave, sediment is brought into suspension, and the sand bed mobilizes.
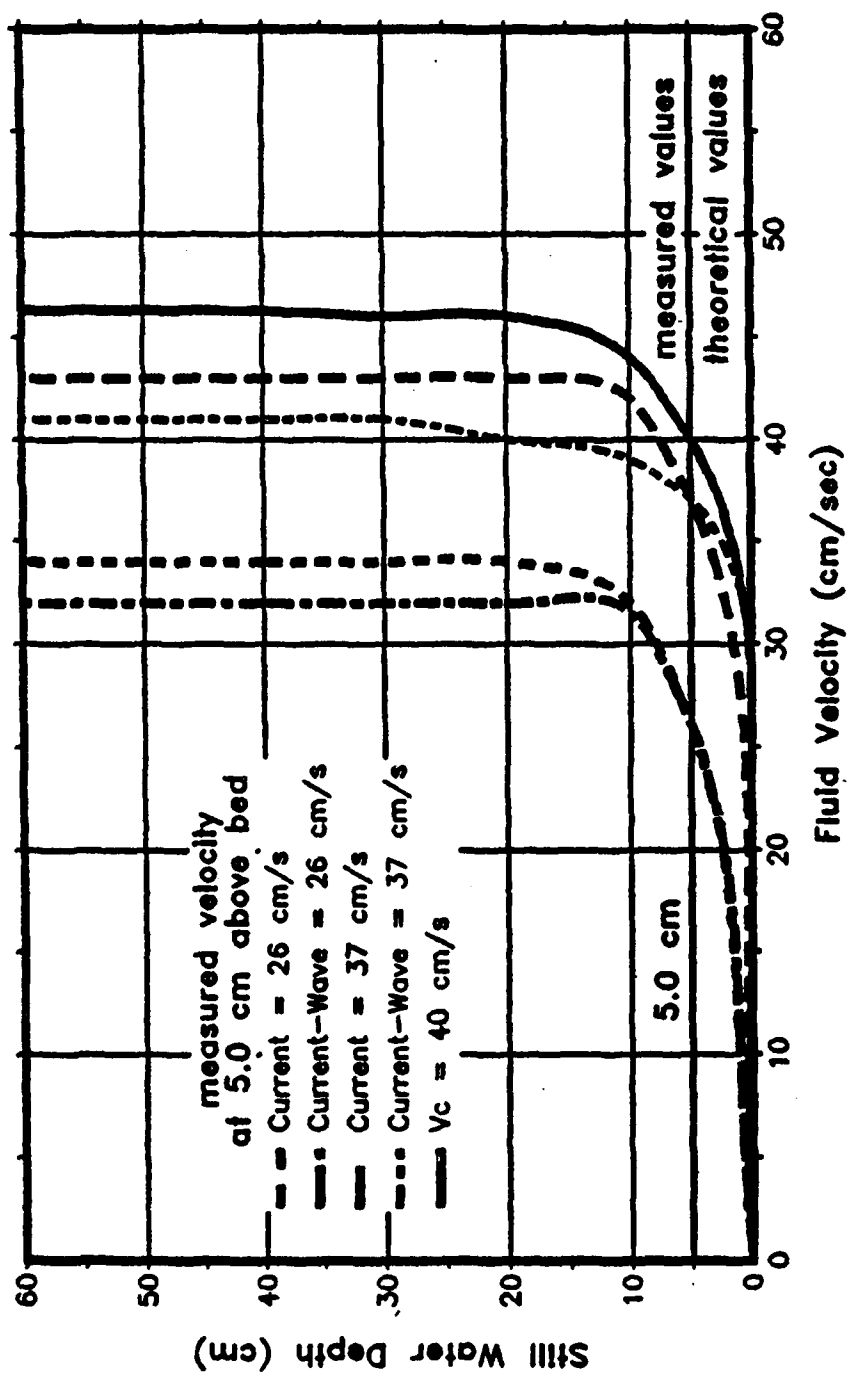
Fig 18. Velocity profiles.

At the onset of each test, the sand bed was leveled and the tank slowly filled with water. Fresh sand was added to the bed between tests, and manually compacted to a thickness of 0.2 m. This was an attempt to control the bed density without taking compaction measurements, ensuring the same bed density for all tests and prevented bed liquefaction.

Equilibrium bed developed as the tank filled with water. The equilibrium bed was characterized with small sand ripples, approximately 2-5 mm high, 2 mm wide and about 4-8 cm apart. The bed remained in equilibrium until the pipes were placed on the bed. Once the test flow depth of 60 cm was reached, the test current was established and measured.

Pipes were placed in the tank once the depth and current were established. For tests with current and wave, the wave generator was preset and started immediately after the pipes were in place. Pipe placement methodology was the same for each test. Each pipe was placed in the tank sequentially; the first pipe is the leading pipe. Scour began immediately.

Velocity profiles were measured and recorded for each test at about one meter upstream of the leading pipe. The profiles shown on Fig. 18 represent averages of all flow conditions for each applicable case. All the profiles shown in Fig. 18 are measured values. The wave gauge was located downstream of the pipe test area. Fig. 16 shows the typical test section layout.

Each test was run between 60 and 90 minutes. Initially, scour occurred at a high rate. Scour profiles were traced on sheets of acetate taped to the side of the tank. These scour profiles were taken periodically, with color coded lines representing different times. Generally, the maximum scour depth was reached within the first twenty minutes. The time profiles differ from the final measured centerline profiles because of side wall interference. These profiles indicate the time when the scour hole was at maximum depth. Once the maximum depth was reached, the test was allowed to run for twenty minutes, ensuring equilibrium scour.

A test run was stopped once it became apparent that the scour hole reached its maximum equilibrium depth. The water slowly drained out of the tank once the wave generator was shut down and the flow control valve closed. The pipes were carefully removed from the tank, without disturbing the scoured bed. The centerline profile was measured with the point gauge profiler at intervals of five millimeters or one centimeter. The measured profile was plotted for each test. The measured bed centerline profile and maximum scour depth for each test is included in Appendix II.

CHAPTER VII

ANALYSIS OF RESULTS

Presentation of Data

The Maximum equilibrium scour depths and relative scour depths which were measured during the tests in this study are presented in Table II and III, respectively. The data show greater scour depth for current when compared to similar cases of current and wave action, (oscillatory motion). Table III shows the relative scour depth Sd/D decreasing with increasing pipe diameter. The pipe spacing is the clear width between outer pipe diameters.

With two pipes in contact with the bed, there were three cases of no scour. Scour was not evident when 3.0 cm pipes were exposed to current and wave action. The small pipe diameter and oscillatory motion allowed for the pipe to capture sediment. The turbulence resulting from vortex shedding was influenced when an additional pipe was placed in the wake of the leading pipe. Where no scour occurred, little or no vortex shedding occurred behind the leading pipe. There was insufficient turbulence in the space between the pipes to keep sediment in suspension for transport. Thus, sediment was deposited between the cylinders. The oscillatory motion contributes to deposition by moving sediment back between the pipes. The sediment entrained between pipes settled out of suspension. In currents, sediment was transported in the direction of the current.

Table II. Maximum Scour Depth.
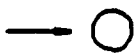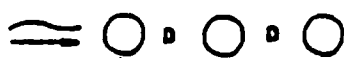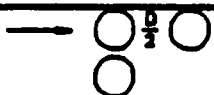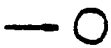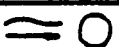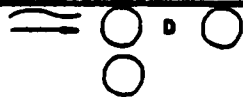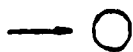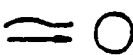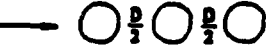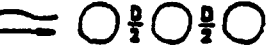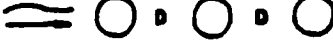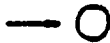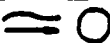
MAXIMUM SCOUR DEPTH —Sd— (cm)						
TEST CONFIGURATION	U = 0.37 m/s			U = 0.26 m/s		
	PIPE DIAMETER — D — (cm)					
	3	6	9	3	6	9
→ ○	2.15	3.75	4.60	1.55	2.20	2.25
≈ ○	1.45	3.05	3.90	1.20	2.00	2.00
→ ○ $\frac{D}{2}$ ○	1.75	3.25	4.95	1.05	2.15	2.25
≈ ○ $\frac{D}{2}$ ○	1.40	2.80	3.70	no scour	2.05	2.15
→ ○ D ○	2.40	3.80	5.15	1.40	2.20	2.25
≈ ○ D ○	2.15	3.35	4.45	no scour	2.30	2.30
→ ○ $\frac{D}{2}$ ○ $\frac{D}{2}$ ○	1.85	4.35	4.65	1.40	2.35	3.25
≈ ○ $\frac{D}{2}$ ○ $\frac{D}{2}$ ○	1.40	3.80	3.60	0.85	1.80	2.25
→ ○ D ○ D ○	2.65	4.65	5.10	1.45	2.00	3.75
≈ ○ D ○ D ○	1.95	4.10	3.95	1.10	1.90	2.50
→ ○ $\frac{D}{2}$ ○ (vertical stack)	1.50	3.05	4.40	**NOTES :**		
≈ ○ $\frac{D}{2}$ ○ (vertical stack)	0.75	2.95	3.95	→ ○ current only		
→ ○ D ○ (vertical stack)	2.40	3.90	4.35	≈ ○ current & wave		
≈ ○ D ○ (vertical stack)	no scour	3.05	4.05	height = 6 cm length = 1.0 m period = 1.2 sec		

Table III. Relative Scour Depth.

RELATIVE SCOUR DEPTH (Sd/D)						
TEST CONFIGURATION	U = 0.37 m/s			U = 0.26 m/s		
	PIPE DIAMETER – D – (cm)					
	3	6	9	3	6	9
→ ○	0.72	0.63	0.51	0.52	0.37	0.25
≈ ○	0.48	0.51	0.43	0.40	0.33	0.22
→ ○ D/2 ○	0.58	0.54	0.55	0.35	0.36	0.25
≈ ○ D/2 ○	0.47	0.47	0.41	0	0.34	0.24
→ ○ D ○	0.80	0.63	0.57	0.47	0.37	0.25
≈ ○ D ○	0.72	0.56	0.49	0	0.38	0.26
→ ○ D/2 ○ D/2 ○	0.62	0.73	0.52	0.47	0.39	0.36
≈ ○ D/2 ○ D/2 ○	0.47	0.63	0.40	0.28	0.30	0.25
→ ○ D ○ D ○	0.88	0.78	0.57	0.48	0.33	0.42
≈ ○ D ○ D ○	0.65	0.68	0.44	0.37	0.32	0.28
→ ○ D/2 ○ (stacked)	0.50	0.51	0.49	NOTES :		
≈ ○ D/2 ○ (stacked)	0.25	0.49	0.44	→ ○ current only		
→ ○ D ○ (stacked)	0.80	0.6?,	0.48	≈ ○ current & wave		
≈ ○ D ○ (stacked)	0	0.51	0.45	height = 6 cm length = 1.0 m period = 1.2 sec		

In most cases of multiple pipes, the vortex shedding from the leading pipe is influenced by the presence of additional pipes. This is seen in the scour profiles presented in Appendix II. In most cases, sediment deposition occurs in the space between multiple pipe configurations. The deposition of sediment between pipes is the result of reduced turbulence in the wake of the leading pipe. Interruption of the vortex shedding by additional pipes results in less turbulence, or a smooth wake. Thus, sediment deposition occurs in the space between pipes.

Subtle variations in scour profiles and relative scour depths are apparent when comparing current only to current and wave action profiles of similar cases. Compared with current only, current and wave action results in a more active bed with less relative scour. This paradox is attributed to the oscillatory wave motion, disturbing capability of wave and wave energy transmitted to the bed.

The disturbing capability of the wave is described by the wave steepness, (H/gT^2). In oscillatory motion, sediment is lifted into suspension and moved in oscillatory motion. The pipe spacing reduces the vortex shedding, thus producing less turbulence. The wave pushes a particle back into the scour hole where there is less fluid motion. Sediment in suspension begins to settle, sediment deposition results, and the scour profile develops. The developing scour profile influences the flow streamlines.

Flow streamlines around multiple cylinders during scour is complex. Streamlines are in a dynamic state, influenced by the changing scour profile and cylinder shape. The developing scour profile alters the flow streamlines. The streamlines adjust to the scour profile. Equilibrium occurs when fluid velocity becomes less than the critical velocity of sediment movement. In equilibrium, streamlines are uniform and the scour hole profile is static.

Data Verification

Data verification is achieved by comparing the single pipe case test results of this study with results presented by Nalluri and Ibrahim (1986), as shown in Figs. 4-7 and Figs. 19-22. In Figs. 19-22 the single pipe results of this study are plotted along with the data of Nalluri and Ibrahim. These plots indicate good correlation between the single pipe cases of this study and the study of Nalluri and Ibrahim.

Figs. 19 and 20 show the relative scour depth plotted against the pipe Froude number and sediment Froude Number, respectively. Flow velocity is part of the Froude Number, which represents an inertia-gravity force system. The relative scour depth Sd/D increases with increasing pipe and sediment Froude Number.
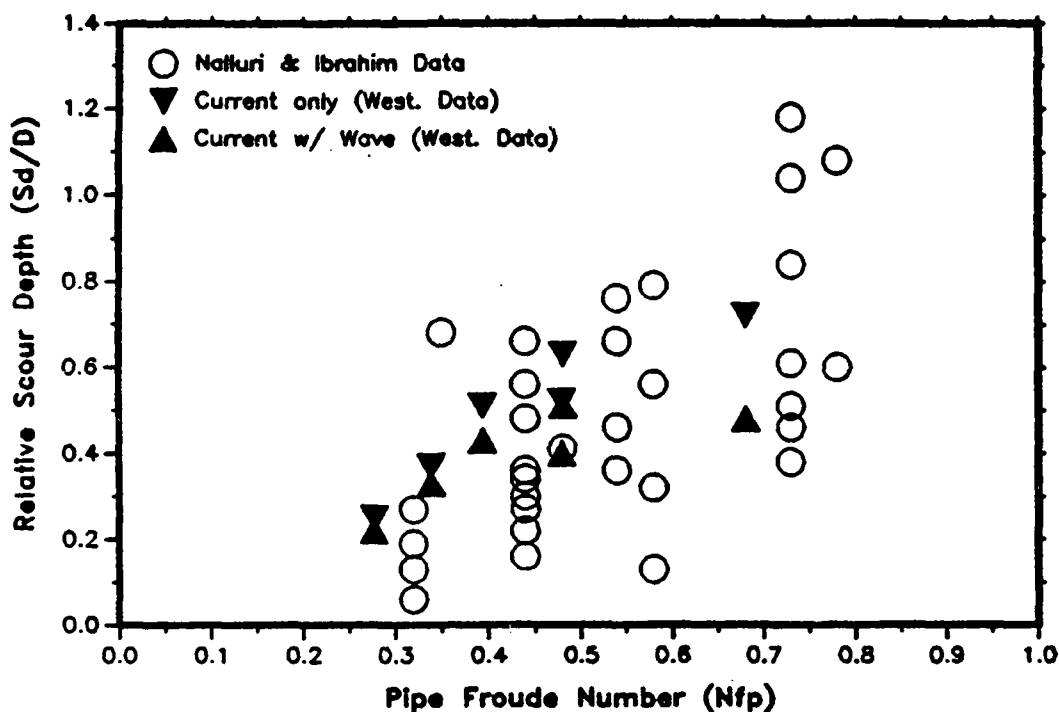
Fig. 19. Influence of pipe Froude Number $(\bar{U}/\sqrt{gD})$ on scour.
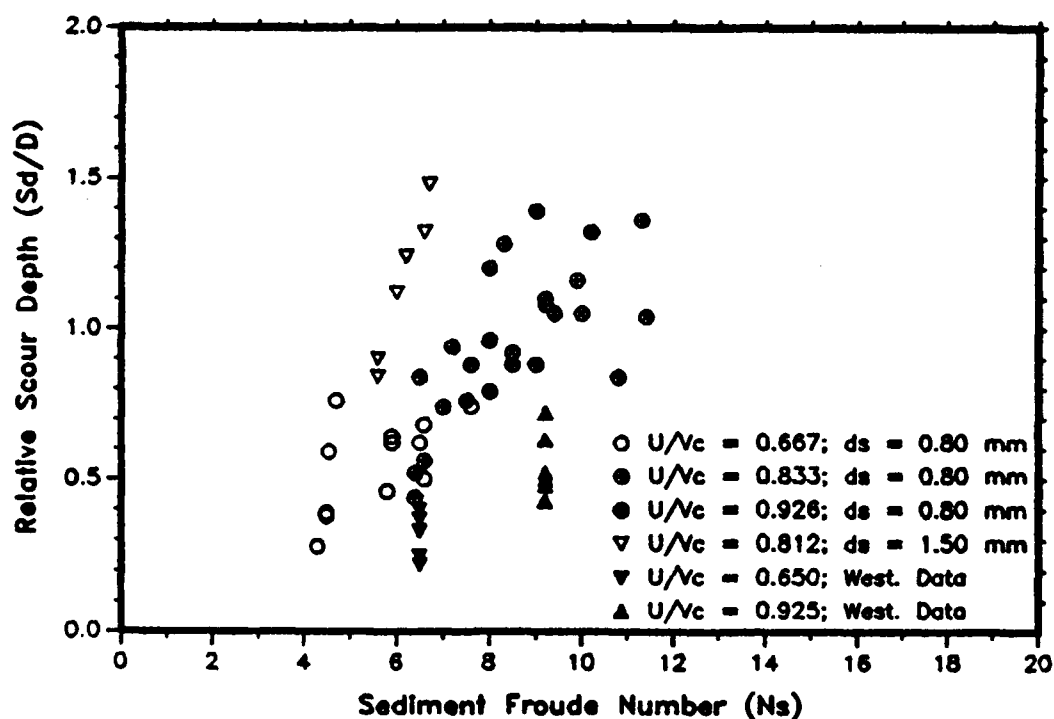
Fig. 20. Influence of sediment Froude Number $(\bar{U}/\sqrt{g\Delta d_s})$ on scour.
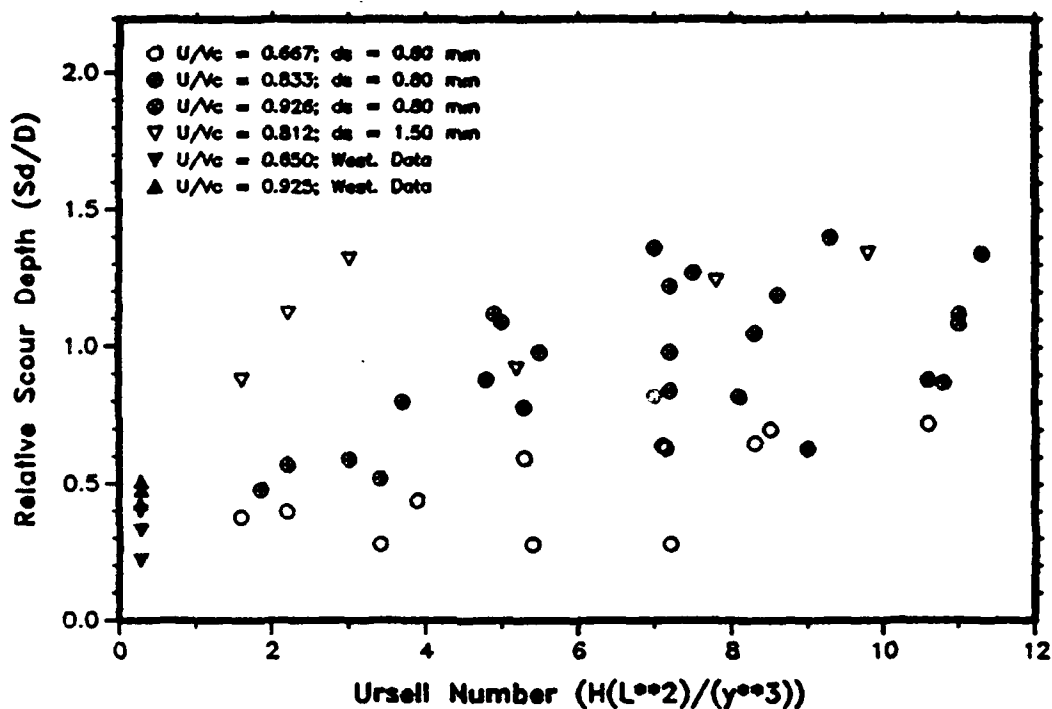
Fig. 21. Influence of wave Ursell Number (HL^2/y^3) on scour.
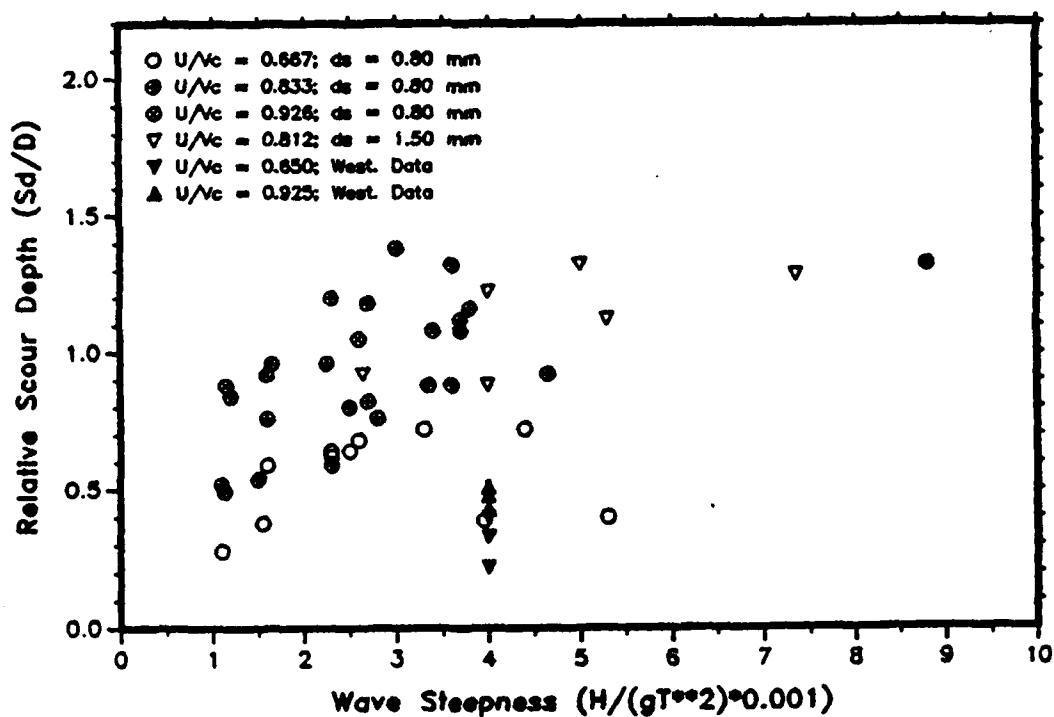
Fig. 22. Influence of wave steepness (H/gT^2) on scour.

Fig. 21 shows the influence of the wave Ursell Number, $U_r = HL^2/y^3$, which represents the relative magnitude between H/L and y/L. $U_r < 1$ corresponds to a region of intermediate to deep water. The data from this study represent intermediate to deep water conditions. The data of Nalluri and Ibrahim (1986) are for shallow water conditions.

Fig. 22 shows wave steepness, H/gT^2, which represents the disturbing capability of the wave. The waves used in this study are longer than the waves used by Nalluri and Ibrahim (1986), and therefore plot at lower Sd/D values.

Pipe Spacing Relationship

The relationship between pipe spacing and scour depth achieved with the data in this study are dimensionless plots of the product of pipe Reynolds Number (Nrp) and sediment Froude Number (Ns) against relative scour depth (Sd/D). Scour is a function of pipe geometry, sediment size and flow conditions. The Reynolds Number and Froude Number represent applicable scaling laws.

The dimensionless product of pipe Reynolds Number and sediment Froude Number account for the most significant parameters which influence scour. Plots developed between Sd/D and $(Nrp)(Ns)$ have a constant sediment Froude Number (Ns) since the sediment is the same in all cases. The pipe Reynolds Number is variable and contributes to the decreasing Sd/D.

Fig. 23–26 are plots of tests with $U = 0.37$ m/sec. Fig. 27–30 are plots of tests with $U = 0.26$ m/sec. These are plots of $(Nrp)(Ns)$ against (Sd/D) . The solid line in each figure is the single pipe case, representing a relative datum line. The lines represent a linear least square fit for a set of three data points. Statistically speaking, more data points are required for definitive conclusions, therefore, the lines represent only general trends.

Fig. 23 represents a trend where the 1/2 diameter pipe spacing results in less scour than both the single pipe case and full diameter case. Similar results are obtained in Fig. 24, current and wave. The 1/2 diameter pipe spacing results in less scour than the single pipe case and full diameter case. Comparing Fig. 23 with Fig. 24 shows a general trend for greater relative scour in the current only case.

Fig. 25 represents a general trend where the 1/2 diameter pipe spacing results in less relative scour than the full diameter pipe spacing. When compared to the single pipe case, there is no apparent trend. The full diameter spacing results in greater scour than both single pipe and 1/2 diameter spacing cases. In Fig. 26, the full diameter pipe spacing is about the same as the 1/2 diameter spacing. Both the 1/2 and full diameter spacing result in greater relative scour than the single pipe case. Comparing Fig. 25 with Fig. 26 shows a general trend for greater relative scour in the current only case.
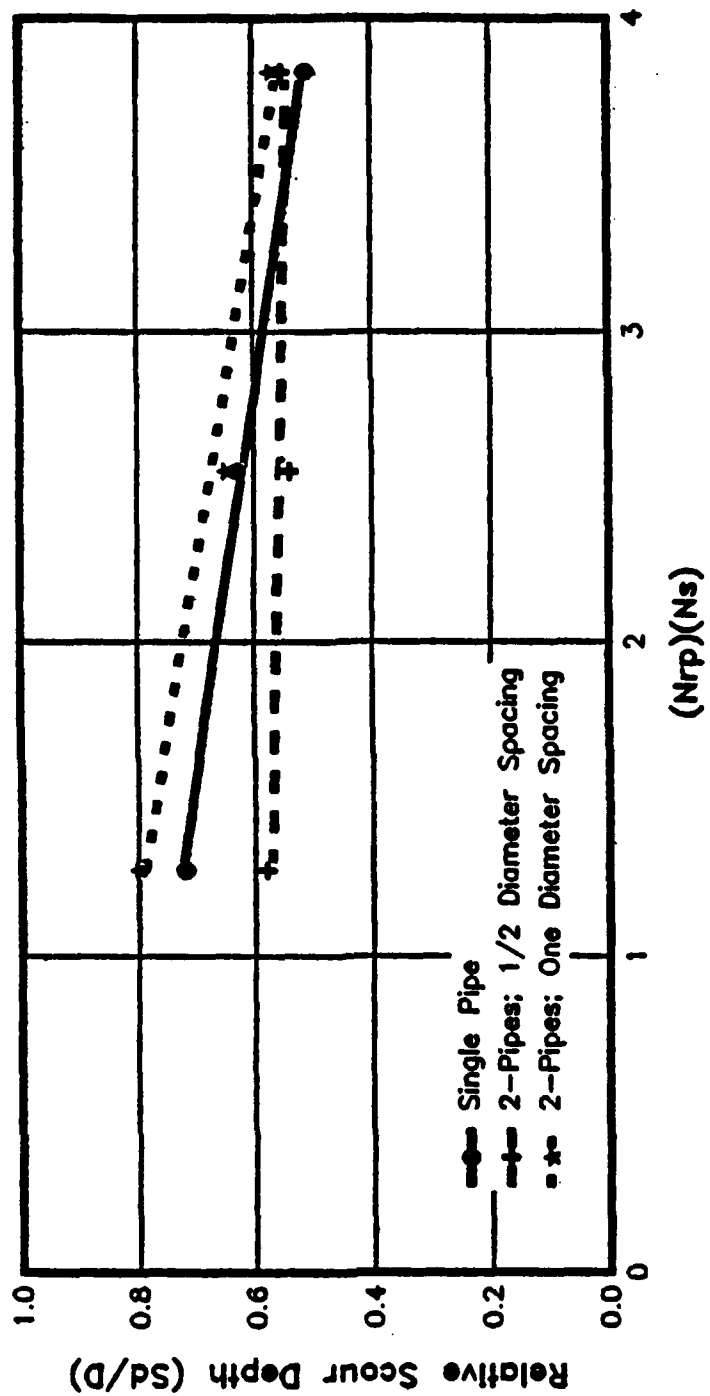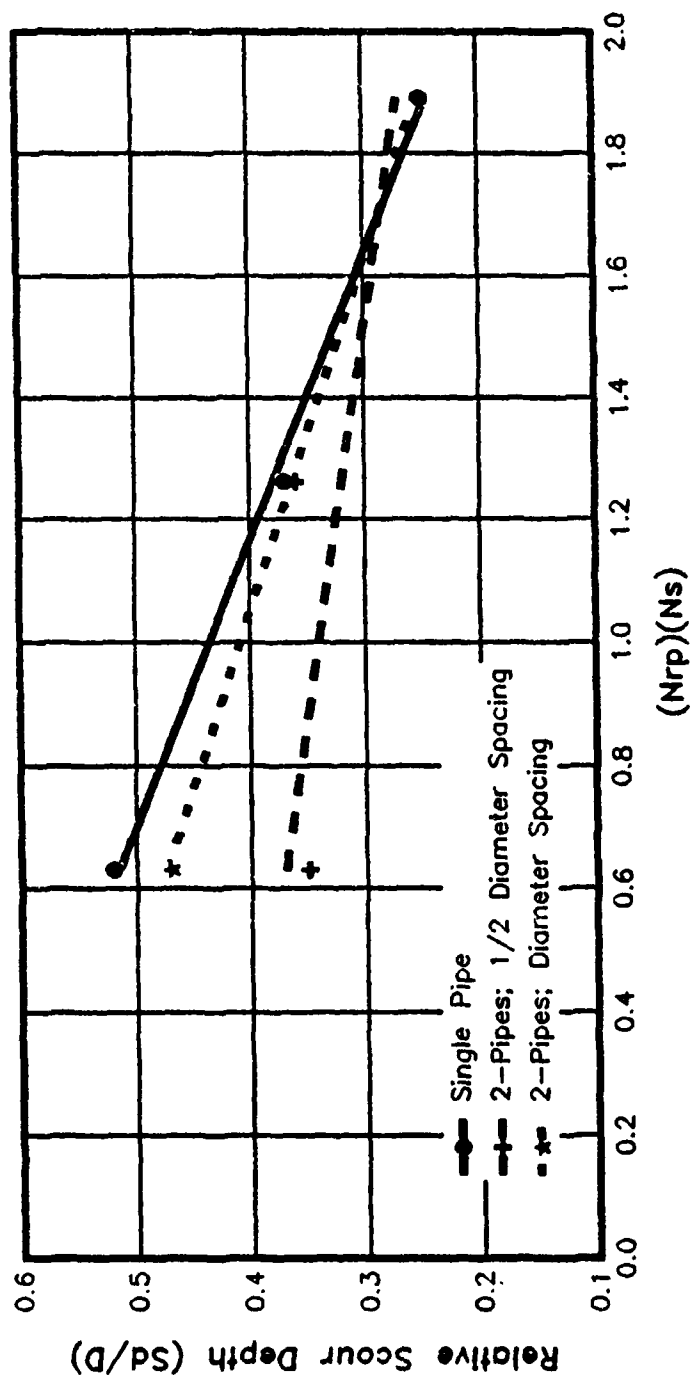
Fig 23. Single vs 2-pipe system; current only.
$(U = 0.37m/sec)$
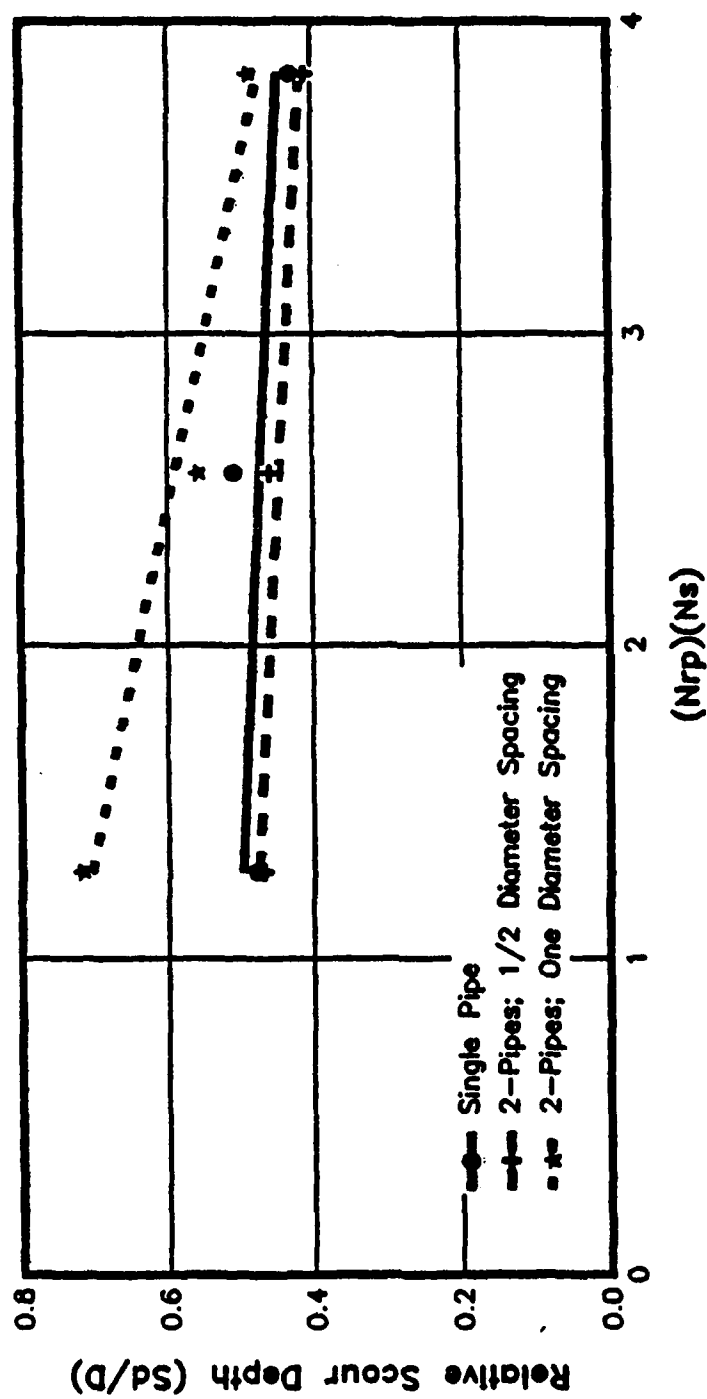
Fig 24. Single vs 2-pipe system; current and wave.
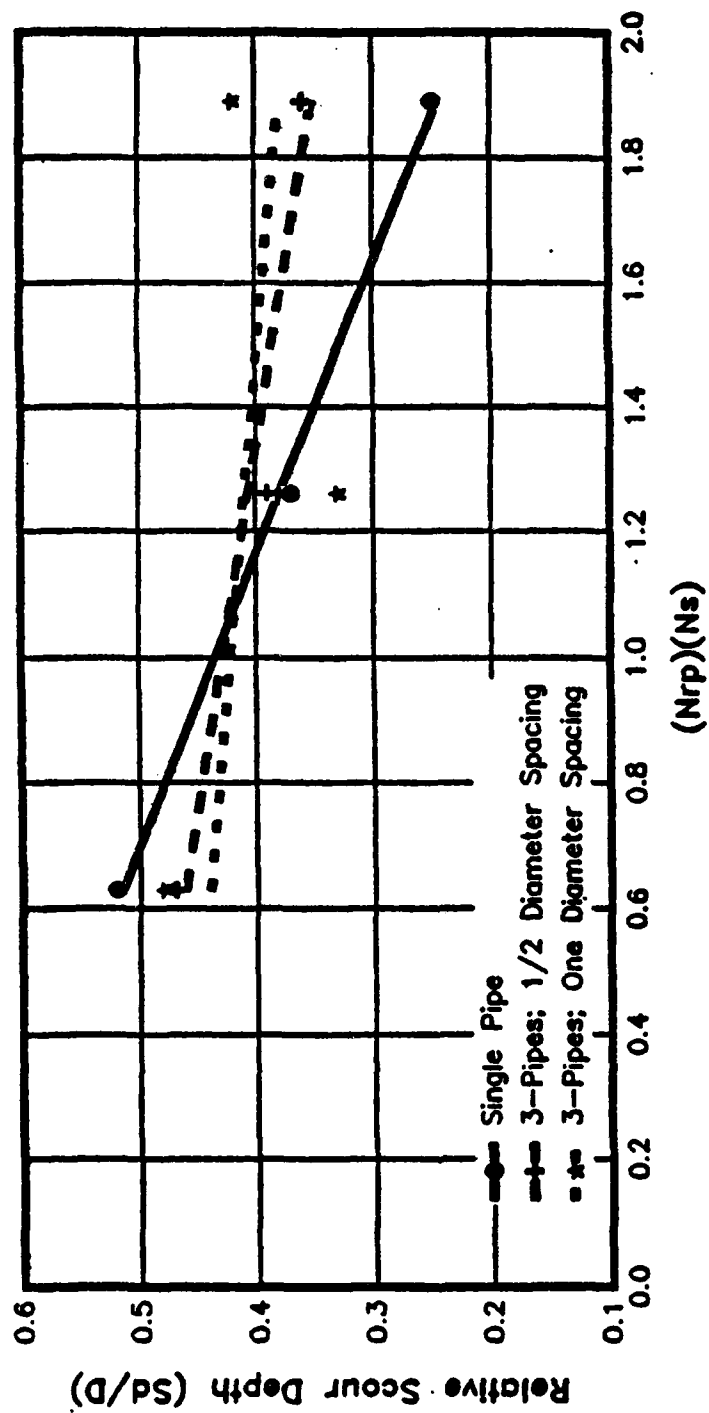($U = 0.37$ m/sec, $L = 1.0$ m, $H = 6.0$ cm, $T = 1.2$ sec)
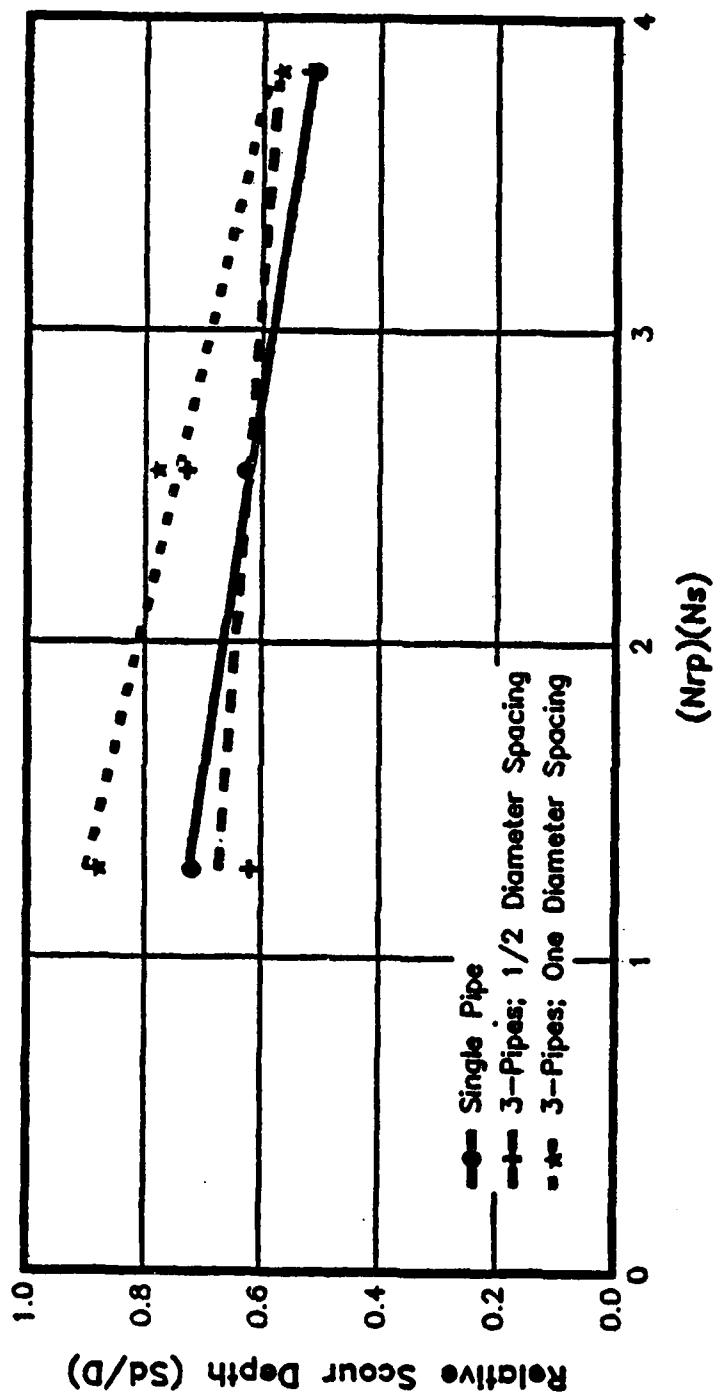
Fig 25. Single vs 3-pipe system; current only.
$(U = 0.37m/sec)$
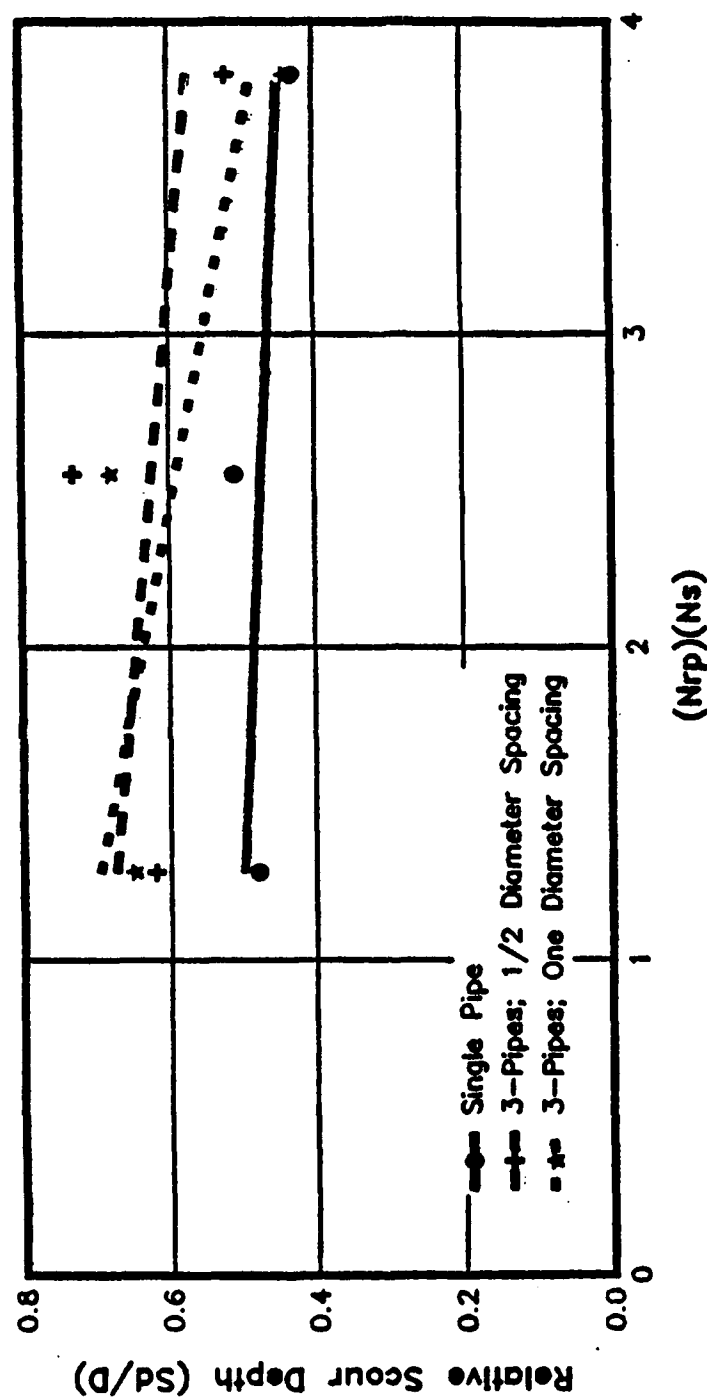
Fig 26. Single vs 3-pipe system; current and wave.
($U = 0.37$ m/sec, $L = 1.0$ m, $H = 6.0$ cm, $T = 1.2$ sec)

In Figs. 23–26, the general trend is that 1/2 pipe diameter pipe spacing results in less relative scour than the full diameter pipe spacing. The 1/2 diameter pipe spacing for 2–pipe systems results in less relative scour than both the single pipe case and the full diameter case. The 1/2 diameter spacing of the 3–pipe system appears to result in greater relative scour than the single pipe case. The full diameter spacing for a 3–pipe system results in greater relative scour than the single case. This may be due to the wide profile characteristic of a 3–pipe system.

Figs. 27–30 are plots with $U = 0.26$ m/sec. In these cases the bed was less dynamic than in the set of tests with $U = 0.37$ m/sec. The general trend is similar. The 1/2 diameter spacing results in less relative scour than the full diameter spacing for 2–pipe systems. In Fig. 28 the trend lines connect two data points. This is the case where there was no scour of the 2–pipe system, 3 cm diameter pipes. The no scour points are plotted at $(Sd/D = 0.0)$.

Figs. 23–30 show a trend for decreasing Sd/D with increasing $(Nrp)(Ns)$. Since Ns is constant, this trend is due to Nrp, which represents increased inertia. Conceptually, inertia is the tendency of a body to resist acceleration. Reynolds Number is an inertia–viscous force ratio. Increasing the pipe diameters increases the pipe Reynolds Number (Nrp) and results in greater system inertia.

In the model test, pipe diameters varied while sediment size remained constant. The larger pipe diameters yield a higher pipe Reynolds Number. Table II shows that Sd/D decreases as D increases for each set of test configurations.

Fig 27. Single vs 2-pipe system; current only.
$(U = 0.26m/sec)$
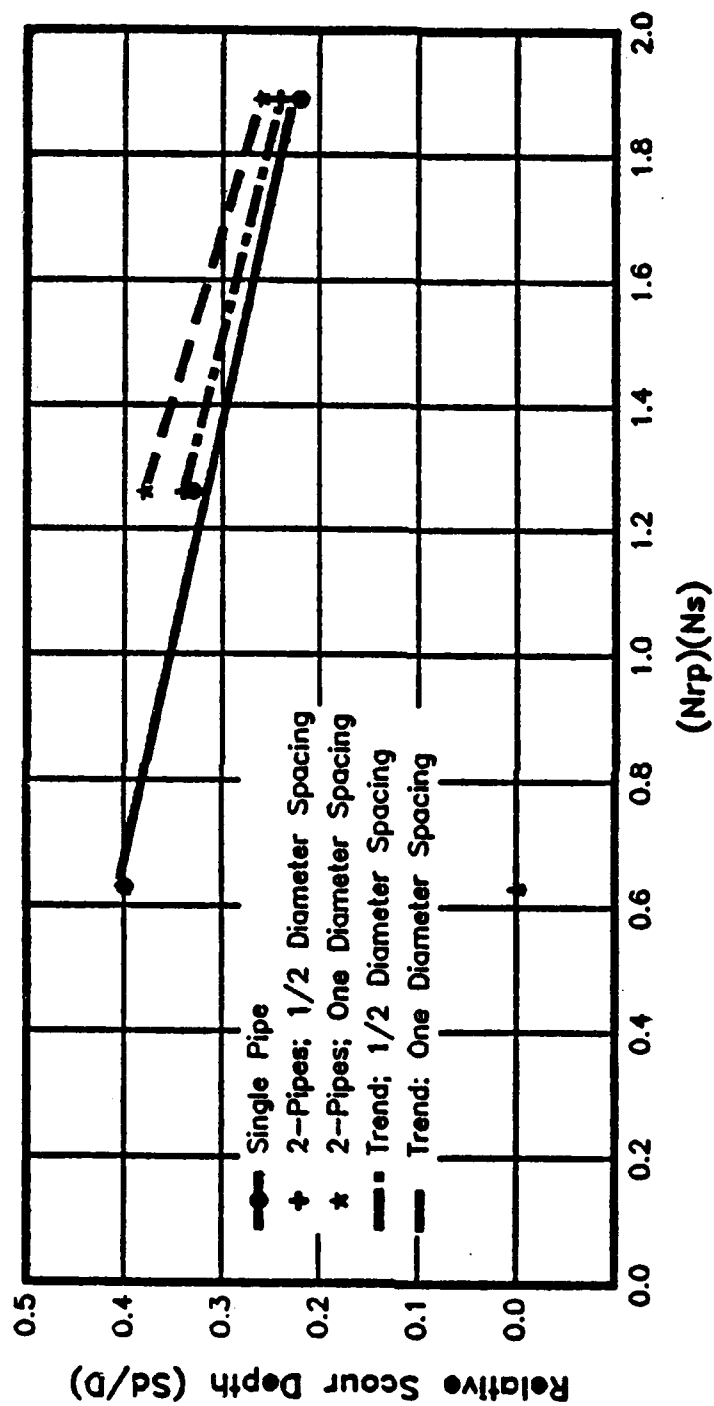
Fig 28. Single vs 2-pipe system; current and wave.
($U = 0.26$ m/sec, $L = 1.0$ m, $H = 6.0$ cm, $T = 1.2$ sec)

72

Fig 29. Single vs 3-pipe system; current only.
(*U* = 0.26*m/sec*)
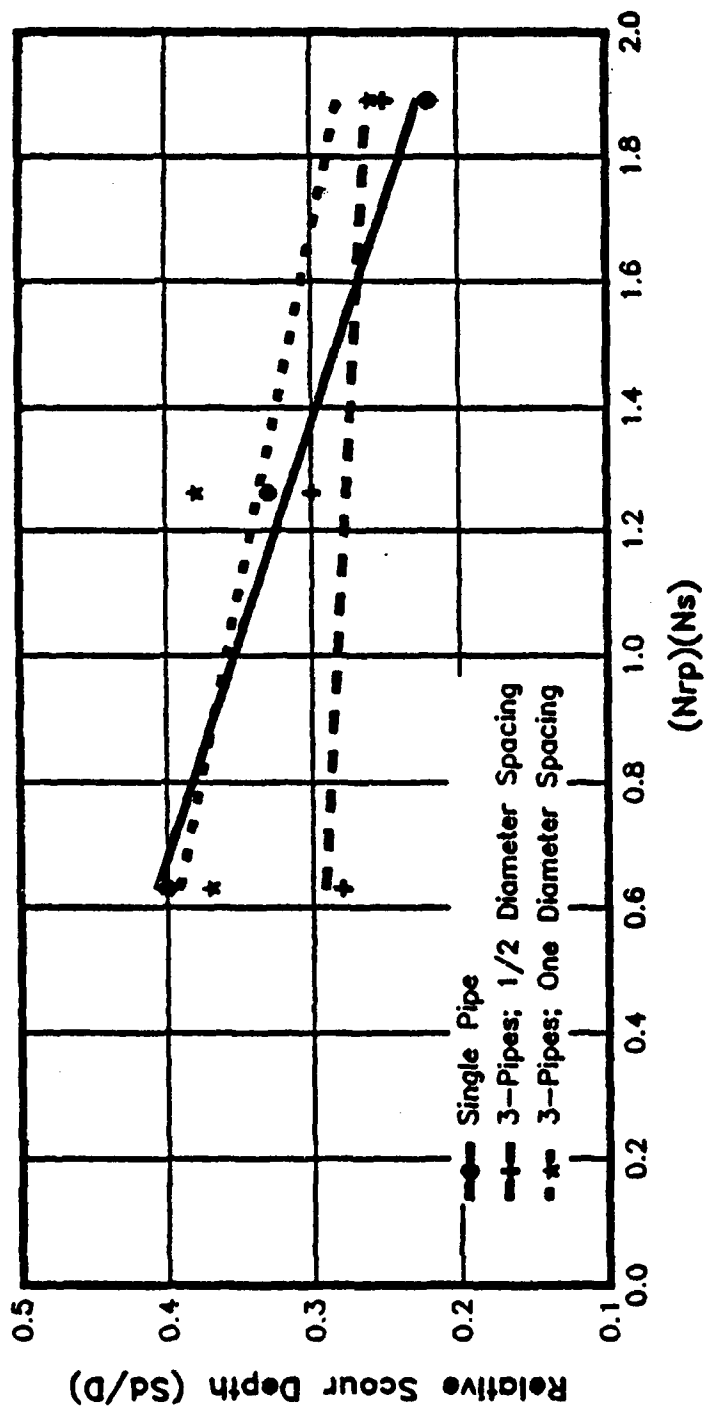
Fig 30. Single vs 3-pipe system; current and wave.
$(U = 0.26 \ m/sec, L = 1.0 \ m, H = 6.0 \ cm, T = 1.2 \ sec)$

The trend for decreasing Sd/D as $(Nrp)(Ns)$ increases is attributed to increasing pipe diameter, which is a function of Nrp.

The scour profiles presented in Appendix II show a variation in scour profiles obtained between the two test currents. Although the 3-pipe system results in greater relative scour depths, scour depth beneath additional pipes appears to be less. This is especially true for the $U = 0.26$ m/sec cases. The general trend for the relative scour depth to be greater in the 3-pipe system is because the scour hole profile is wider. Inspection of the 3-pipe configurations with $U = 0.26$ m/sec (Appendix II) reveals many cases where the third pipe behind the leading pipe has minimal if any scour. When examining the profiles in Appendix II, note the distortion of the axis scales.

The equilibrium bed consisted of ripple formations, discussed in Chapter VI. The ripples migrate in the direction of the current. The migration is not visible, but apparent when comparing time profiles. Tests with current and wave action resulted in a more active bed. In these cases, sediment is transported from upstream of the leading pipe. As the sediment is transported through the pipe test section, there is some sediment deposition. In some cases sediment was deposited in the vicinity in front of the leading pipe. This combined with the migration of bed ripples accounts for sediment deposition in front of the leading pipe in several cases. The buried pipes had no apparent effect on stabilizing the bed.

Scour Rate

Initially, scour occurs at a high rate. Fig. 31 shows three time stages of scour for test number 64. Test 64 was conducted on a single 9 cm pipe exposed to current and wave action with $U = 0.26m/sec$. The maximum equilibrium scour depth is established early, with equilibrium profile at a later time. In most tests the maximum equilibrium scour depth was reached within twenty minutes, and the equilibrium scour profile within ninety minutes.

Fig. 32 shows three time stages for test number 70. Test 70 is a three pipe system with 1/2 diameter spacing between pipes. Test 70 is exposed to the same flow conditions as test 64. The maximum depth below the leading pipe is established early. The third pipe experiences sediment deposition. This is due to the reduced turbulence in the wake of the second pipe. The rate of scour may be a function of the effective sediment size, as well as flow conditions. Fig. 31 and Fig. 32 are typical examples of the scour rates observed in this study. Also note that the direction of flow in Fig. 31 and 32 is from right to left.

(a) Scour profile after 10 minutes.

(b) Scour profile after 40 minutes.

(c) Scour profile after 90 minutes.

Fig. 31. Test number 64: scour profile development.
($U = 0.26\ m/sec$, $L = 1.0\ m$, $H = 6.0\ cm$, $T = 1.2\ sec$)
(Pipe diameter = 9 cm)
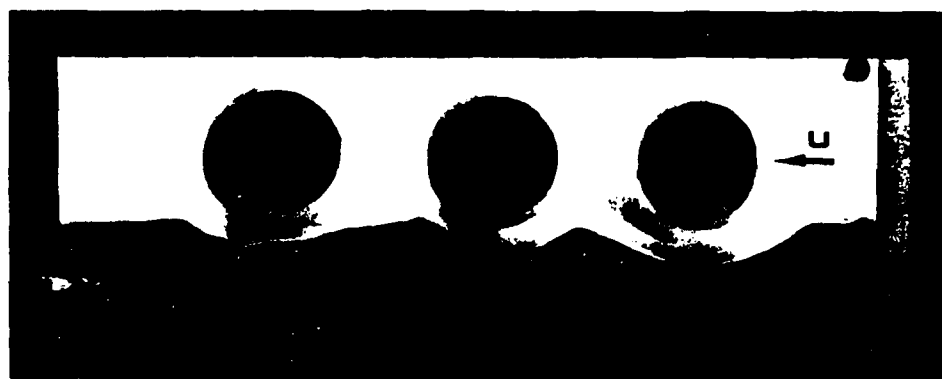
(a) Scour profile after 10 minutes.
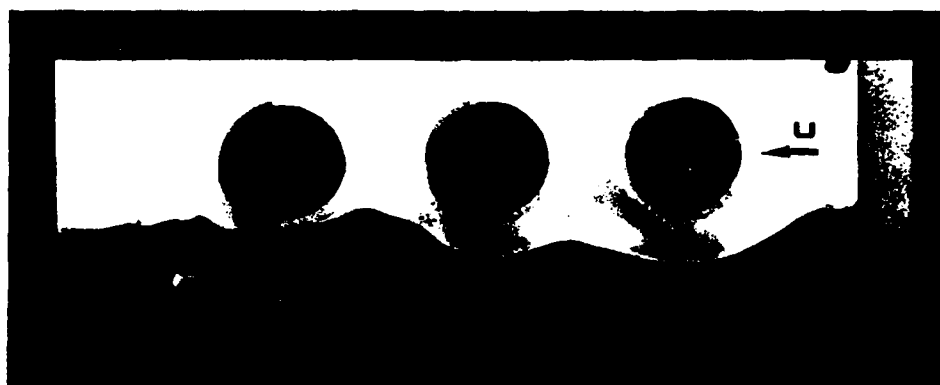
(b) Scour profile after 40 minutes.

(c) Scour profile after 90 minutes.

Fig. 32. Test number 70: scour profile development.
($U = 0.26 \ m/sec$, $L = 1.0 \ m$, $H = 6.0 \ cm$, $T = 1.2 \ sec$)
(Pipe diameter $= 9$ cm; spacing $= 4.5$ cm)

CHAPTER VIII

SUMMARY OF CONCLUSIONS
AND RECOMMENDATIONS

One of the major problems of placing pipelines in the ocean is pipeline scour, which is a threat to pipeline stability. As more pipelines are placed in the ocean, many adjacent to one another, scour will continue to be a problem. Research objectives of this study were to determine the relationship between pipe geometry and scour depth, and examine scour hole dimensions under multiple pipes. Pipeline scour was reviewed, followed by a theoretical and descriptive presentation of pipeline scour.

Seventy-two model tests were conducted on multiple pipelines in contact with a sand bed. Model tests were conducted in a two-dimensional wave-current flume facility. Multiple pipe systems were exposed to unidirectional flow and unidirectional flow with oscillatory motion. The model testing investigated pipe spacing and its relationship to scour. A major influence on scour was believed to be vortex shedding in the wake of the pipe. Vortex shedding was disrupted by placing additional pipes behind the leading pipe. A scour profile was developed for each test.

Model testing resulting in the following conclusions:

(1) For two pipe systems, 1/2 pipe diameter pipe spacing between pipes results in less scour depth than full diameter spacing. This is due to interruption of the vortex shedding occurring behind the leading pipe. At a full diameter spacing, the vortex shedding has enough space to develop. The 1/2 diameter spacing blocks the vortex action, preventing its full development.

(2) Unidirectional flow with oscillatory motion results in less scour than unidirectional flow. Oscillatory motion contributes to deposition by moving sediment back into the scour hole, between pipes. Since there is less turbulence between pipes, the sediment settles out of suspension.

(3) The scour rate is high initially, then decreases until equilibrium is reached. Maximum scour depth was usually reached within twenty minutes during the model tests, and equilibrium profile was attained in about ninety minutes.

(4) A relationship exists between relative scour depth, Sd/D, and pipe Reynolds Number, Nrp. Relative scour depth Sd/D decreases with increasing pipe Reynolds Number Nrp.

(5) Wave characteristics affected scour by disturbing and mobilizing the bed. The effect was a mass transfer in the direction of the current.

Following are recommendations for further research:

(1) A larger data base contributes in developing definitive conclusions. Additional research should concentrate on one set of pipe configurations. Collect additional data for one set of configurations at various pipe spacings for analysis.

(2) Conduct a series of tests on different sediment sizes and pipe configurations. This may result in an improved relationship between pipe spacing and sediment size, and establish correlation between scour rate and sediment size. This will also develop the relationship between the product $(Nrp)(Ns)$. By varying pipe Reynolds Number and sediment Froude Number, a relationship between relative scour depth, pipe sizes and sediment sizes will be determined.

(3) Investigate various waves and the effect of the Keulegan–Carpenter number on multiple pipe systems. Varying wave characteristics will develop stronger relationships on the affect of waves on scour.

REFERENCES

Bijker, E.W., and Leeuwestein, W. (1983). "Interaction Between Pipelines and the Seabed Under the Influence of Waves and Currents", *Seabed Mechanics, Symposium Proceedings*, International Union of Theoretical and Applied Mechanics and International Union of Geodesy and Geophysics, London, England, pp 235–242.

Bruschi, R., Cimbali, W., Leopardi, G., and Vincenzi, M. (1986). "Scour Induced Free Spans Analysis ", *Proceedings of the 5th International Symposium on Offshore Mechanics*, American Society of Mechanical Engineering, New York, New York, pp 656–669.

Dahlberg, R. (1983). *Geotechnical Aspects of Coastal and Offshore Structures*, A.A. Balkema, Rotterdam, Netherlands, pp 166–168.

Einstein, H.A. (1942). "Formulas for Transportation of Bed Load", *Transactions*, ASCE, Vol. 107, pp 798–878.

Fredsoe, J., Mao, Y., and Summer, B.M. (1988). "Interaction Between Vibrating Pipe and Erodible Bed", *Journal of Waterway, Port, Coastal and Ocean Engineering Division*, ASCE, 114(1), pp 81–93.

Herbich, J., Dunlap, W., Schiller, R., and Watanabe, R. (1984). *Seafloor Scour, Design Guidelines for Ocean-Founded Structures*, Marcel Dekker, Inc., New York, New York, pp203-204.

Hulsbergen, C.H. (1984). "Stimulated Self-Burial of Submarine Pipelines", *Proceedings of the 16th Annual Offshore Technology Conference*, OTC-paper 4667, Dallas, Texas, pp 171–178.

Ibrahim, A., and Nalluri, C. (1986). "Scour Around Pipelines Under Marine Environment", *Proceedings of the 5th International Symposium on Offshore*

Mechanics, American Society of Mechanical Engineering, New York, New York, pp 569-575.

Kjeldsen, S. (1973). "Local Scour Near Offshore Pipelines", *Proceedings, Second Conference on Port and Ocean Engineering Under Arctic Conditions*, Reykjavic, Iceland, pp 171-178.

Leeuwestein, W. (1984). "Scour Around Submarine Pipelines", *Petrole Informations*, No. 1602, pp 16-26.

Liu, H.K. (1958). "Mechanics of Sediment-Ripple Formation", *Journal of the Hydraulics Division*, ASCE, Vol. 84, No. HY5, pp 1832-10-1832-12.

Mao, Y. (1986). "Interaction Between a Pipeline and an Erodible Bed", *Dissertation*, Institute of Hydromechanics and Hydraulic Engineering, Technical University of Denmark, Series Paper No. 39.

Shields, A. (1936). "Anwendung der Aehnlichkeitsmechanik und Turbulenz forschung auf die Geshiebewegung", *Mitteilung Preussischen Versuchanstalt Wasser, Erd, Schiffbau*, No. 26, Berlin, (in German).

Simons, D.R., and Şentürk, F., (1977). *Sediment Transport Technology*, Water Resources Publications, Fort Collins, Colorado, pp 409-411.

Vanoni, V.A. (1966). "Sediment Transportation Mechanics: Initiation of Motion, Progress Report of the Task Committee On Preparation of Sedimentation Manual, Committee on Sedimentation", *Journal of Hydraulics Division*, ASCE, Vol. 92, No. HY2, pp 291-315.

Yang, C.T. (1973). "Incipient Motion and Sediment Transport", *Journal of the Hydraulics Division*, ASCE, Vol. 92, No. HY10, pp 1679-1704.

APPENDICES

APPENDIX I

SCOUR.FOR PROGRAM CODE

```
*****************************************************************
                        SCOUR.FOR
   This program calls subprogram WAVE123 which computes
   the fluid velocity directly in front of the pipe.
   It then calculates the maximum scour depth and scour
   hole profile under the pipe. An output file, PROFILE.DAT,
   is created.  PROFILE.DAT is plotted using the VAX/VMS
   PICSURE program.

*****************************************************************

     * Variables

     *UZ3   wave velocity in ft/s
     *Material_constant   dimensionless
     *U_wave     m/s
     *U_current  m/s
     *U_flow     m/s
     *D_pipe     mm
     *Gravity    u/s**2
     *K_s            dimensionless
     *Sand_factor   dimensionless
     *H_init     mm
     *Epsilon    0
     *Number_of_points   Number of points to be outputed
     *Number_of_points
     *Sdmax mm Maximum scour depth
     *X     mm   Position along the sea bed perpendicular to the pipe
     *X_inc mm Sampling increment
     *W     mm   Wave number
     *H     mm   Distance between the bottom of the pipe and the sea bed
     *PI         Circumference constant


     REAL Material_constant
     &,UZ3
     &,U_wave
     &,U_current
     &,U_flow
     &,D_pipe
     &,Gravity
     &,K_s
     &,Sand_factor
     &,H_init
     &,Epsilon
     &,Number_of_points
     &,Sdmax
     &,X
     &,X_inc
     &,W
     &,H
     &,PI
```

SCOUR.FOR PROGRAM CODE – CONTINUED

```
      PARAMETER (PI=3.14159265,Gravity=9.81)

      CALL WAVE123(UZ3)
      WRITE(6,*)'WAVE123 COMPLETED'

      K_s=0.972
      U_wave=UZ3*.3048


C Open file MAIN.DAT as input to read in the following parameters
      OPEN(UNIT=10,FILE='MAIN.DAT',STATUS='UNKNOWN')
      READ(10,*)U_current
      READ(10,*)D_pipe
      READ(10,*)Sand_factor

      Epsilon=H_init / D_pipe

      U_flow = U_wave + U_current

      Sdmax=K_s*(U_flow**2/Gravity)**0.20*D_pipe**0.800

      W=Sand_factor*D_pipe

      Number_of_points= 30


      OPEN(UNIT=20,FILE='PROFILE.DAT',STATUS='NEW')
      WRITE(20,*)'POSITION   DEPTH'
      X=-D_pipe*4
      X_inc=2*ABS(X)/Number_of_points
      X=X-X_inc

      DO I=1,INT(Number_of_points)
         X=X+X_inc
         IF ( ABS(X).LT.(W/2) ) THEN
            H=Epsilon +D_pipe/2 + Sdmax/2*(1+cos(2*PI*X/W))
            ELSE
            H=Epsilon +D_pipe/2
         ENDIF

         H=H-D_pipe/2
         WRITE(6,*)X,H
         WRITE(20,*)X,H
      ENDDO

      CALL EXIT
      END
```

APPENDIX II
TEST PROFILES

TEST No.1: CURRENT
U =0.37 m/sec

PIPE LOCATION

EQUILIBRIUM SCOUR BED

Max Scour Depth=2.15cm

PIPE DIAMETER=3cm

ELEVATION(cm)

LENGTH(cm)
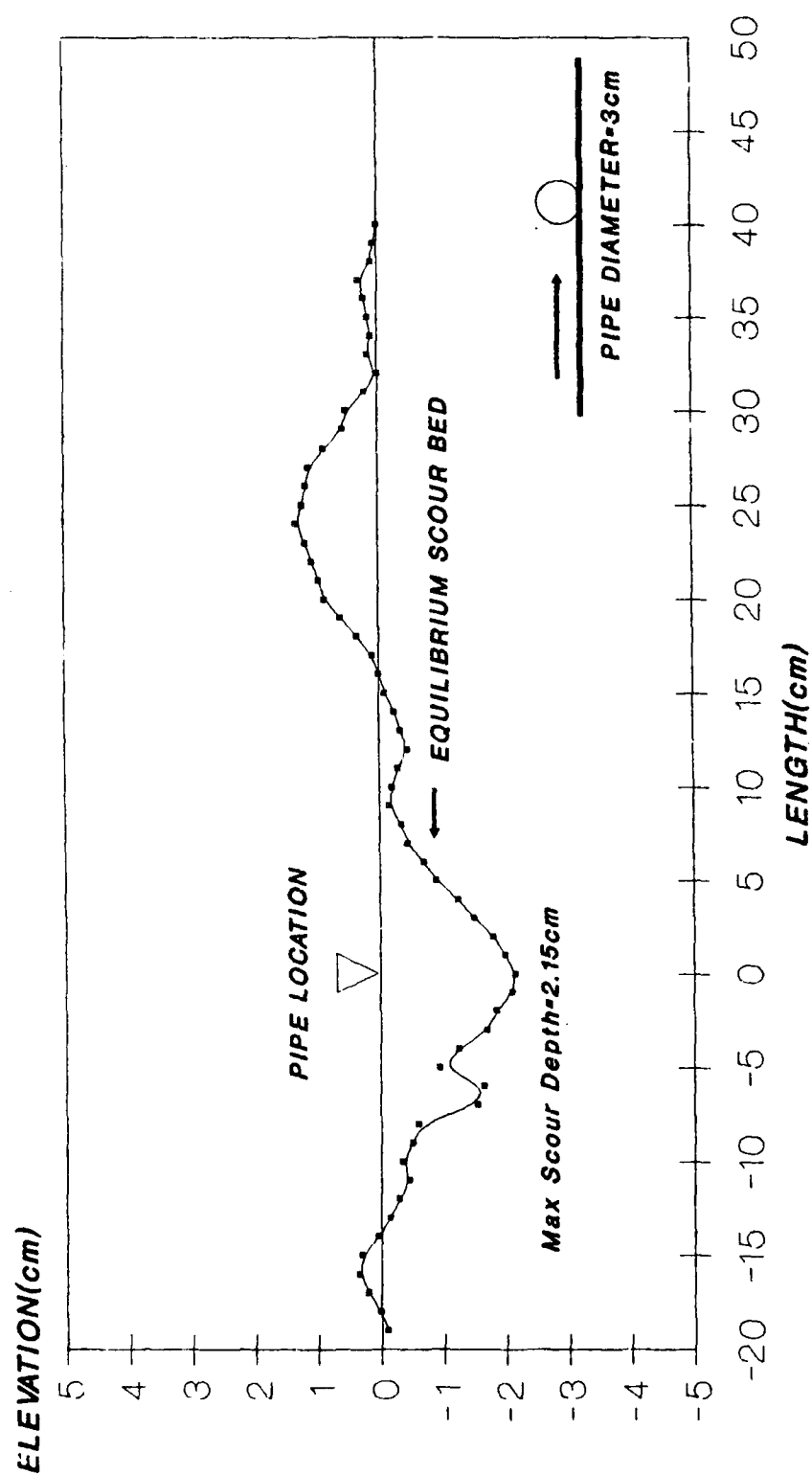
TEST No.2: CURRENT AND WAVE
U= 0.37m/sec, H= 6cm, T= 1.2sec, L= 1.0m
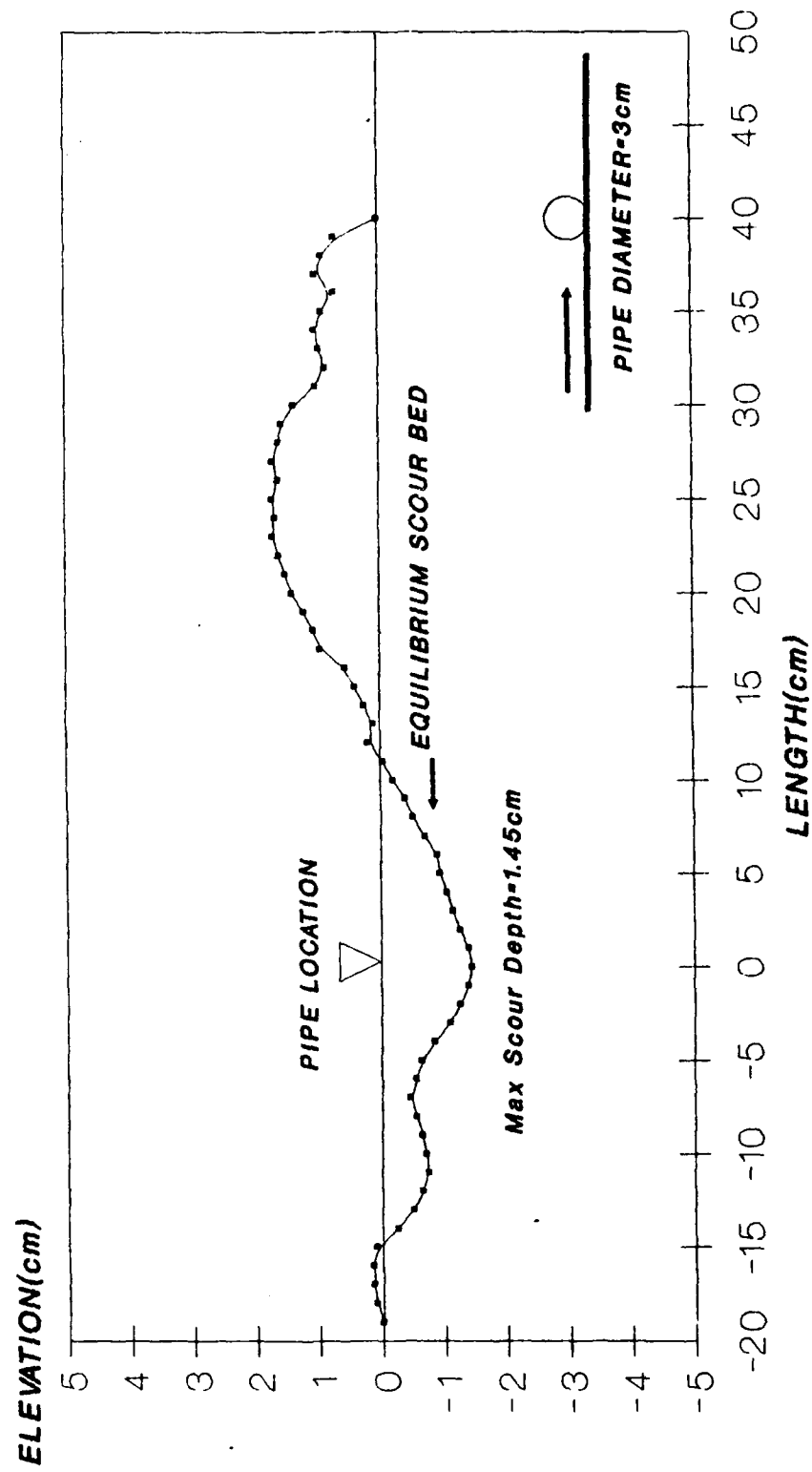
TEST No.3: CURRENT
U= 0.37m/sec
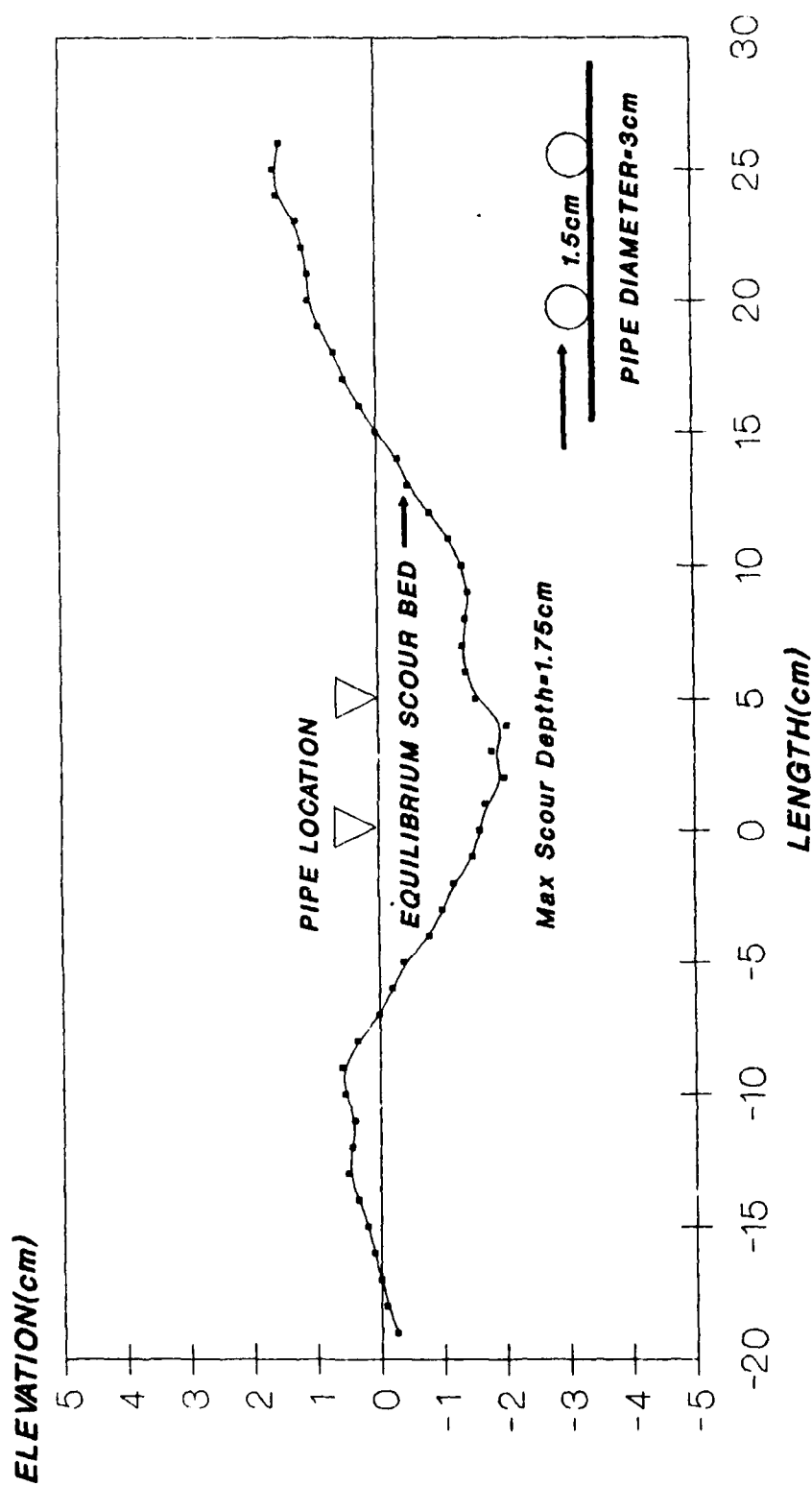
TEST No.4: CURRENT AND WAVE
U= 0.37m/sec, H= 6cm, T= 1.2sec, L= 1.0m

ELEVATION(cm)

PIPE LOCATION

EQUILIBRIUM SCOUR BED

Max Scour Depth=1.40cm

1.5cm

PIPE DIAMETER=3cm

LENGTH(cm)
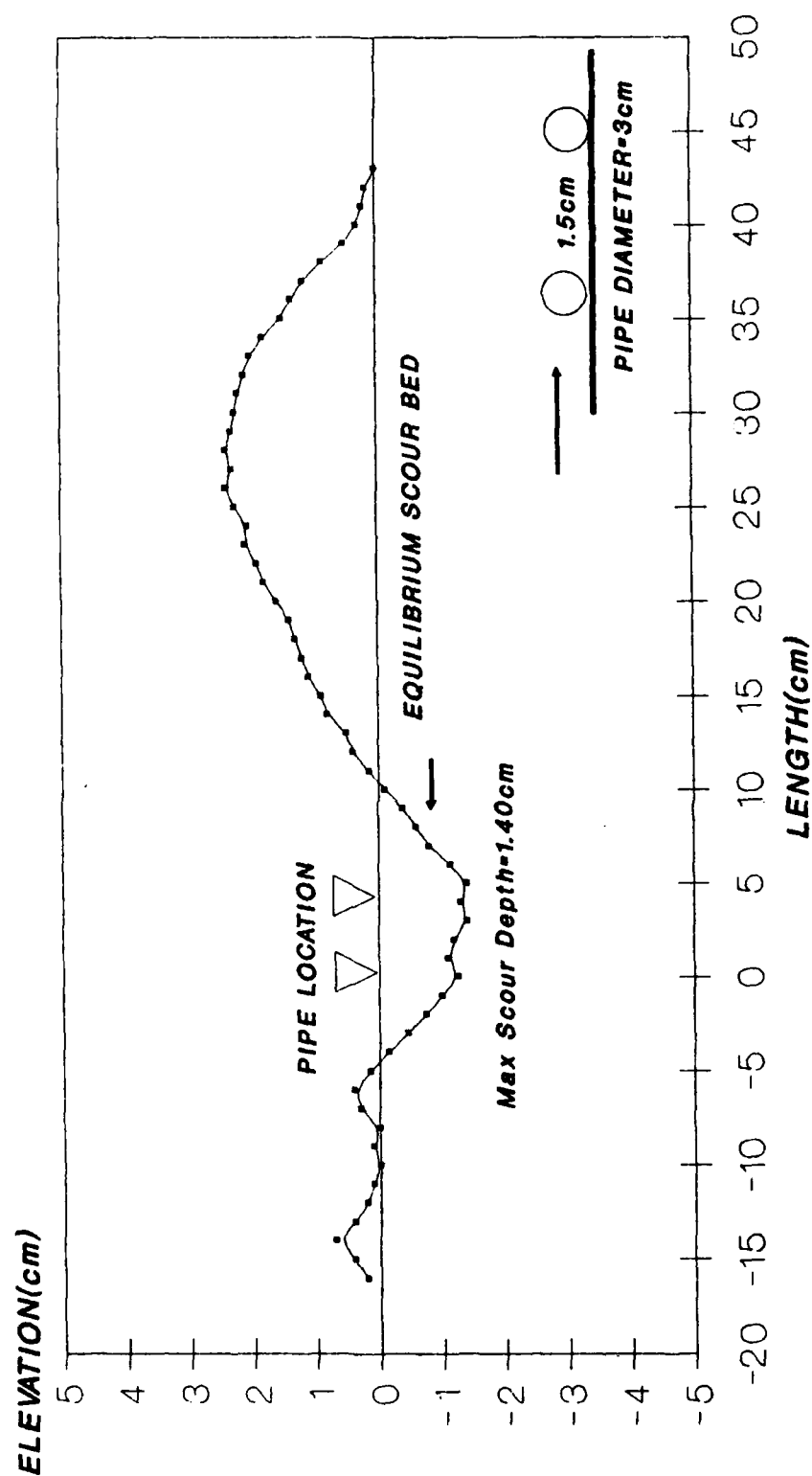
TEST No.5: CURRENT
U= 0.37m/sec
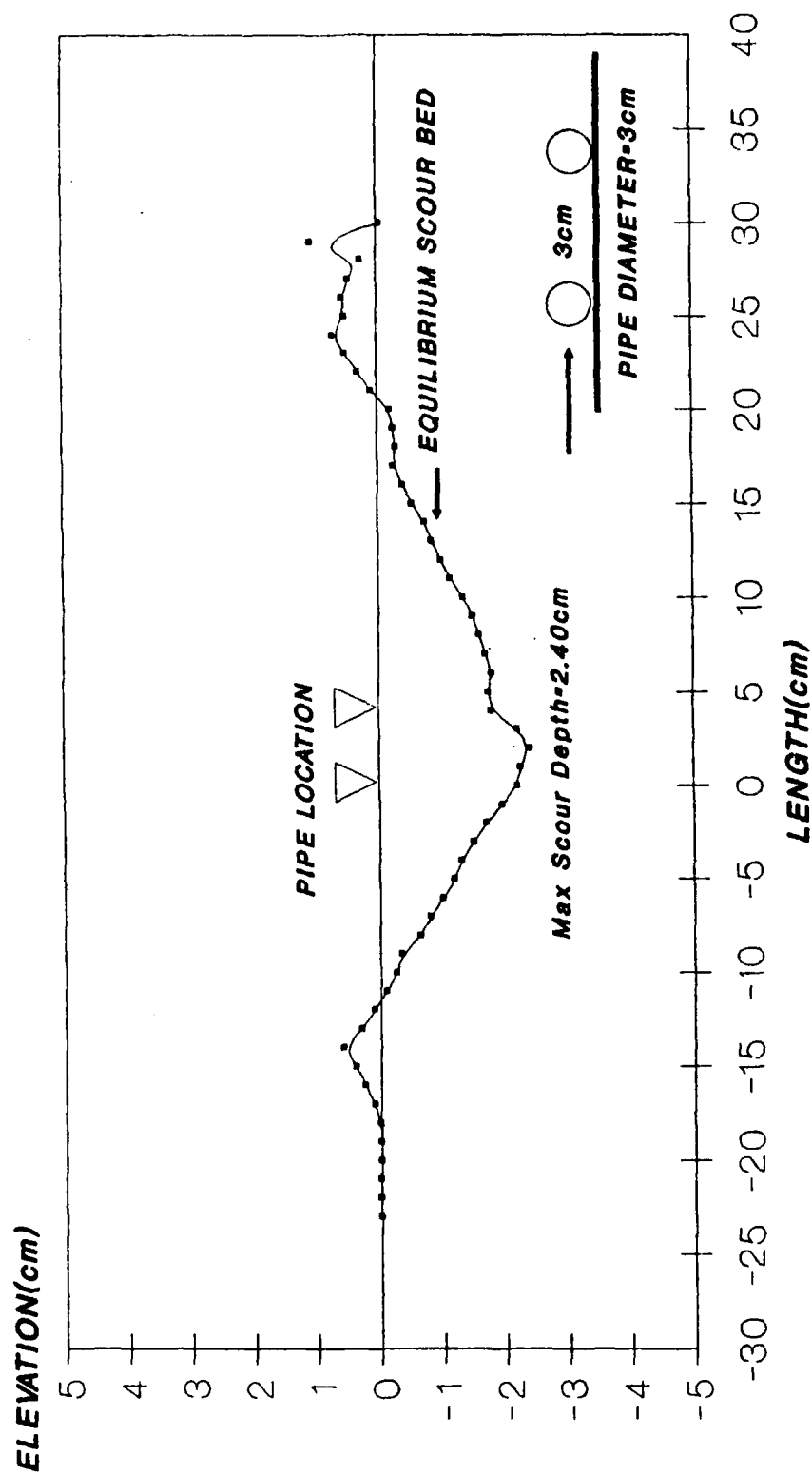
TEST No.6: CURRENT AND WAVE
U= 0.37m/sec, H= 6cm, T= 1.2sec, L= 1.0m
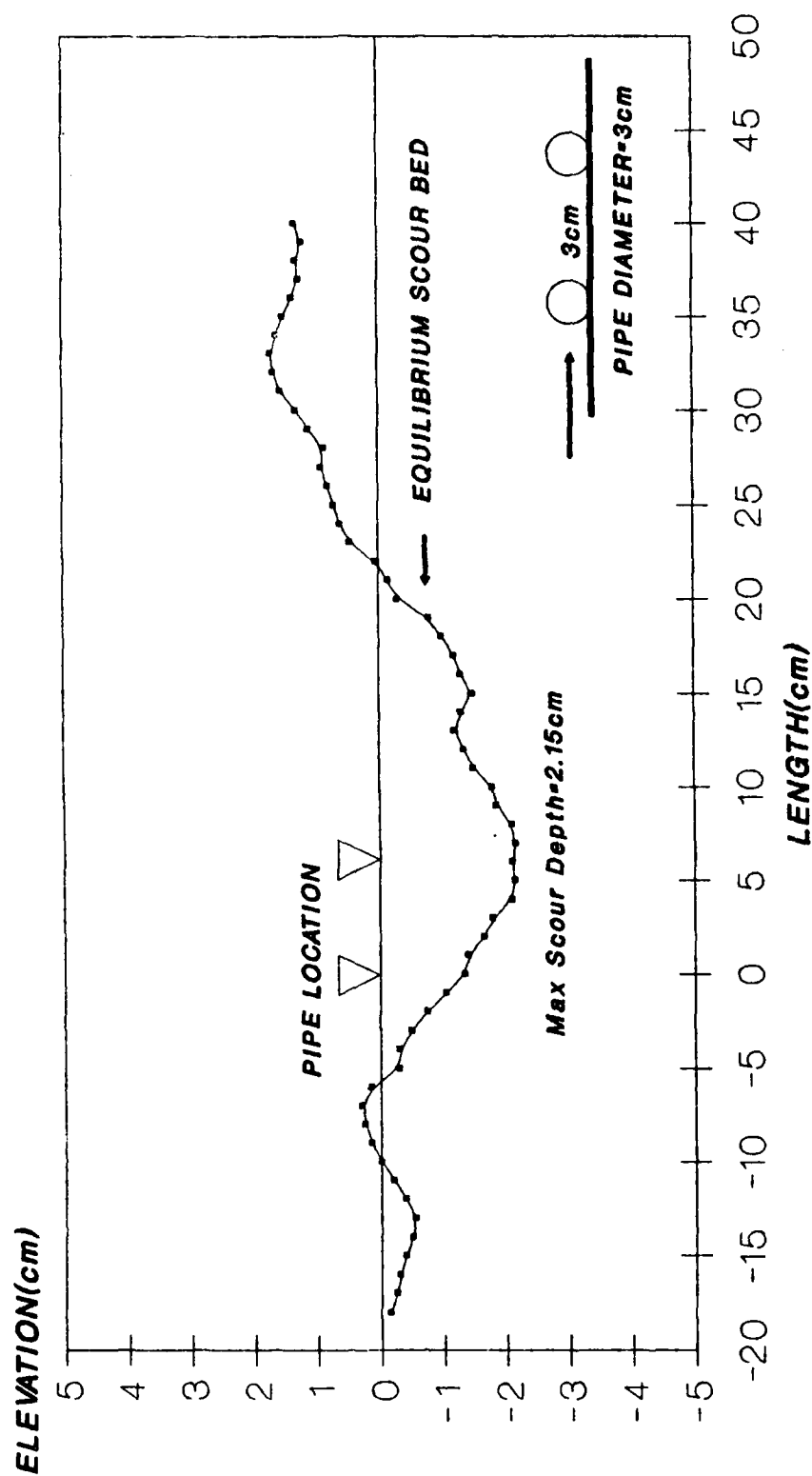
TEST No.7: CURRENT
U= 0.37m/sec
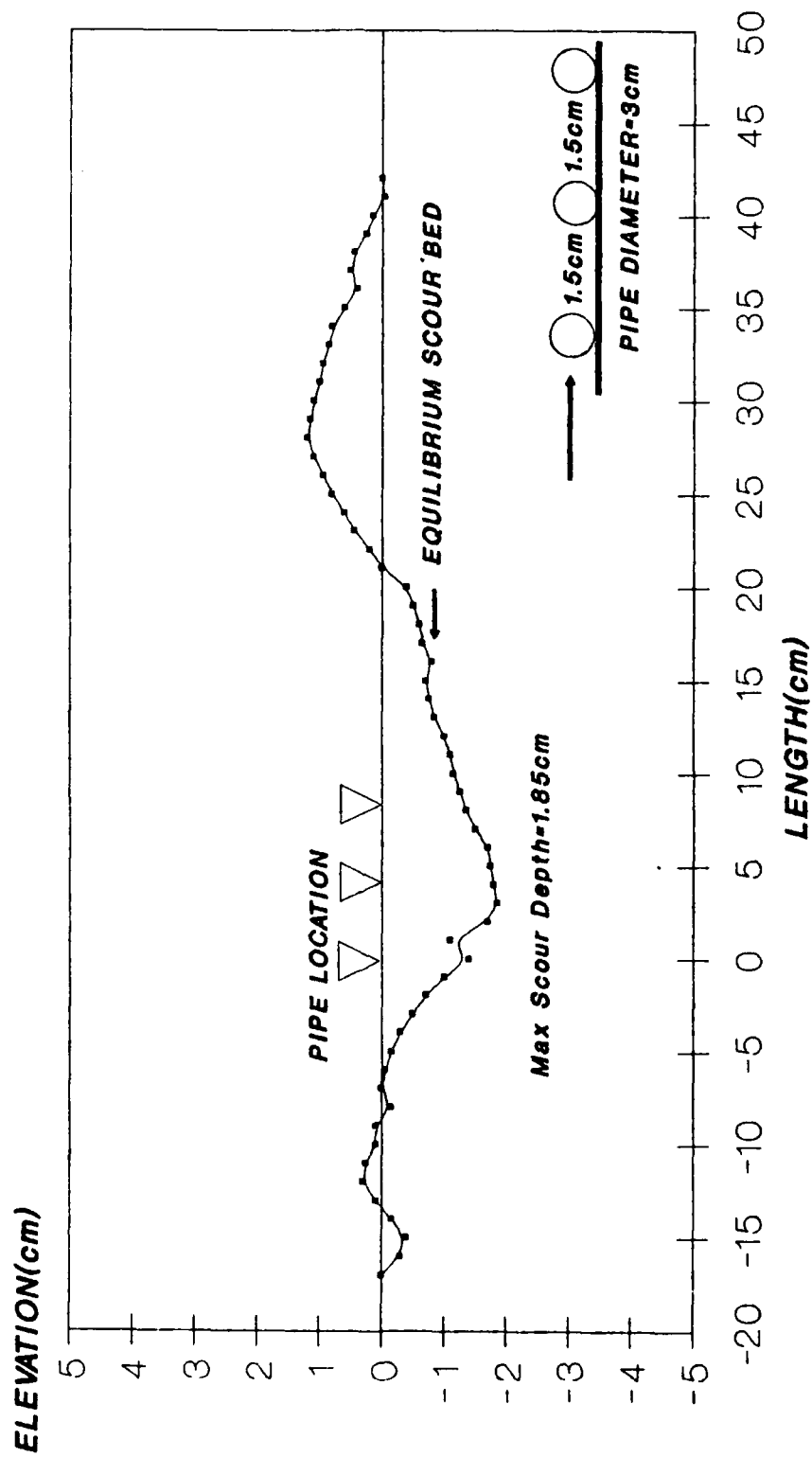
TEST No.8: CURRENT AND WAVE
U= 0.37m/sec, H= 6cm, T= 1.2sec, L= 1.0m

ELEVATION(cm)

PIPE LOCATION

EQUILIBRIUM SCOUR BED

Max Scour Depth=1.40cm

1.5cm 1.5cm 1.5cm

PIPE DIAMETER=3cm

LENGTH(cm)
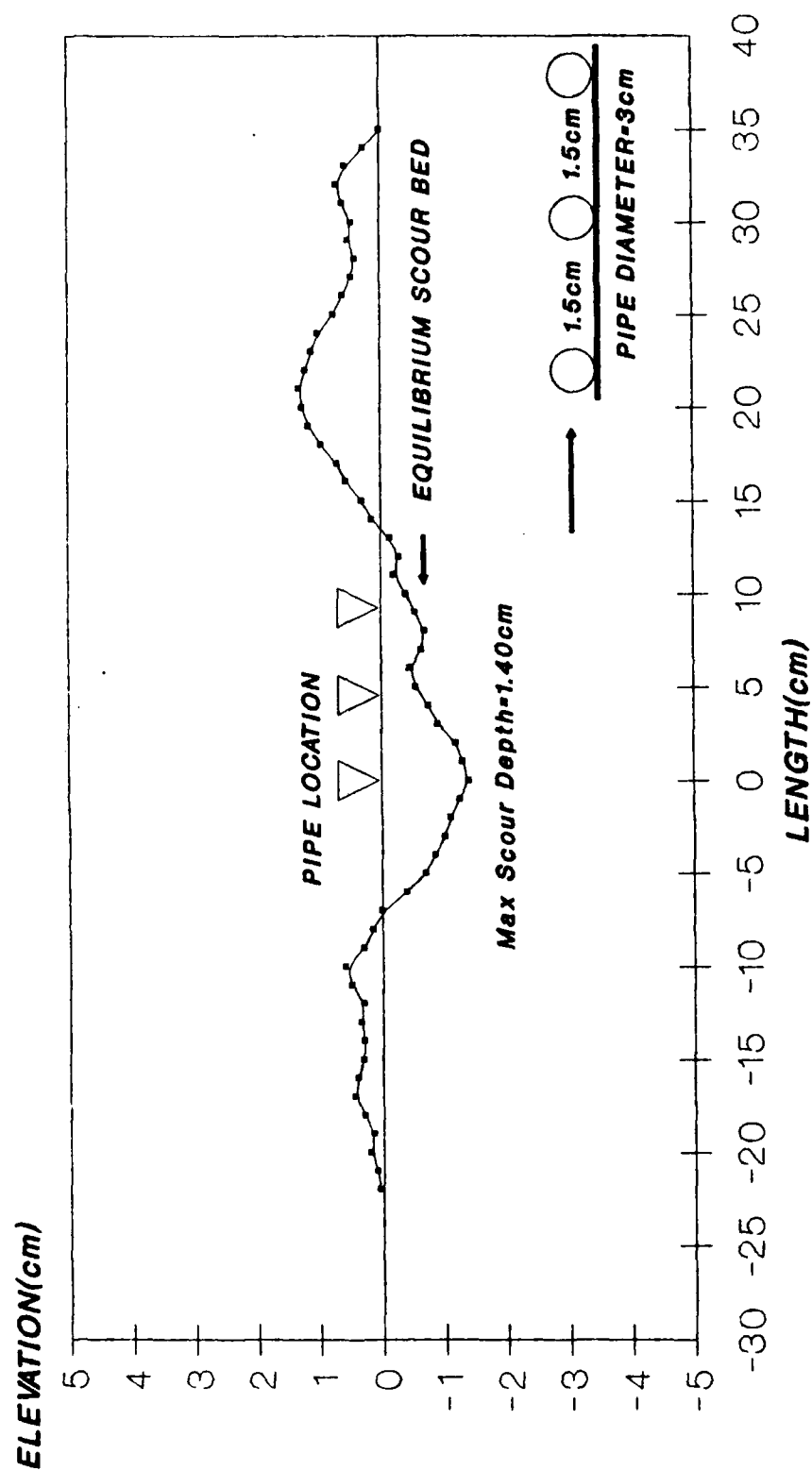
TEST No.9: CURRENT
U= 0.37m/sec

PIPE LOCATION

EQUILIBRIUM SCOUR BED

Max Scour Depth=2.65cm

3cm 3cm

PIPE DIAMETER=3cm

ELEVATION(cm)

LENGTH(cm)
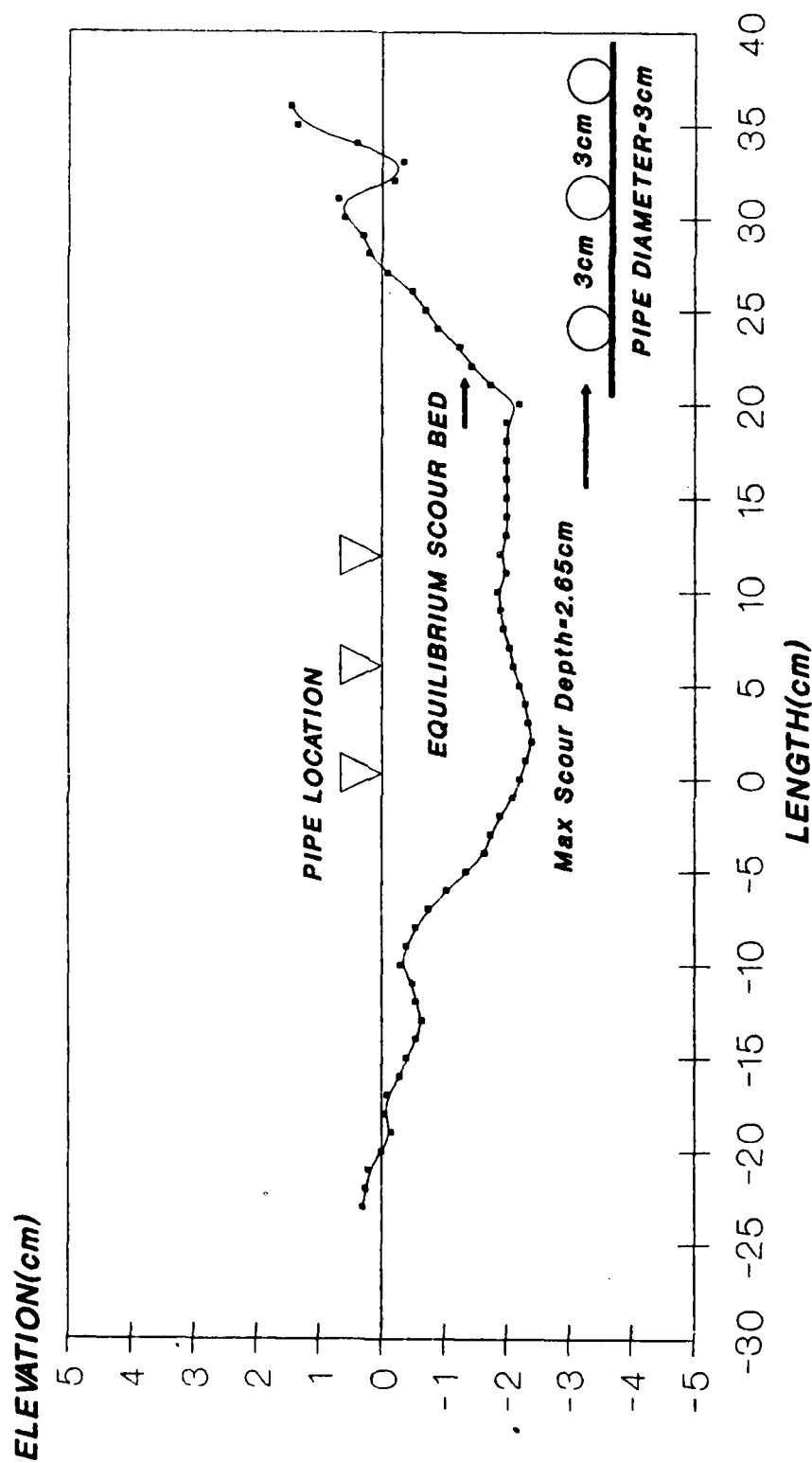
TEST No.10: CURRENT AND WAVE
U = 0.37m/sec, H = 6cm, T = 1.2sec, L = 1.0m

97
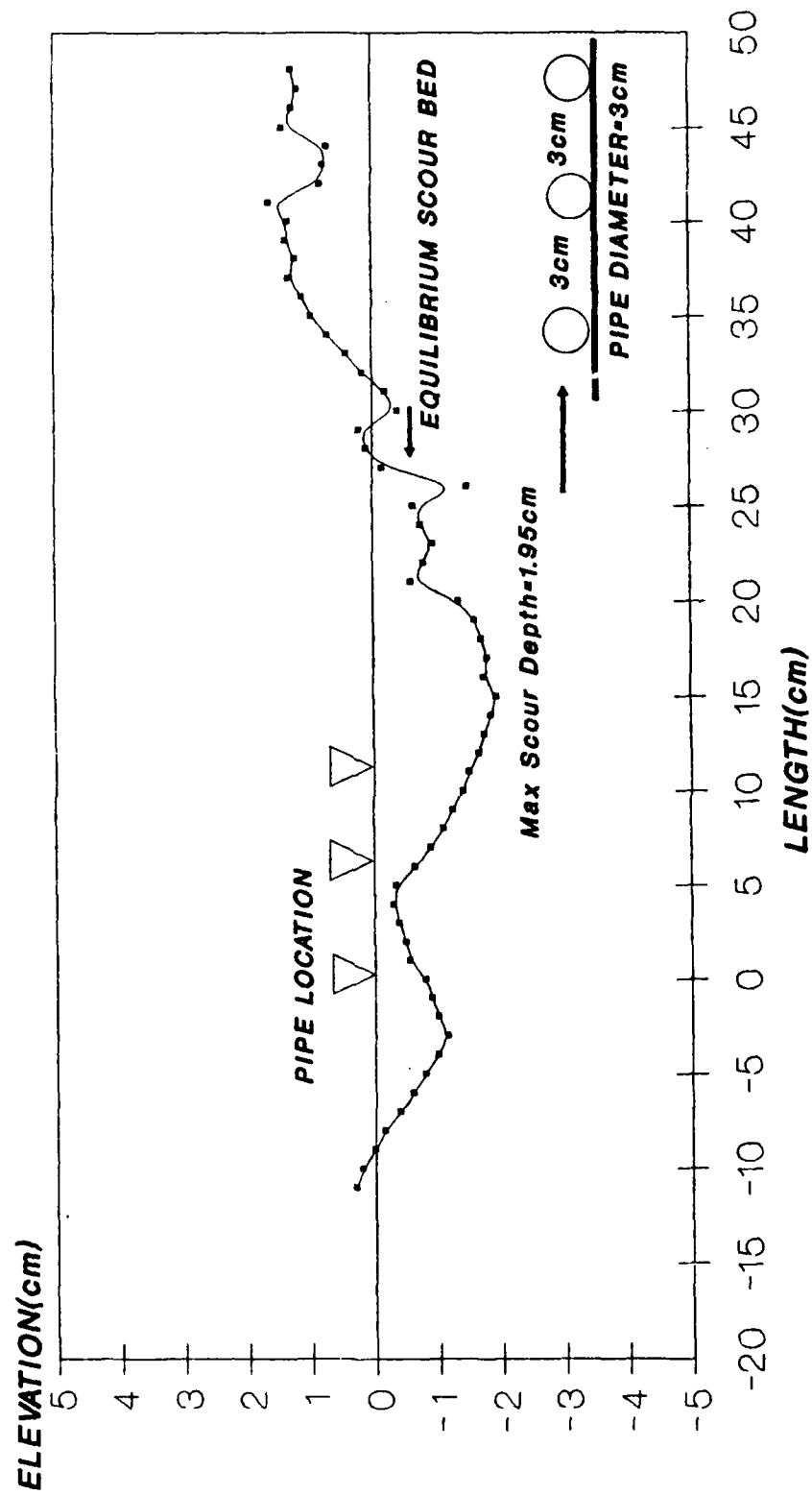
TEST No.11: CURRENT
U= 0.37m/sec

ELEVATION(cm)

PIPE LOCATION

EQUILIBRIUM SCOUR BED

Max Scour Depth=1.5cm

1.5cm

1.5cm

PIPE DIAMETER=3cm

LENGTH(cm)
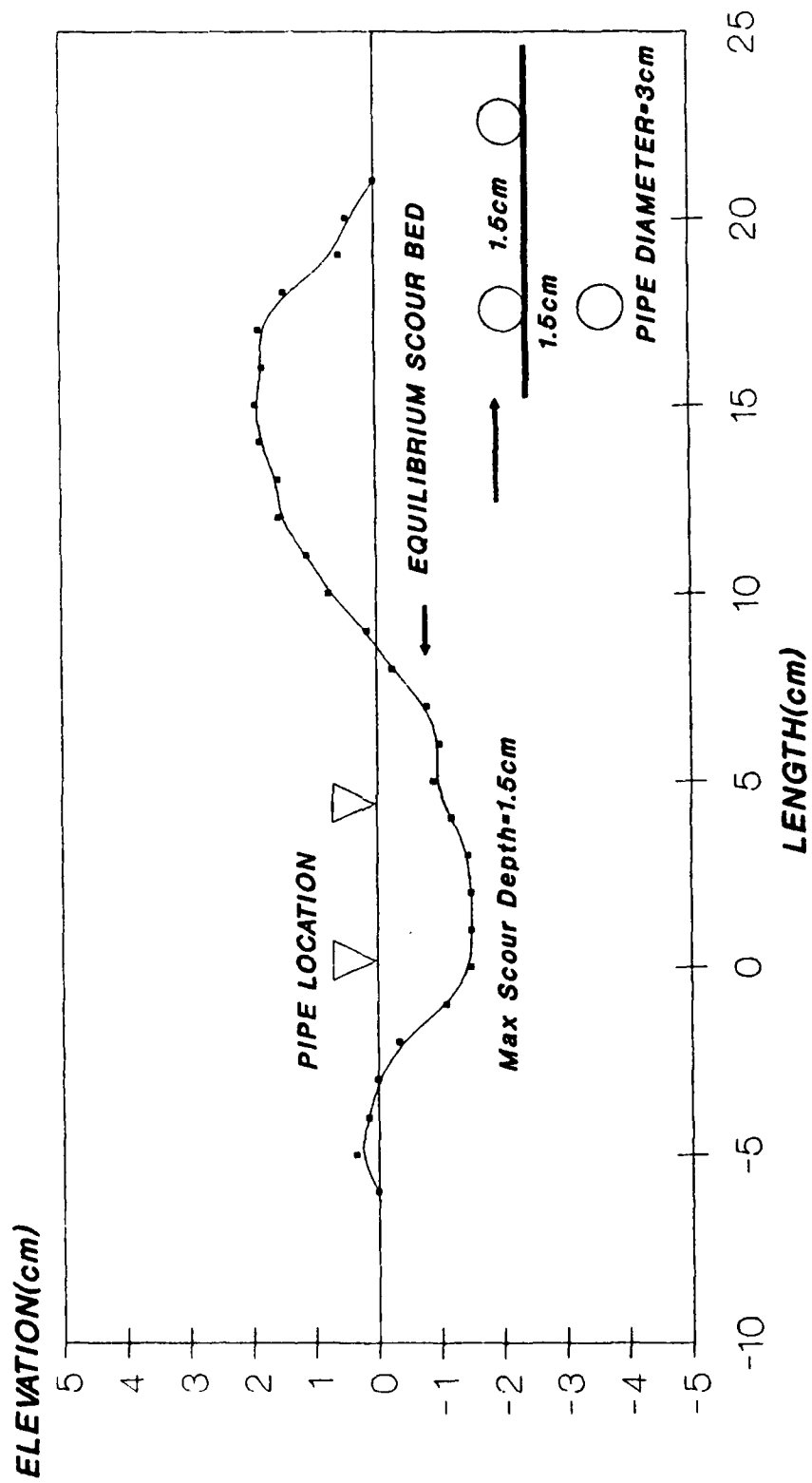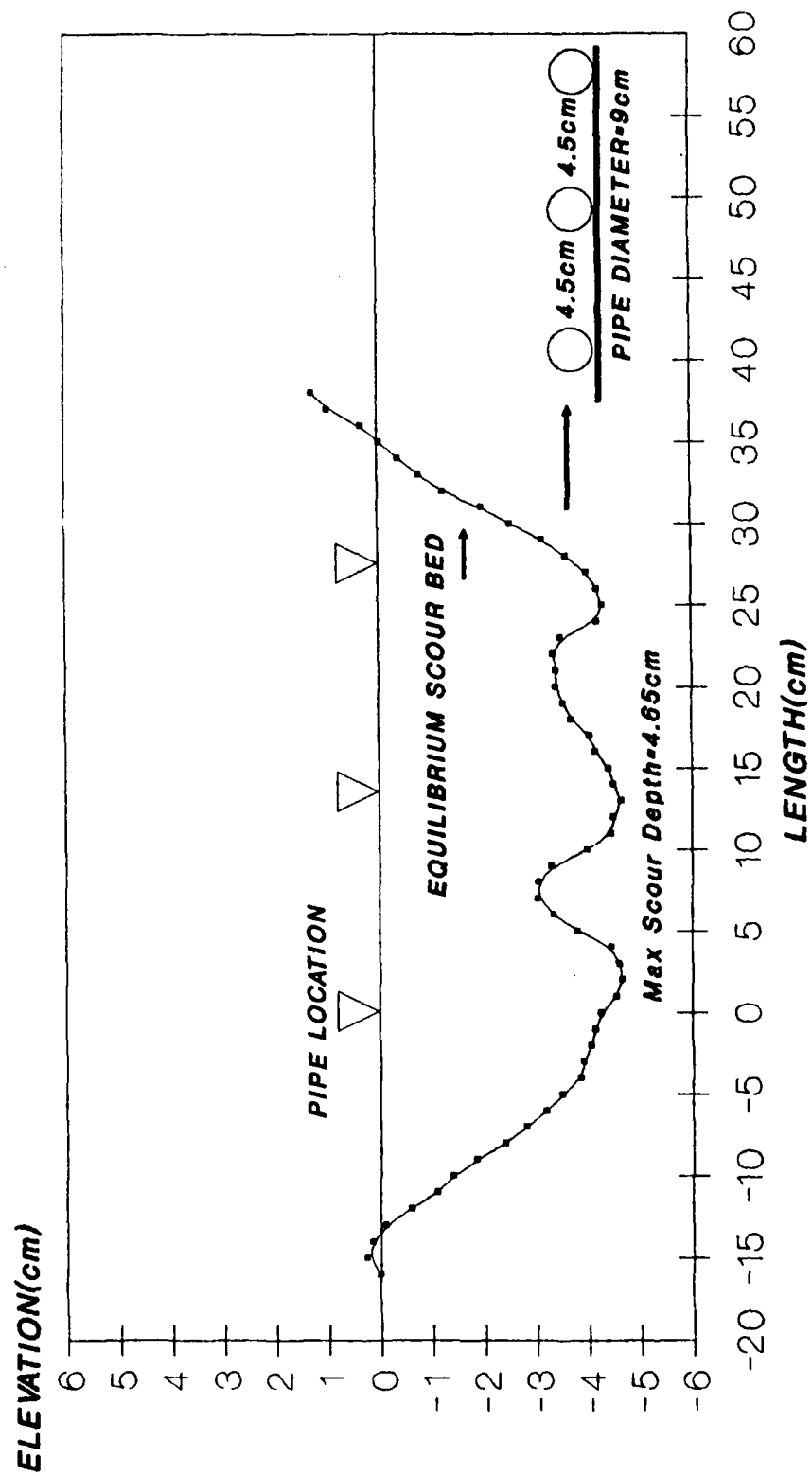
TEST No.12: CURRENT AND WAVE
U= 0.37m/sec, H= 6cm, T= 1.2sec, L= 1.0m
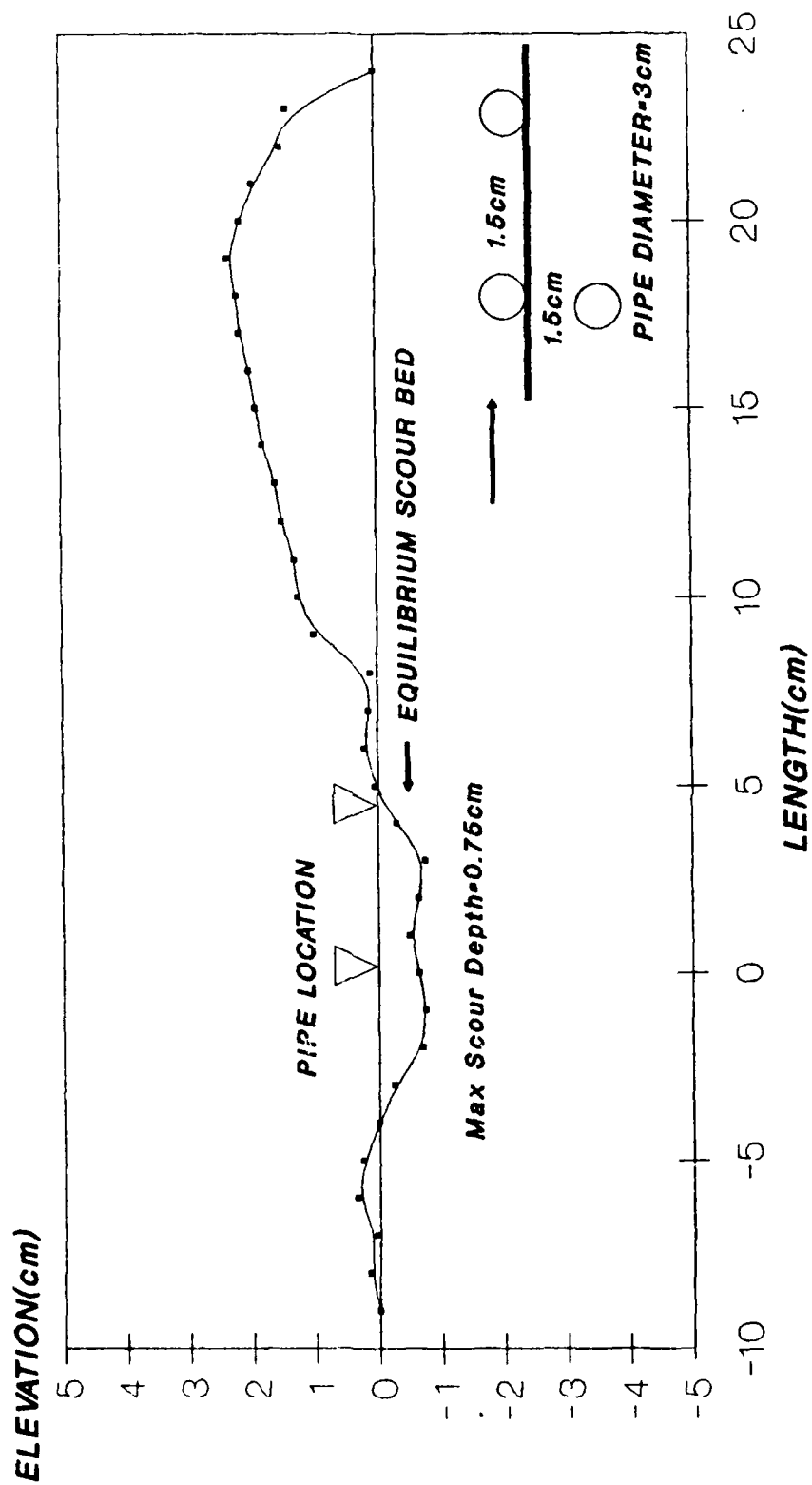
TEST No.13: CURRENT
U= 0.37m/sec

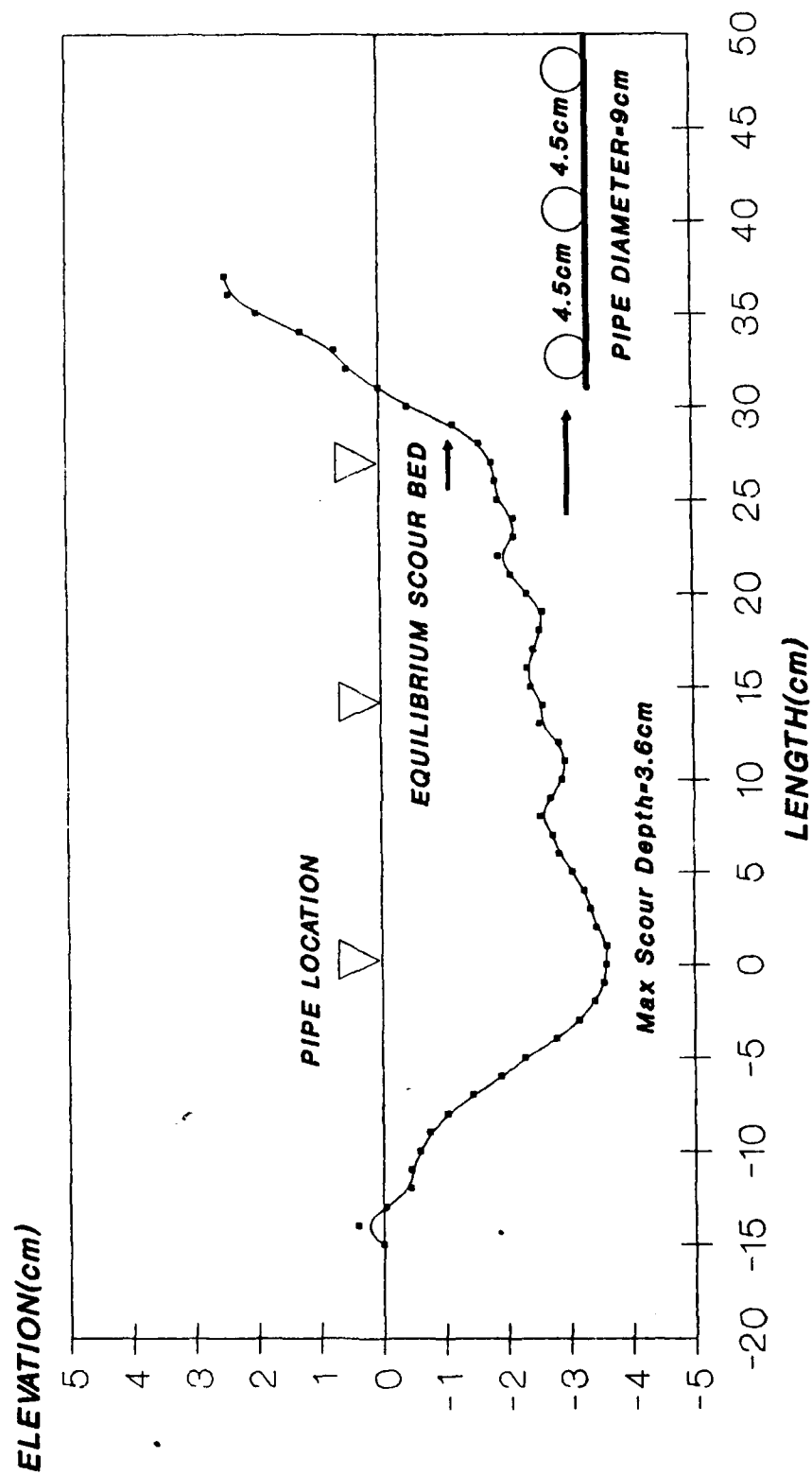# TEST No.14: CURRENT AND WAVE
U= 0.37m/sec, H= 6cm, T= 1.2sec, L= 1.0m

PIPE LOCATION

No Scour, Pipes covered

PIPE DIAMETER=3cm

3cm

3cm

ELEVATION(cm)

LENGTH(cm)
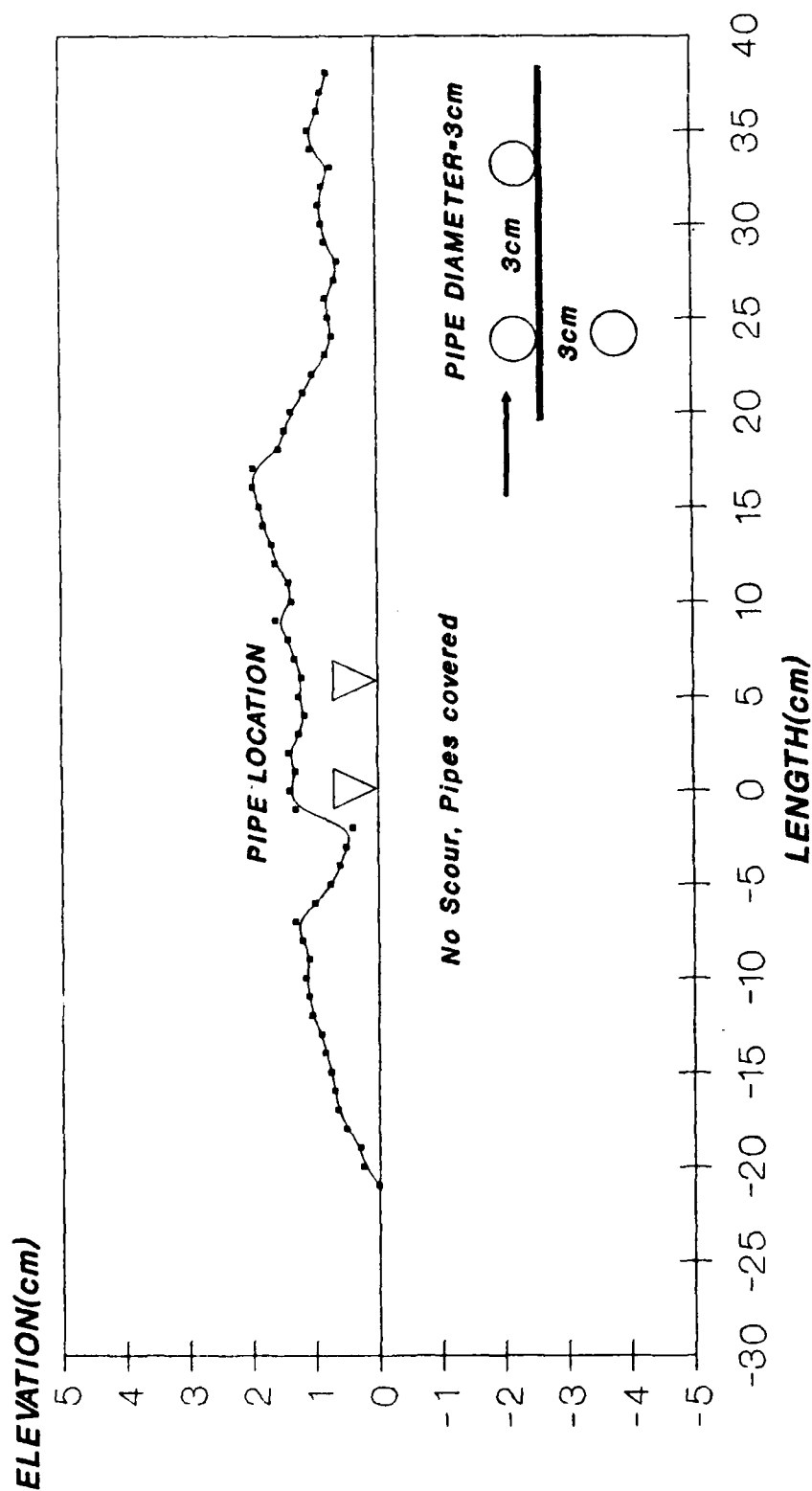
TEST No.15: CURRENT
U= 0.37m/sec

ELEVATION(cm)

PIPE LOCATION

EQUILIBRIUM SCOUR BED

Max Scour Depth=3.75cm

PIPE DIAMETER=6cm

LENGTH(cm)
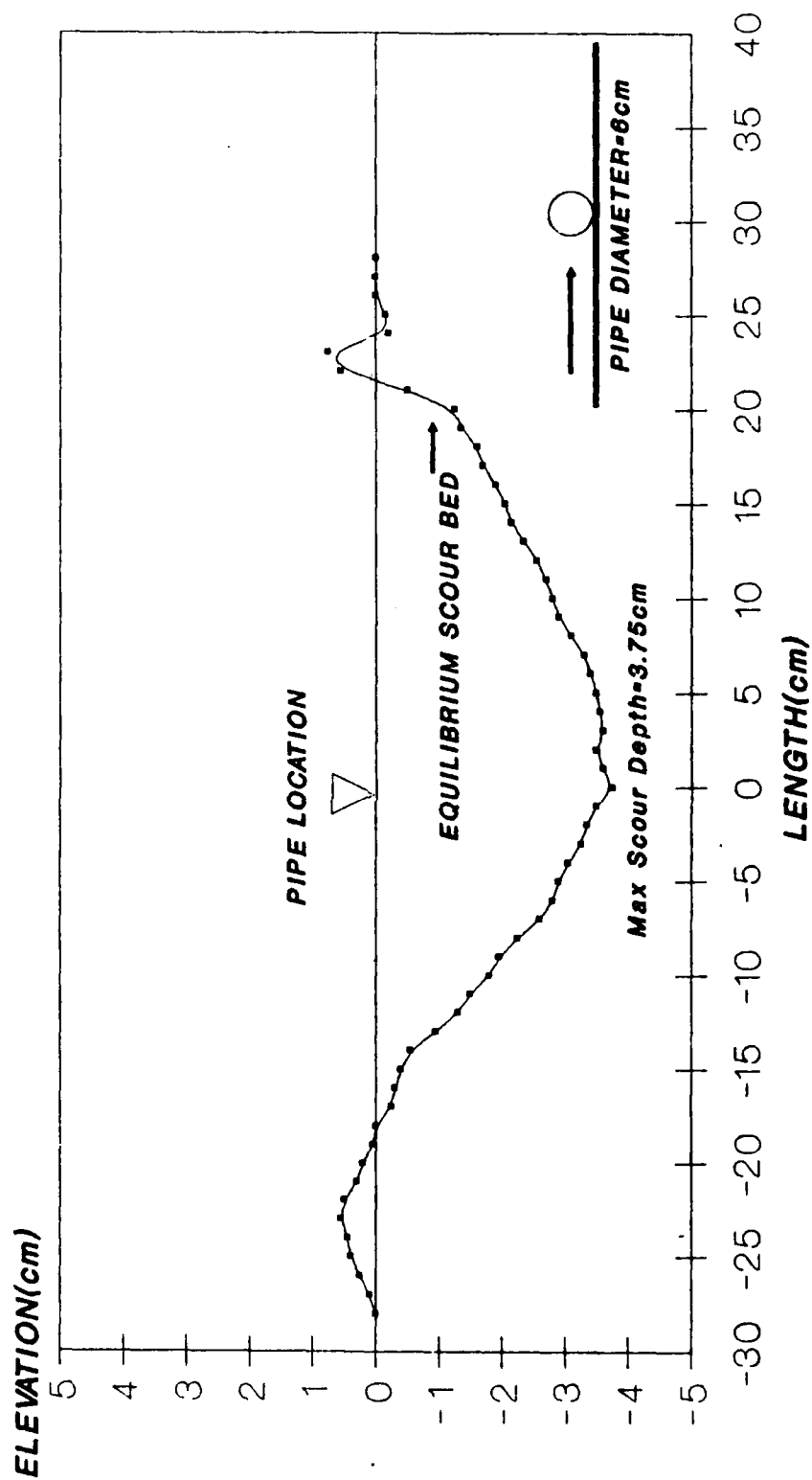
TEST No.16: CURRENT AND WAVE
U= 0.37m/sec, H= 6cm, T= 1.2sec, L= 1.0m

ELEVATION(cm)

PIPE LOCATION

EQUILIBRIUM SCOUR BED

Max Scour Depth=3.05cm

PIPE DIAMETER=6cm

LENGTH(cm)
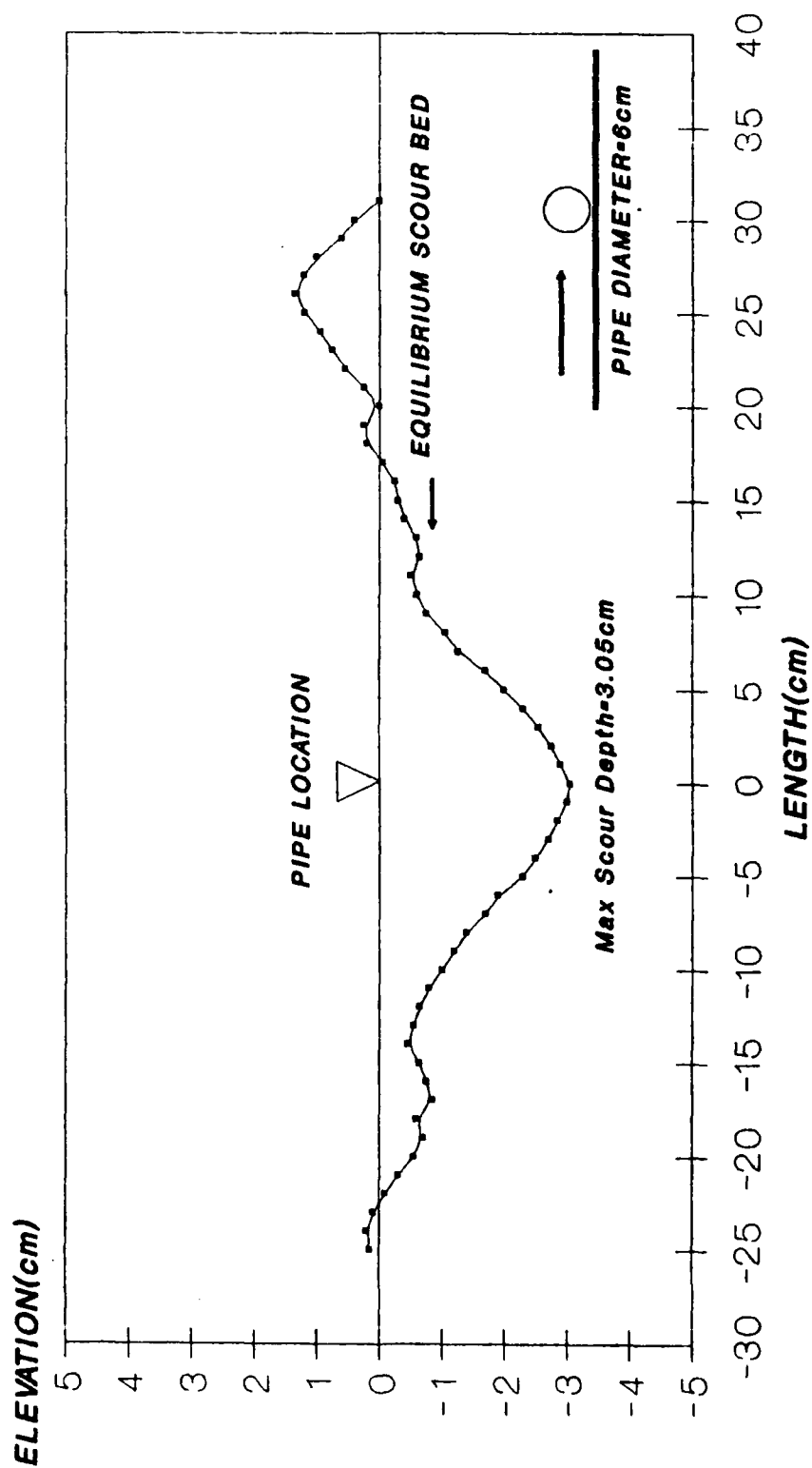
TEST No.17: CURRENT
U= 0.37m/sec
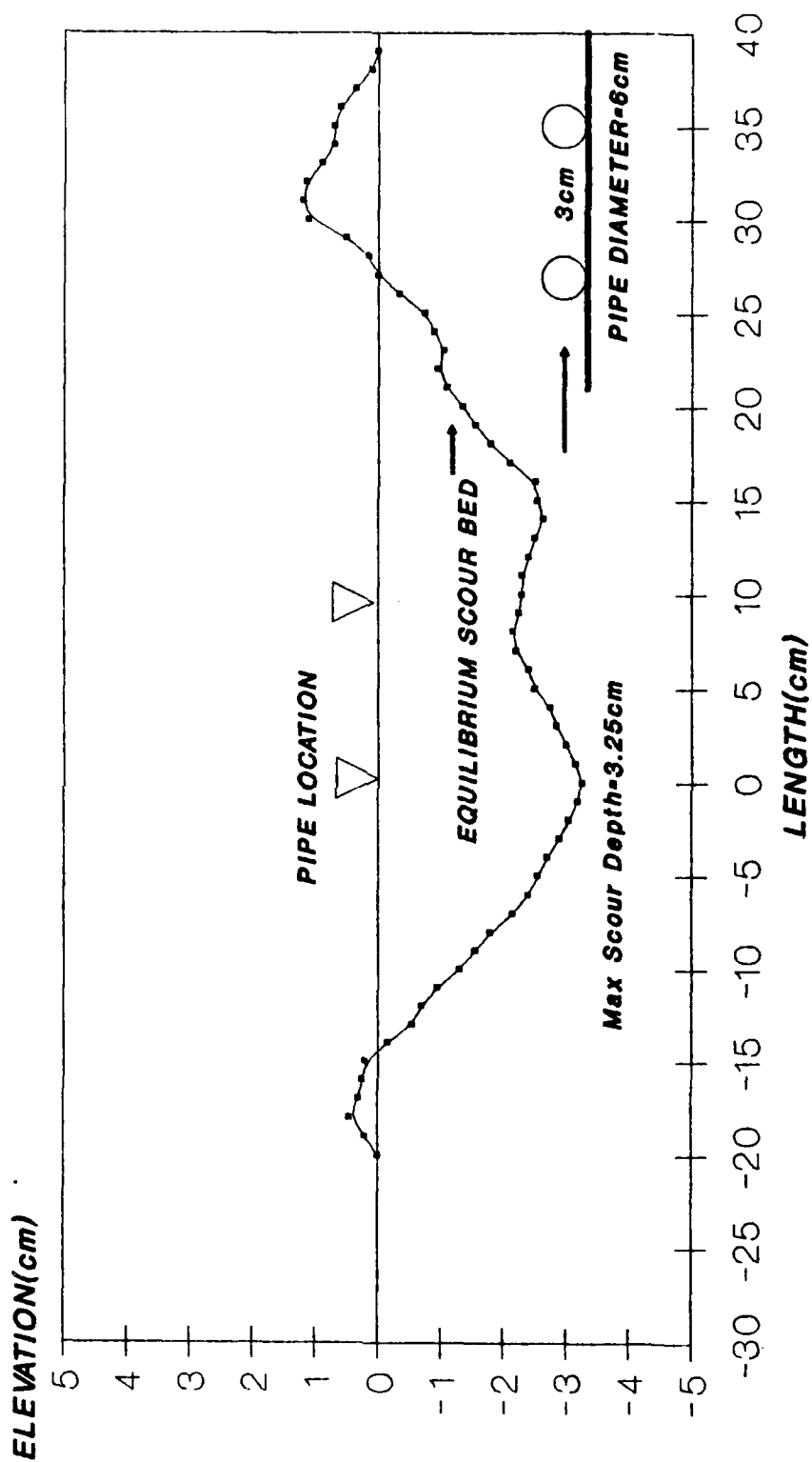
TEST No.18: CURRENT AND WAVE
U= 0.37m/sec, H= 6cm, T= 1.2sec, L= 1.0m

ELEVATION(cm)

PIPE LOCATION

EQUILIBRIUM SCOUR BED

Max Scour Depth=2.80cm

3cm

PIPE DIAMETER=6cm

LENGTH(cm)
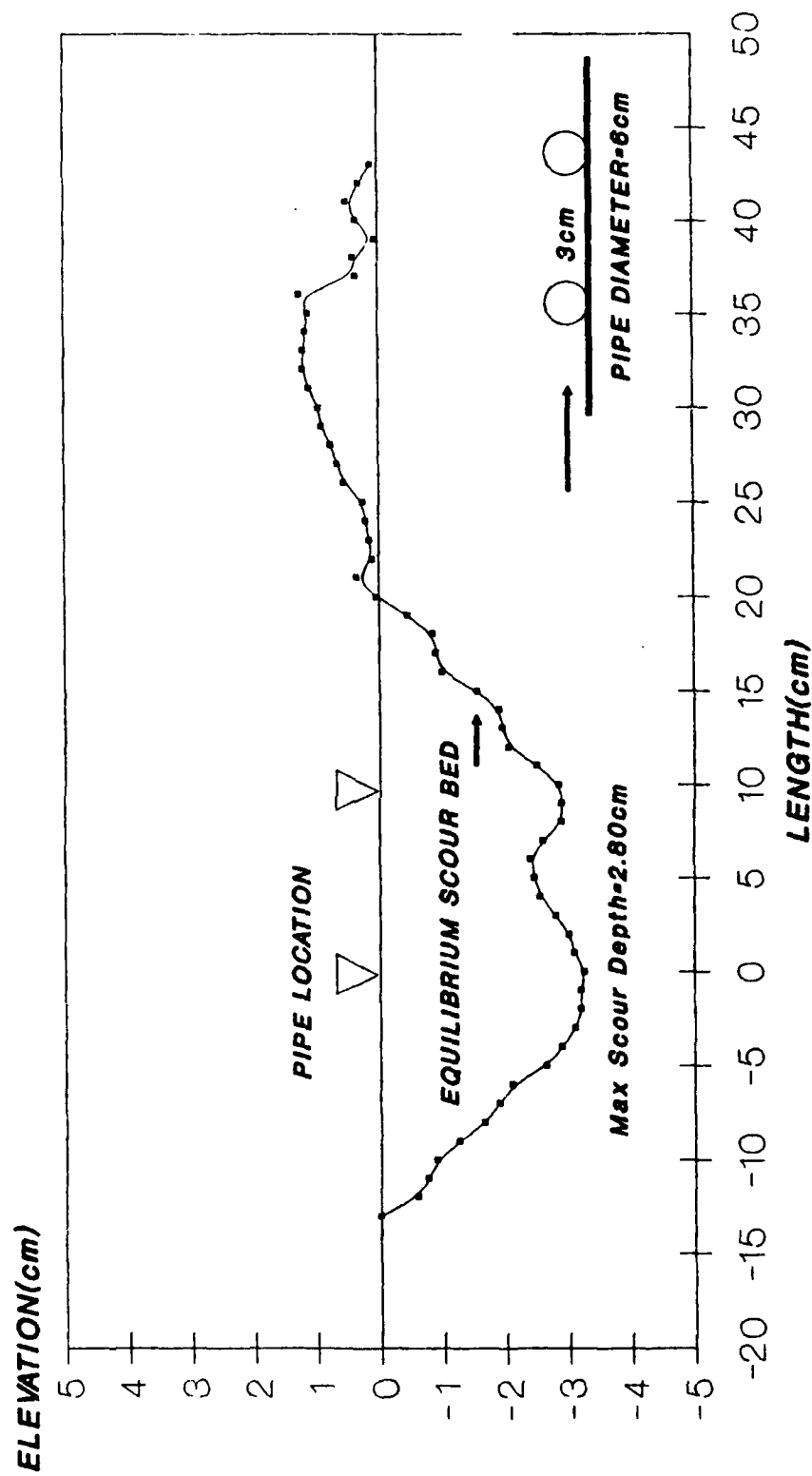
TEST No.19: CURRENT
U= 0.37m/sec
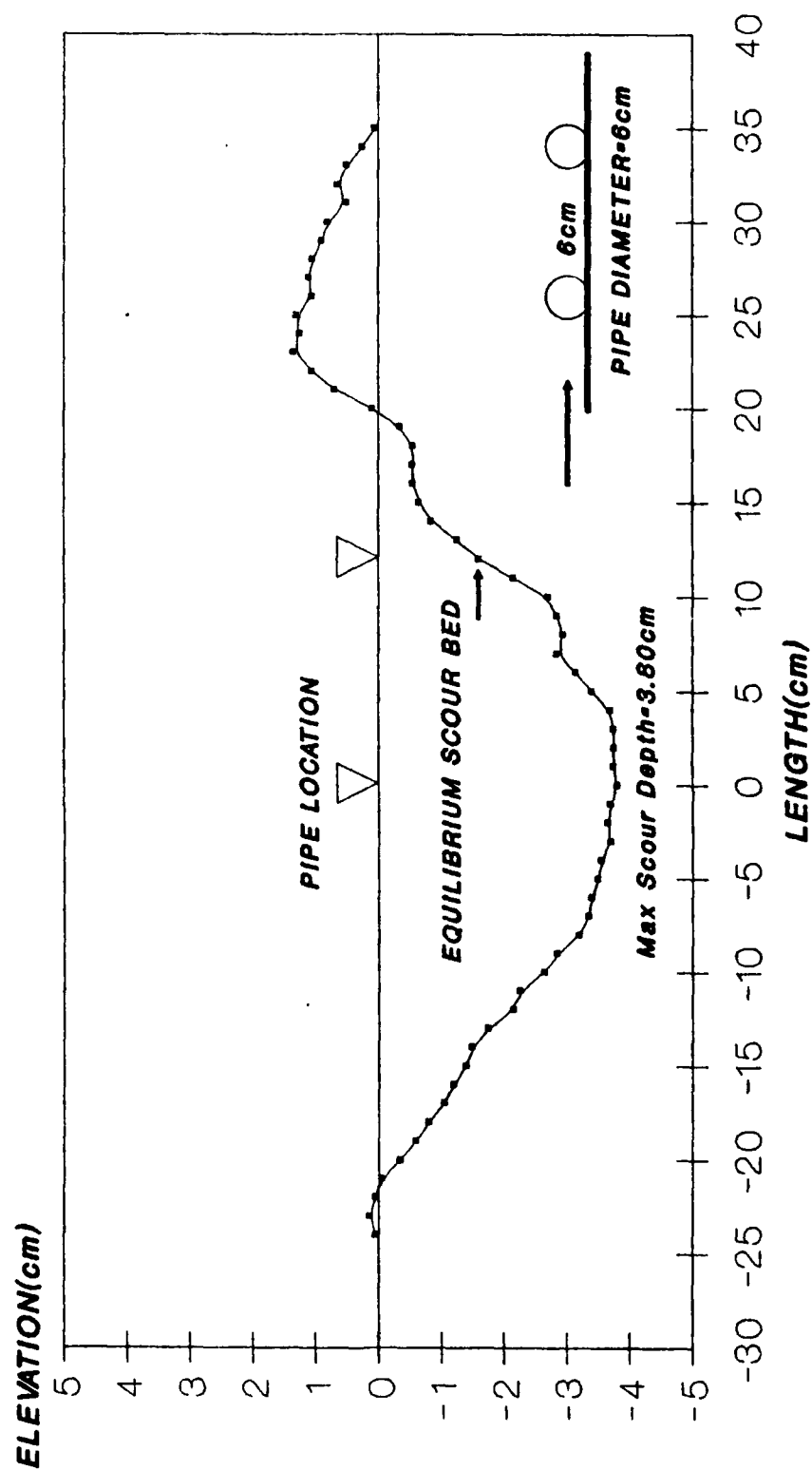
TEST No.20: CURRENT AND WAVE
U= 0.37m/sec, H= 6cm, T= 1.2sec, L= 1.0m

PIPE LOCATION

EQUILIBRIUM SCOUR BED

Max Scour Depth=3.36cm

6cm

PIPE DIAMETER=6cm

ELEVATION(cm)

LENGTH(cm)
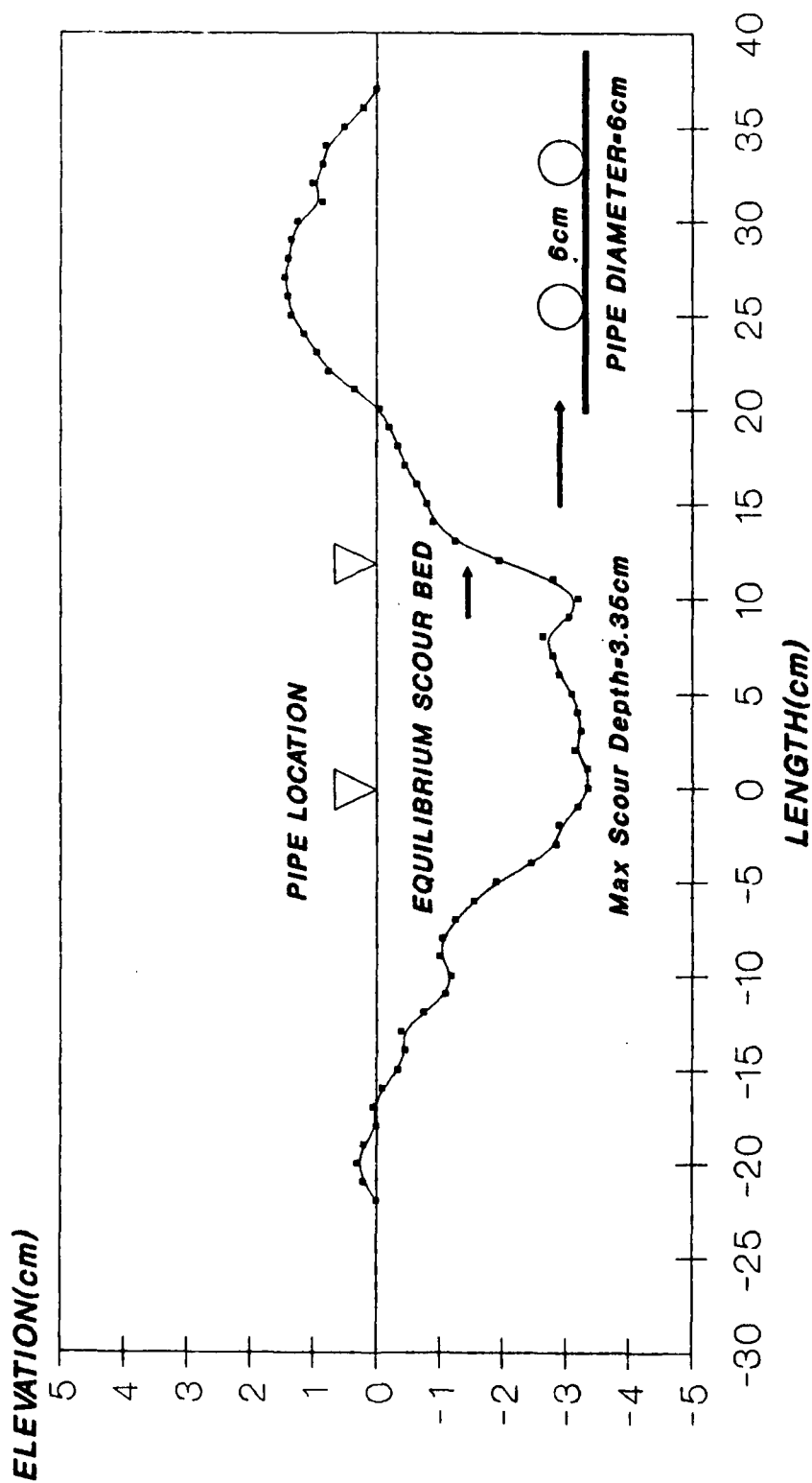
TEST No.21: CURRENT
U= 0.37m/sec

PIPE LOCATION

EQUILIBRIUM SCOUR BED

Max Scour Depth=4.35cm

PIPE DIAMETER=6cm

3cm   3cm

ELEVATION(cm)

LENGTH(cm)
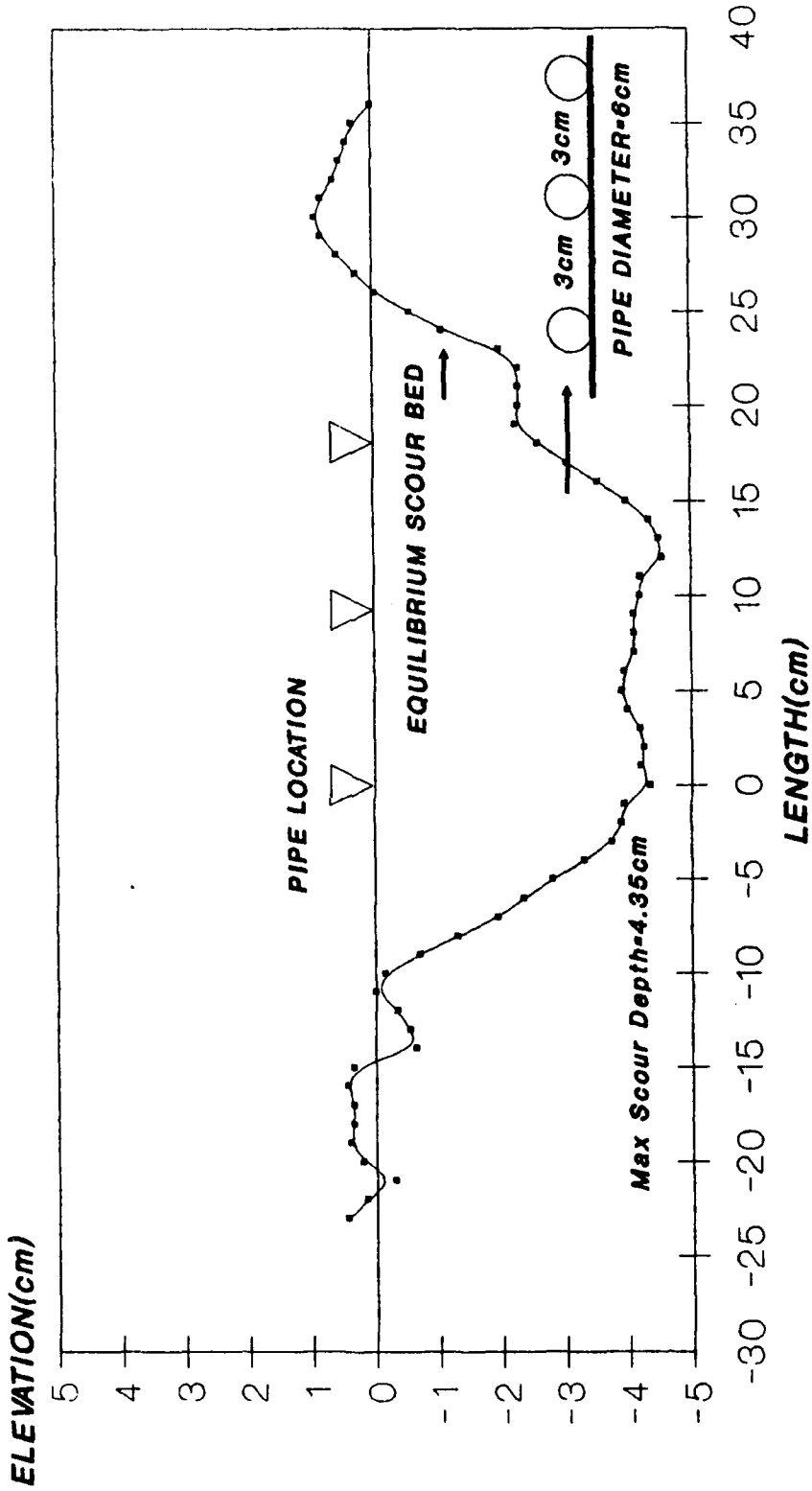
TEST No.22: CURRENT
U= 0.37m/sec

ELEVATION(cm)

PIPE LOCATION

EQUILIBRIUM SCOUR BED

Max Scour Depth=3.8cm

3cm 3cm

PIPE DIAMETER=6cm

LENGTH(cm)

109
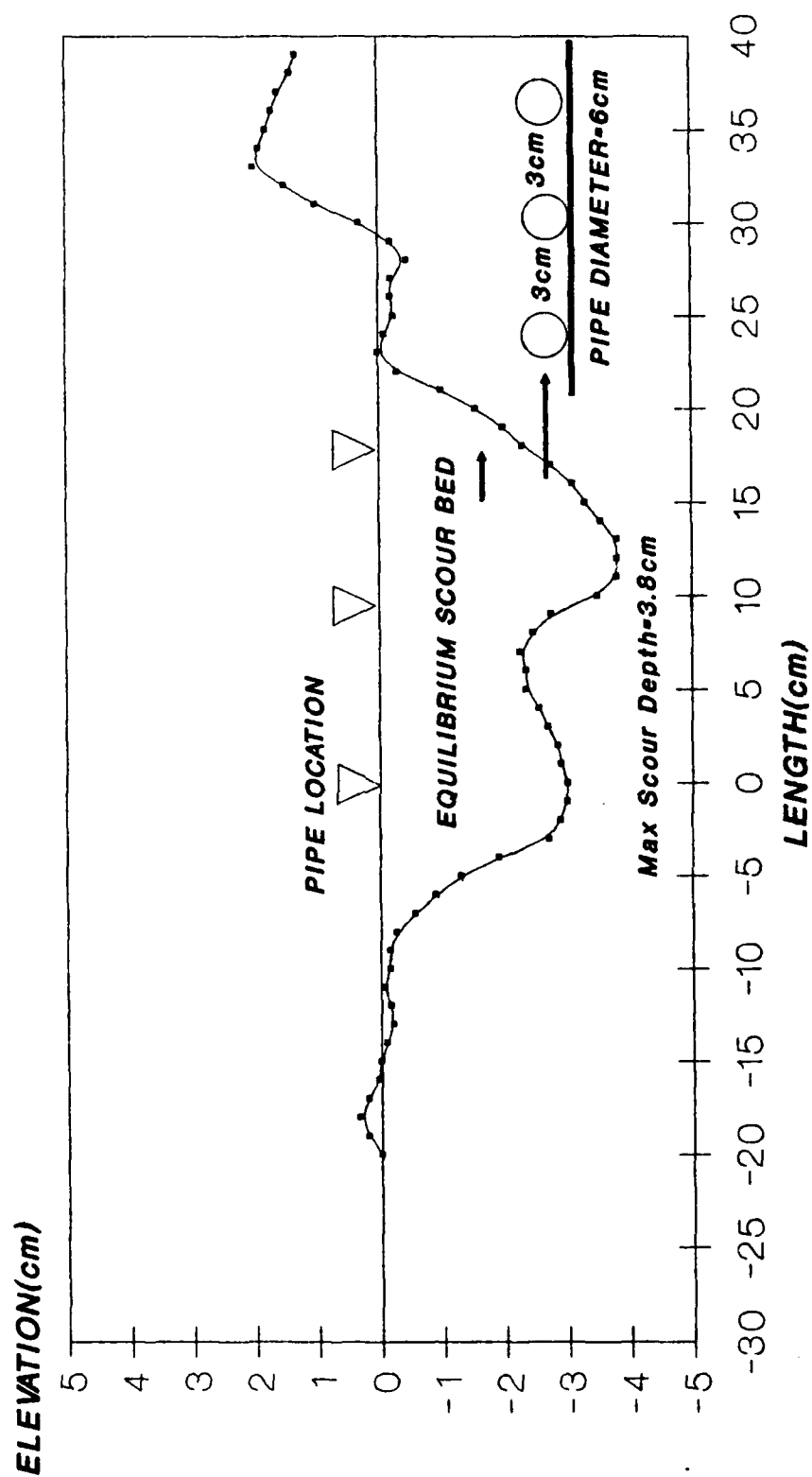
TEST No.23: CURRENT
U = 0.37m/sec
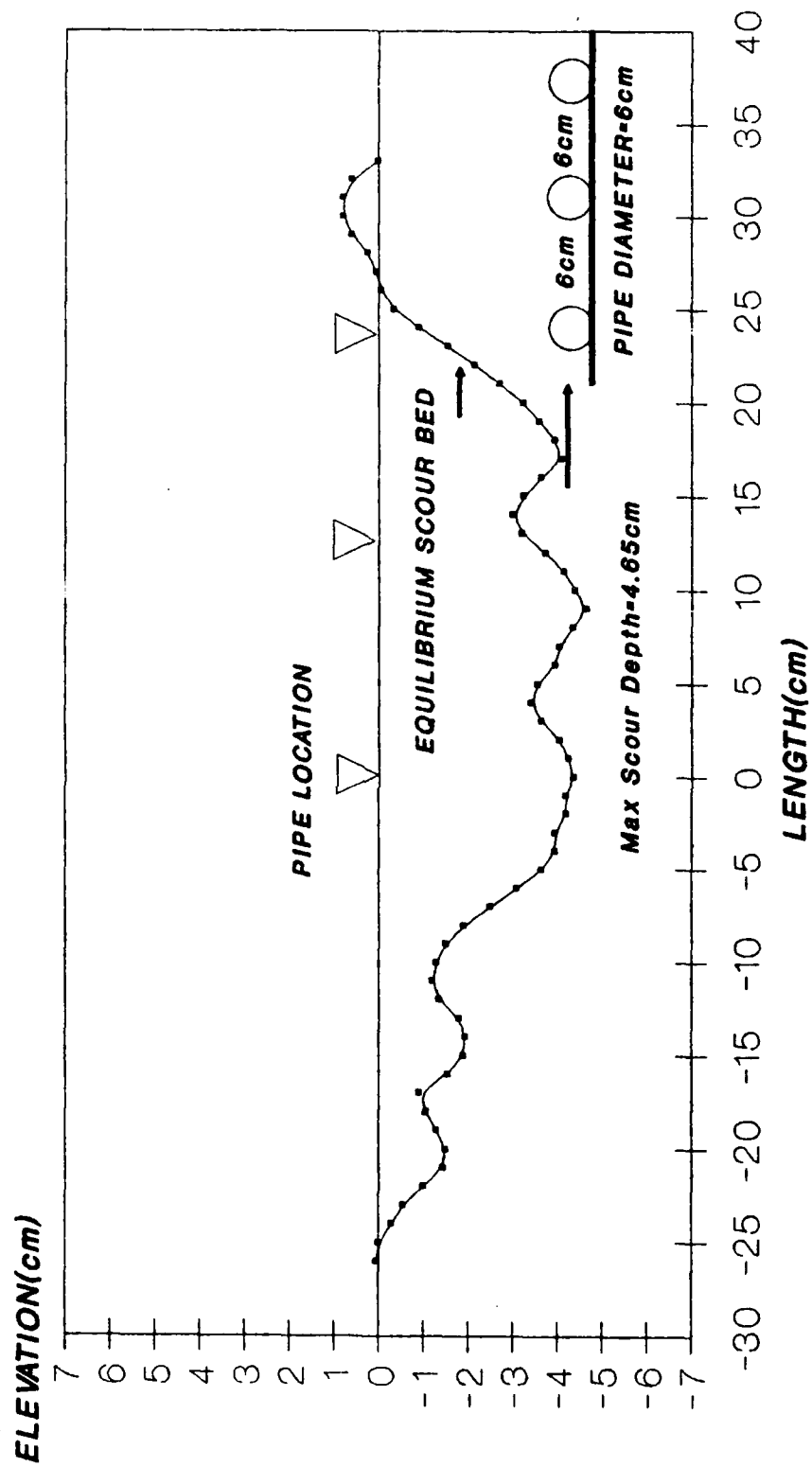
TEST No.24: CURRENT AND WAVE
U= 0.37m/sec, H= 6cm, T= 1.2sec, L= 1.0m

110

111
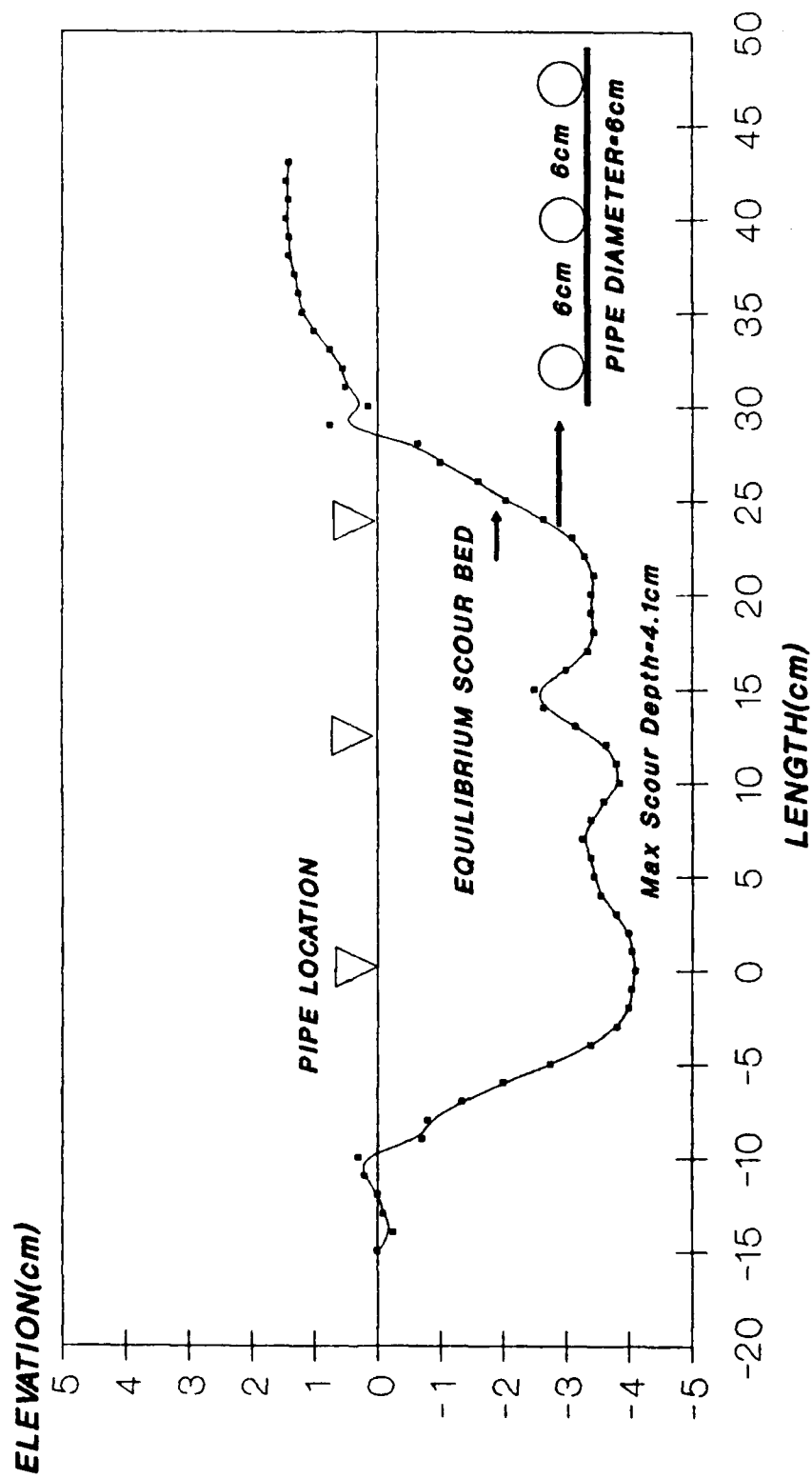
TEST No.25: CURRENT
U = 0.37m/sec
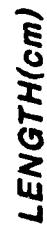
TEST No.26: CURRENT AND WAVE
U= 0.37m/sec, H= 6cm, T= 1.2sec, L= 1.0m
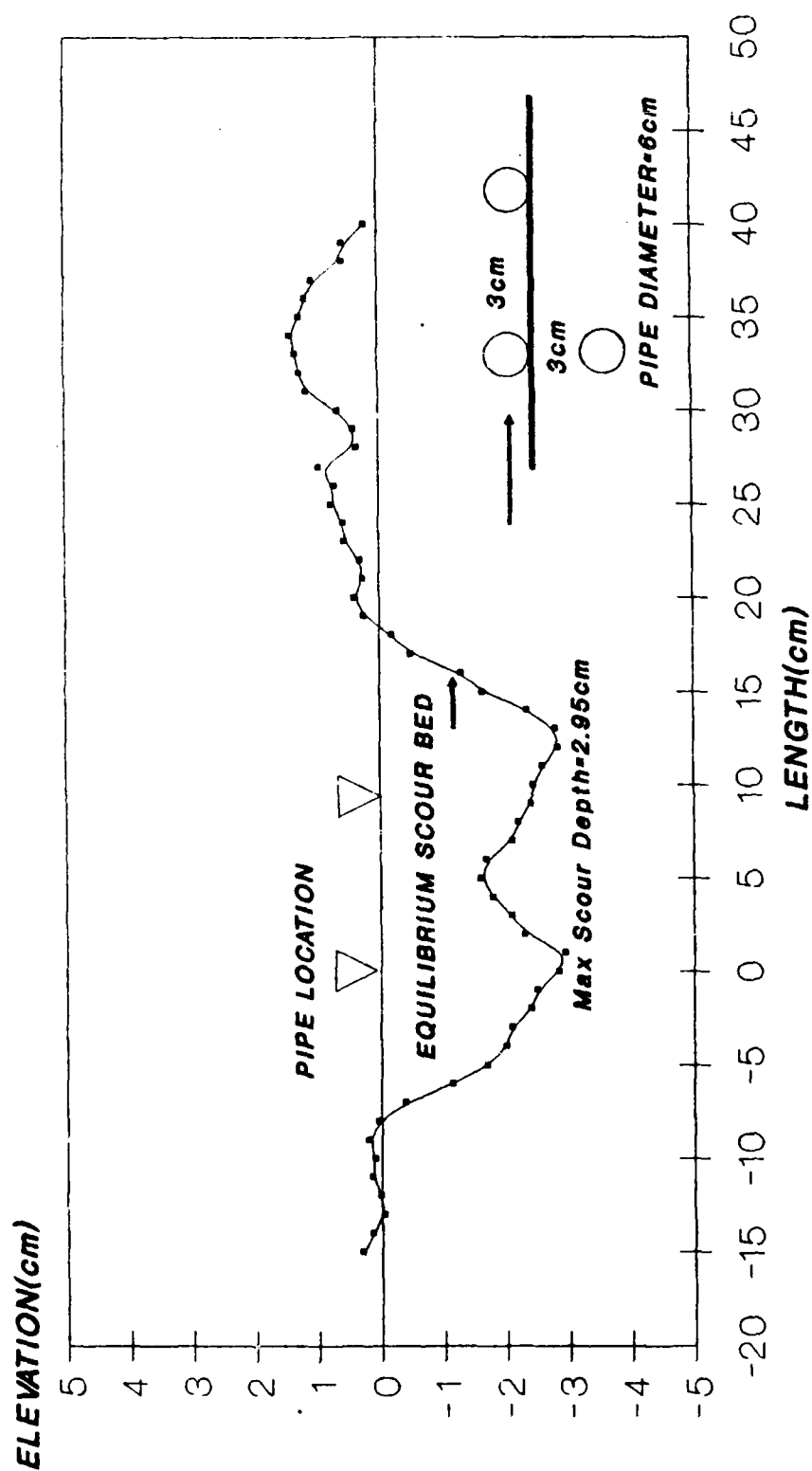
TEST No.27:CURRENT
U= 0.37m/sec
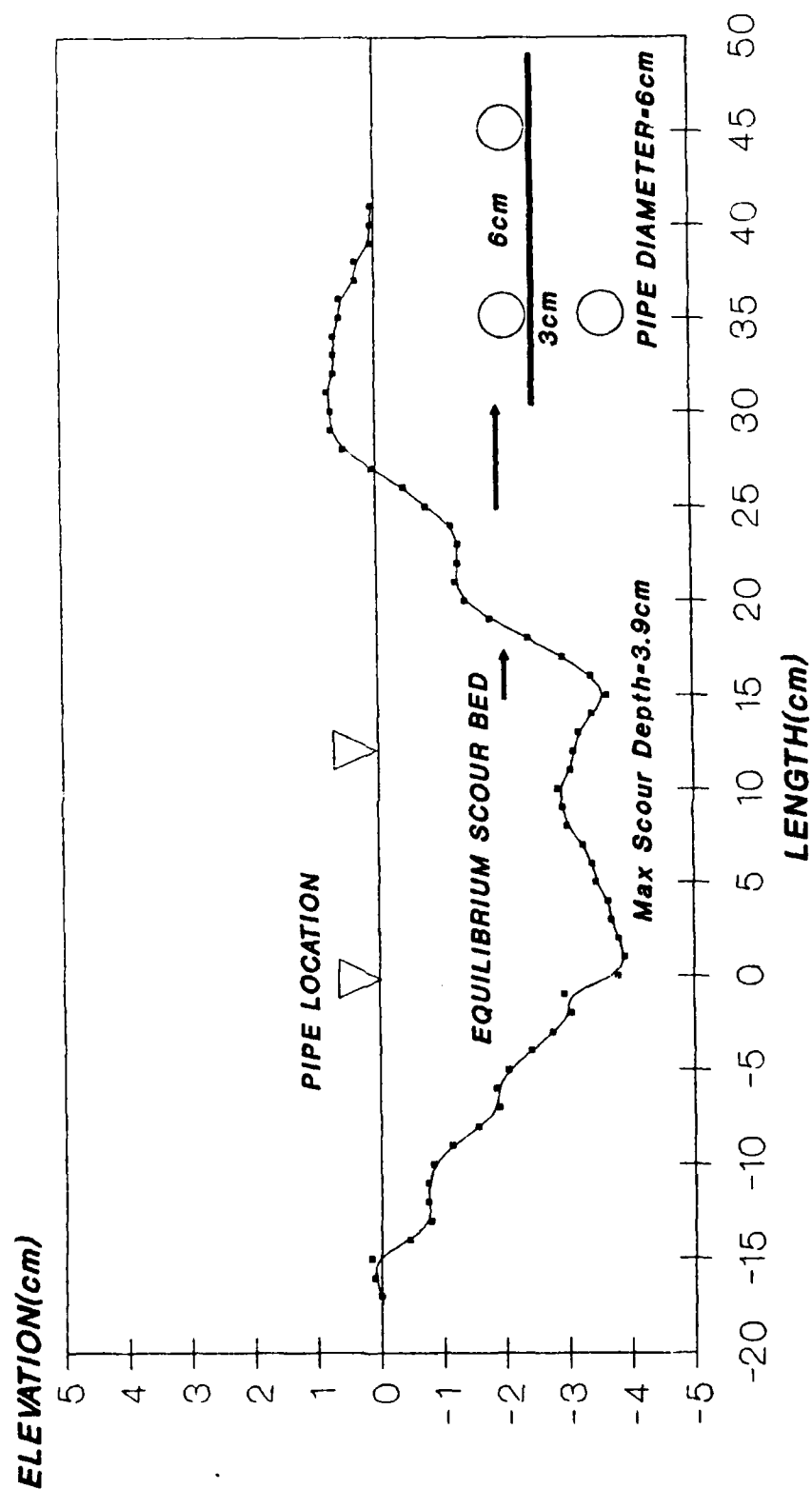
TEST No.28: CURRENT AND WAVE
U= 0.37m/sec, H= 6cm, T= 1.2sec, L= 1.0m

ELEVATION(cm)

PIPE LOCATION

EQUILIBRIUM SCOUR BED

Max Scour Depth=3.05cm

3cm

6cm

PIPE DIAMETER=6cm

LENGTH(cm)
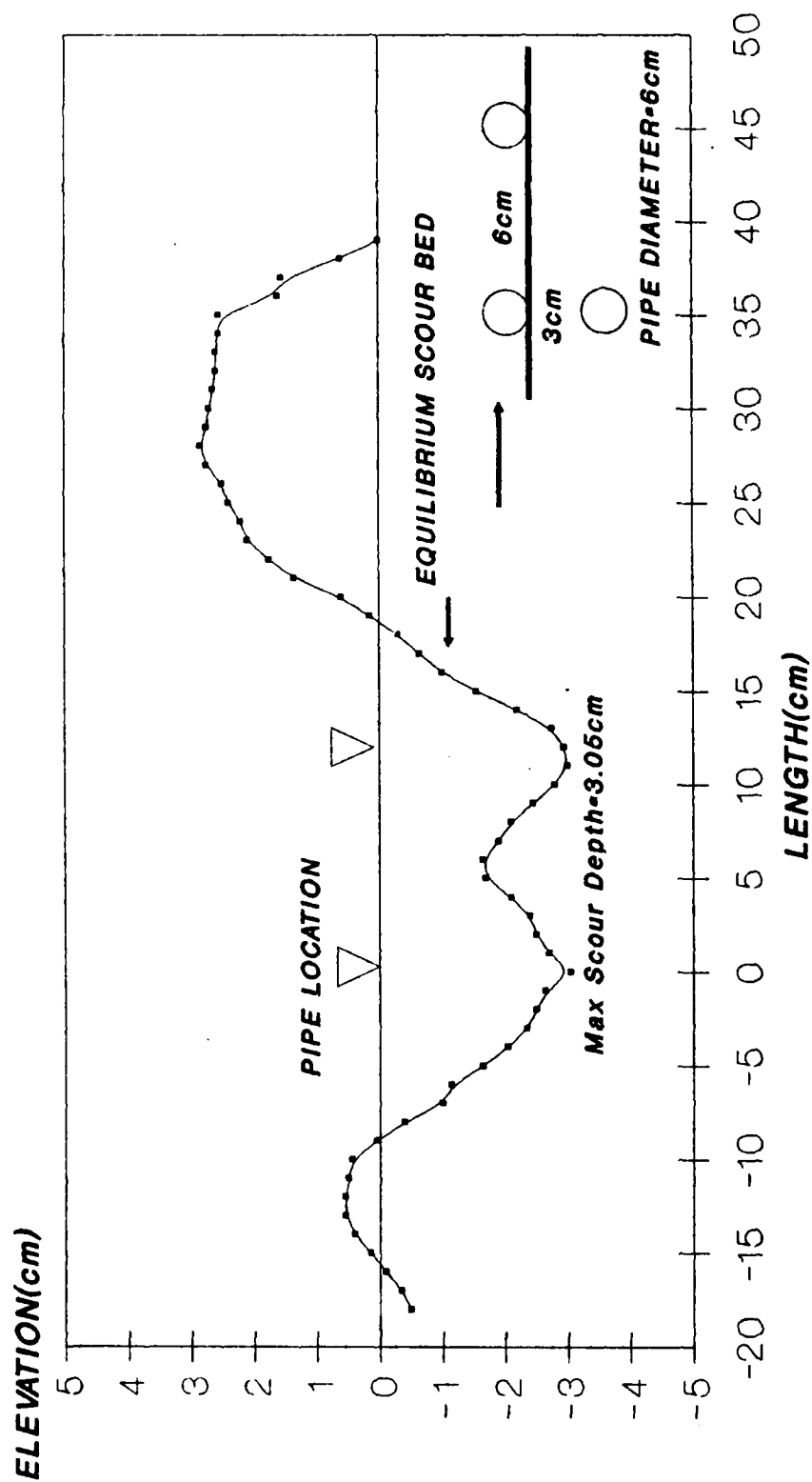
TEST No.29: CURRENT
U= 0.37m/sec
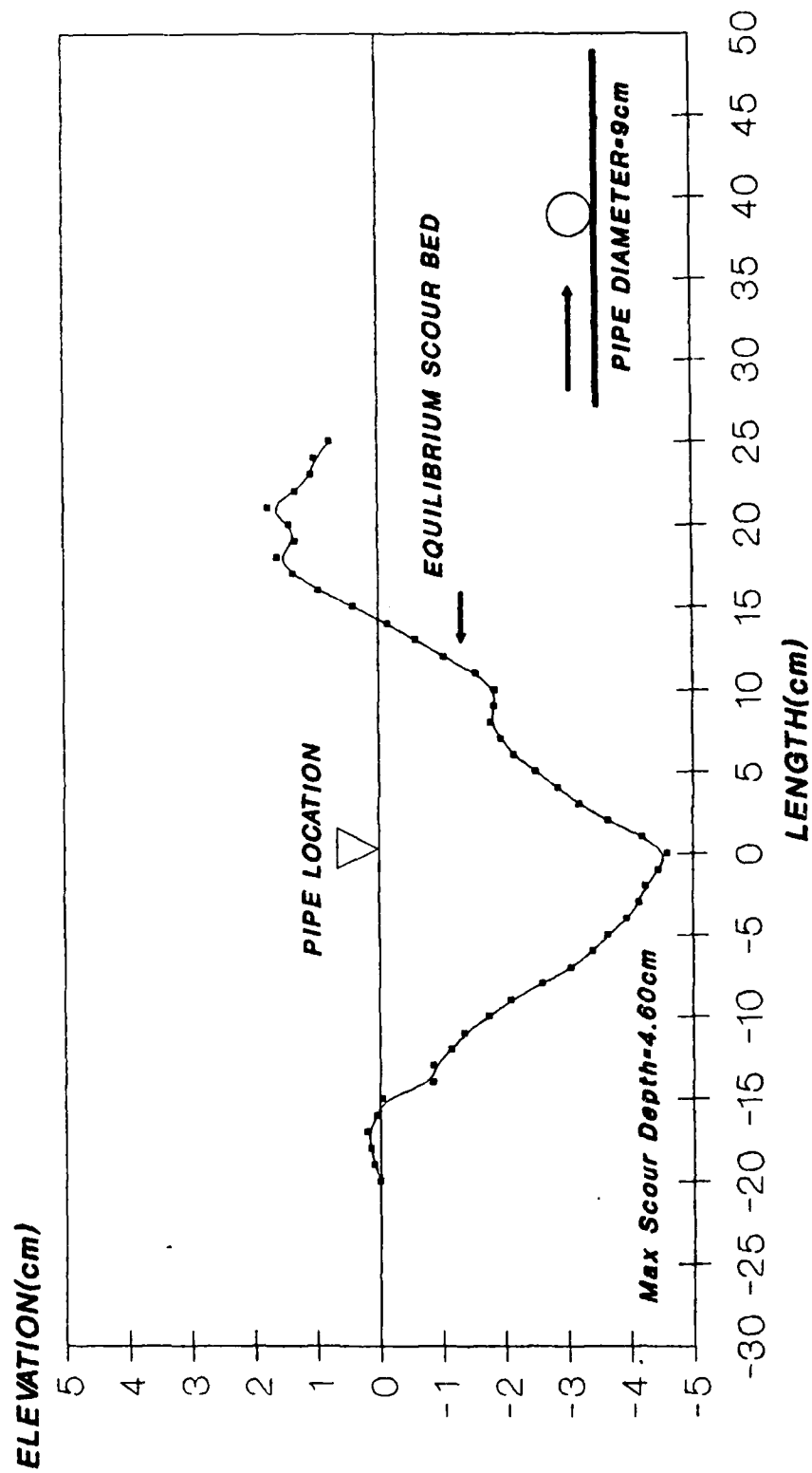
TEST No.30: CURRENT AND WAVE
U= 0.37m/sec, H= 6cm, T= 1.2sec, L= 1.0m

ELEVATION(cm)

PIPE LOCATION

EQUILIBRIUM SCOUR BED

PIPE DIAMETER=9cm

Max Scour Depth=3.90cm

LENGTH(cm)
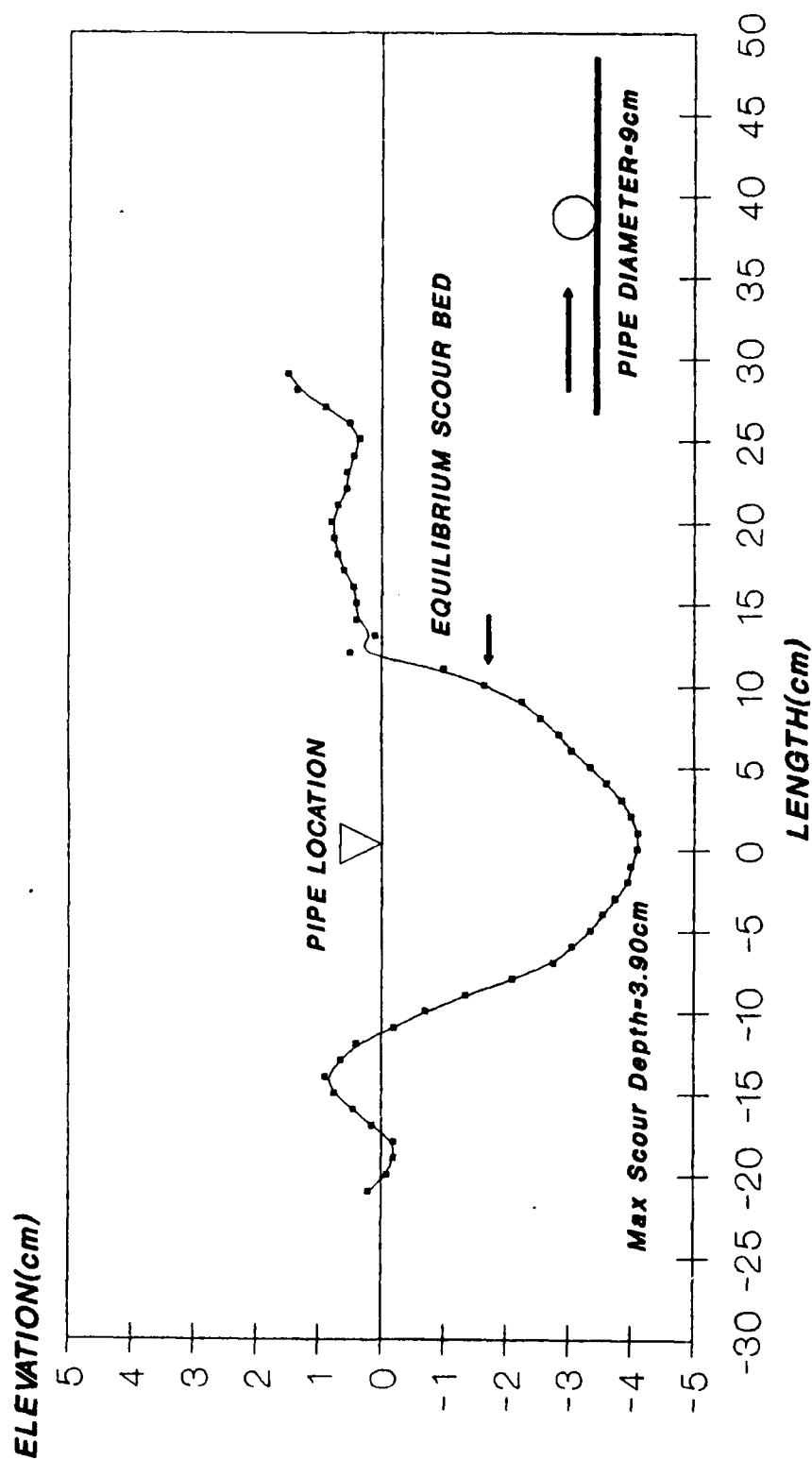
TEST No.31: CURRENT
U= 0.37m/sec

PIPE LOCATION

EQUILIBRIUM SCOUR BED

Max Scour Depth=4.95cm

PIPE DIAMETER=9cm

4.5cm

ELEVATION(cm)

LENGTH(cm)
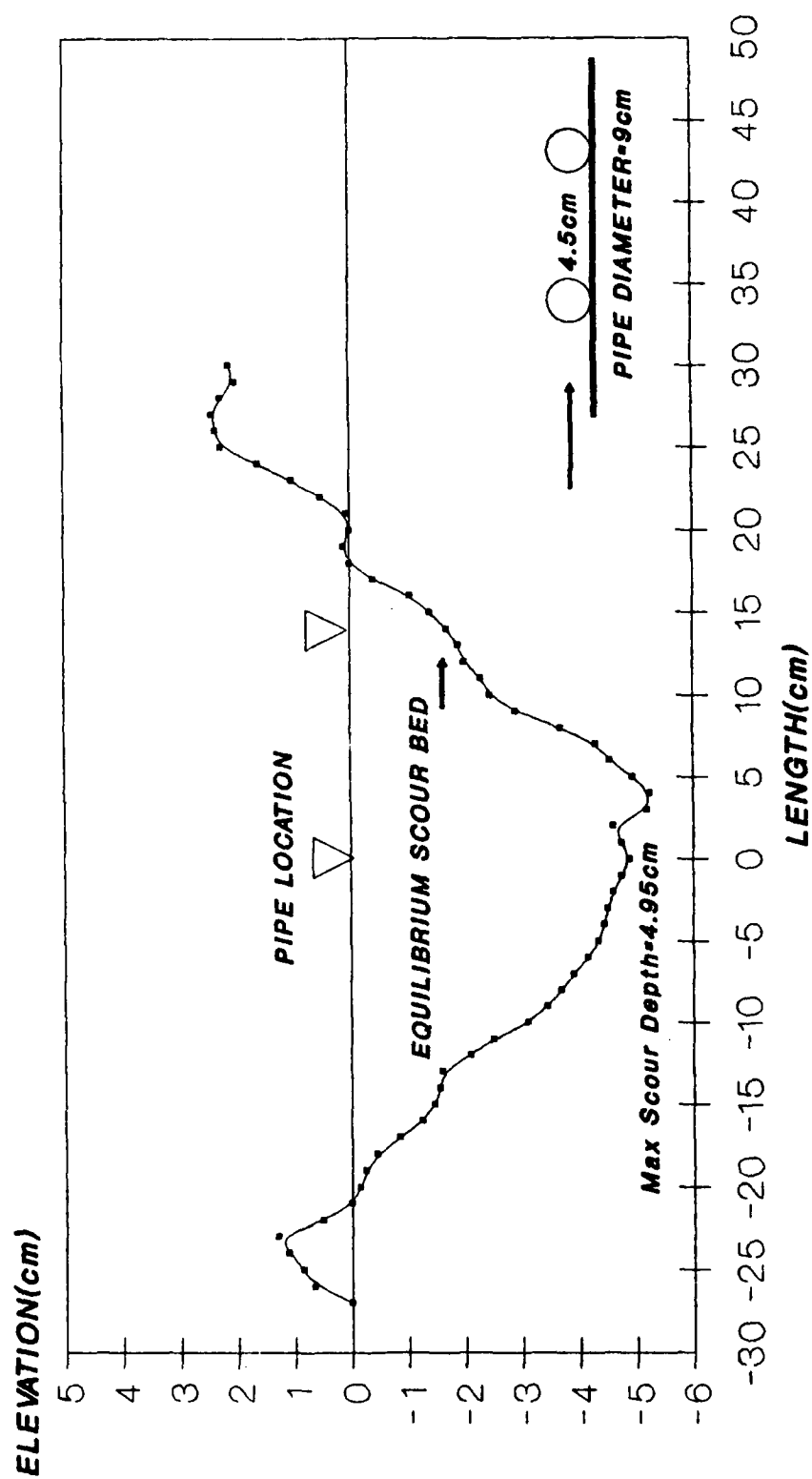
TEST No.32: CURRENT AND WAVE
U= 0.37m/sec, H= 6cm, T= 1.2sec, L= 1.0m

PIPE LOCATION

EQUILIBRIUM SCOUR BED

Max Scour Depth=3.70cm

4.5cm

PIPE DIAMETER=9cm

ELEVATION(cm)

LENGTH(cm)
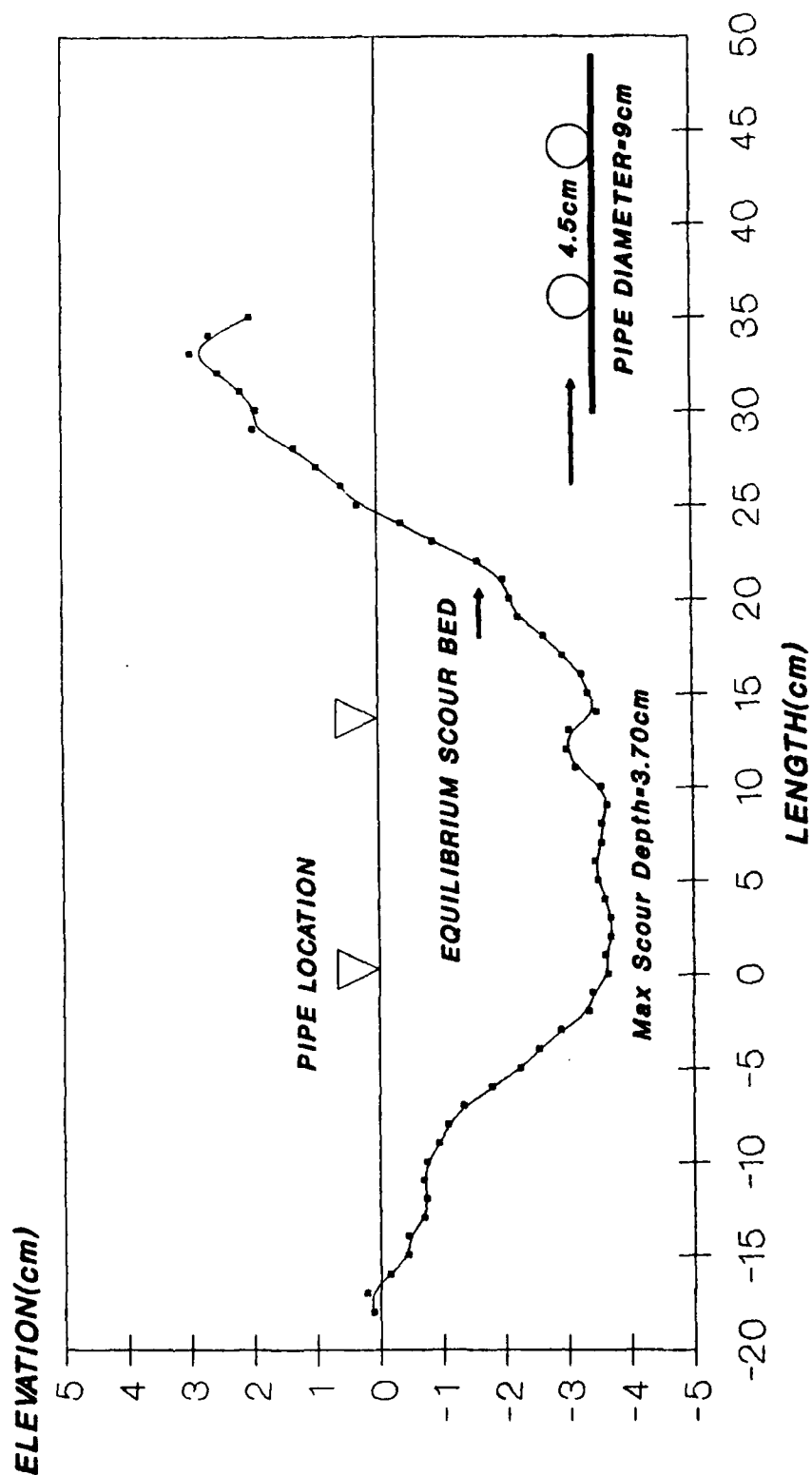
TEST No.33: CURRENT
U = 0.37m/sec

PIPE LOCATION

EQUILIBRIUM SCOUR BED

Max Scour Depth=5.15cm

9cm

PIPE DIAMETER=9cm

ELEVATION(cm)

LENGTH(cm)
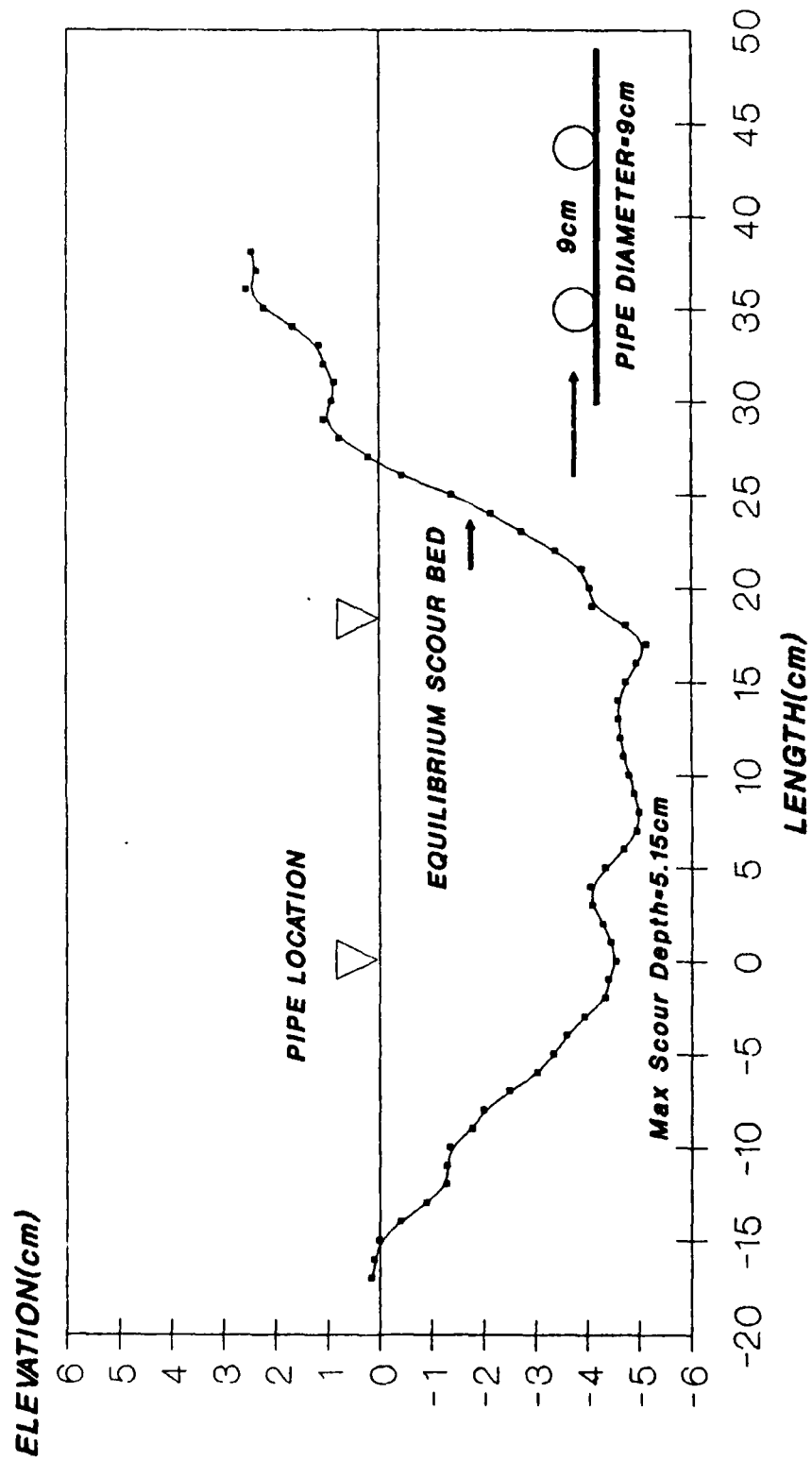
TEST No.34:CURRENT AND WAVE
U= 0.37m/sec, H= 6cm, T= 1.2sec, L= 1.0m

PIPE LOCATION

EQUILIBRIUM SCOUR BED

Max Scour Depth=4.45cm

9cm

PIPE DIAMETER=9cm

ELEVATION(cm)

LENGTH(cm)
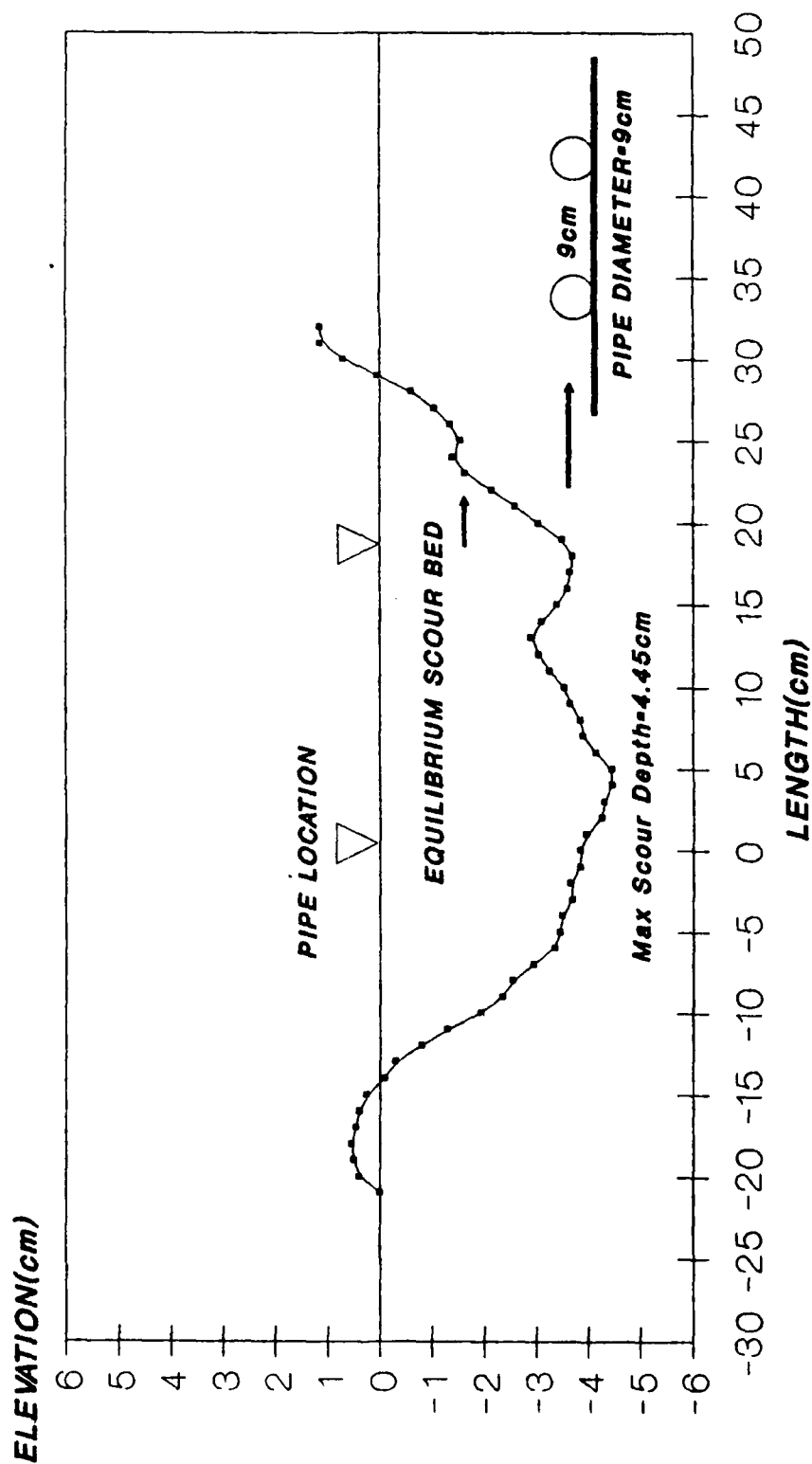
TEST No.35: CURRENT
U= 0.37 m/sec

PIPE LOCATION

EQUILIBRIUM SCOUR BED

Max Scour Depth=4.65cm

4.5cm 4.5cm

PIPE DIAMETER=9cm

ELEVATION(cm)

LENGTH(cm)

TEST No.36: CURRENT AND WAVE
U= 0.37m/sec, H= 6cm, T= 1.2sec, L= 1.0m

TEST No.37: CURRENT
U= 0.37m/sec

PIPE LOCATION

EQUILIBRIUM SCOUR BED

Max Scour Depth=5.10cm

PIPE DIAMETER=9cm

9cm 9cm 9cm

ELEVATION(cm)

LENGTH(cm)

124
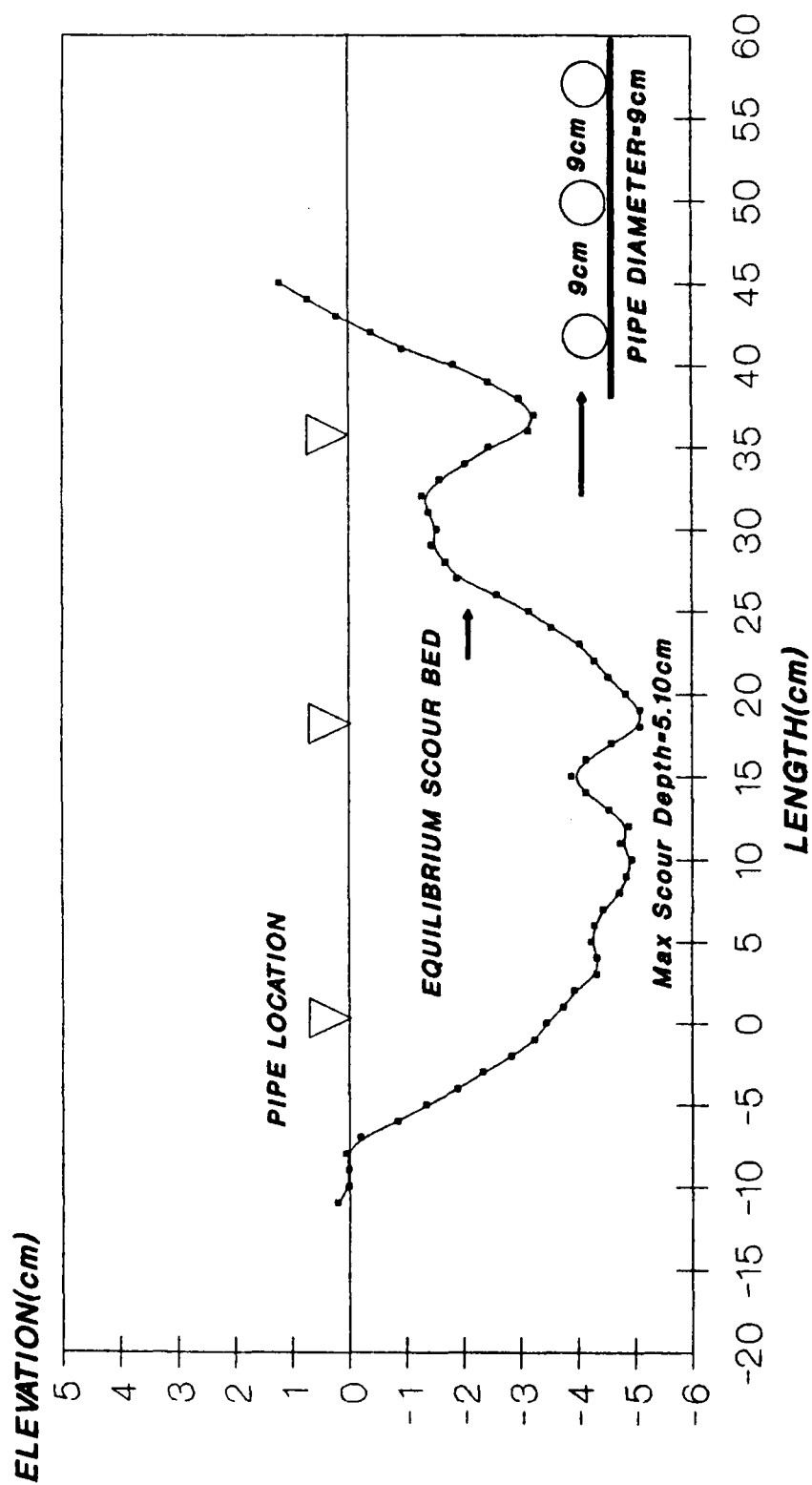
TEST No.38: CURRENT AND WAVE
U= 0.37m/sec, H= 6cm, T= 1.2sec, L= 1.0m

ELEVATION(cm)

PIPE LOCATION

EQUILIBRIUM SCOUR BED

Max Scour Depth=3.95cm

9cm 9cm 9cm

PIPE DIAMETER=9cm

LENGTH(cm)
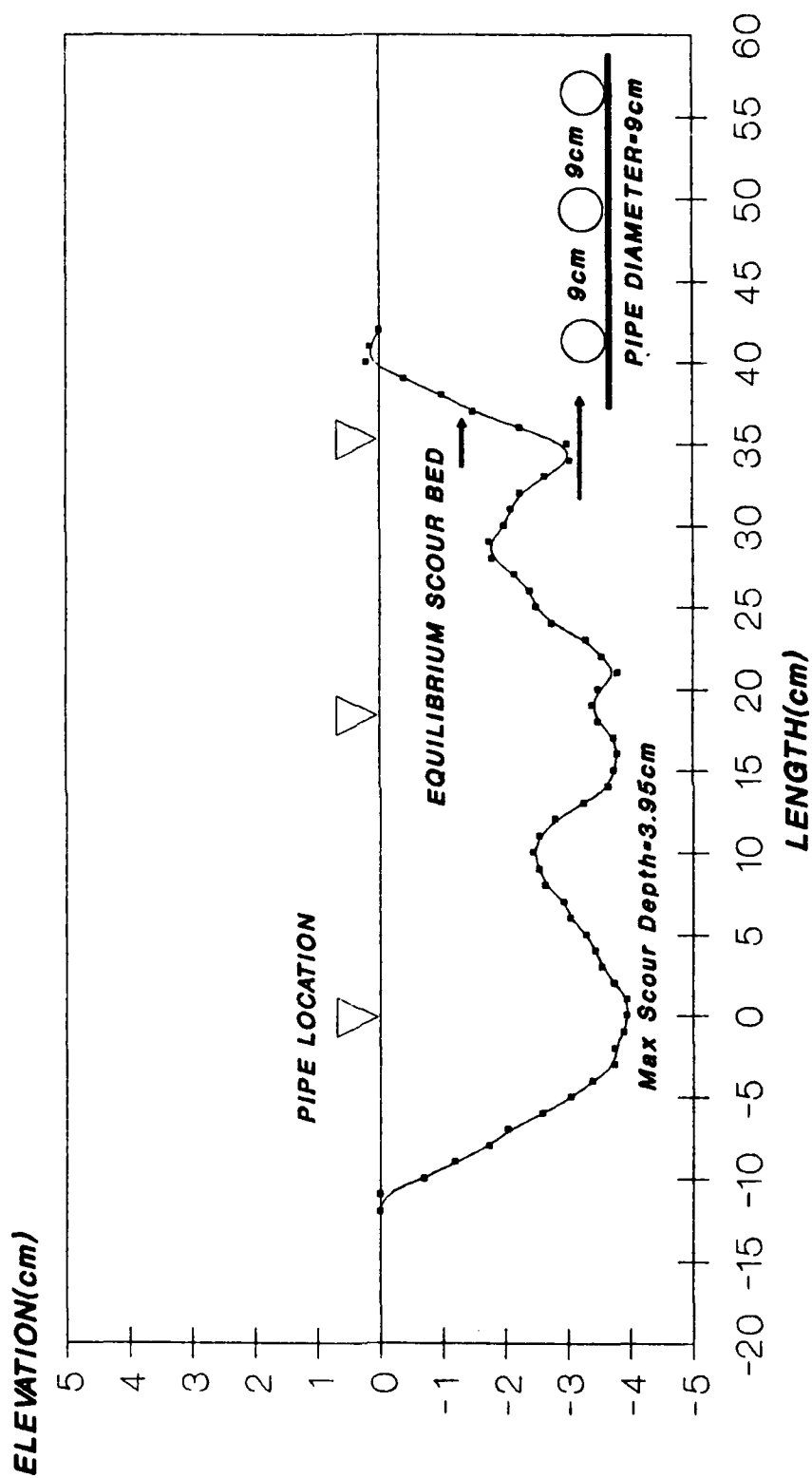
TEST No.39: CURRENT
U= 0.37m/sec

PIPE LOCATION

EQUILIBRIUM SCOUR BED

Max Scour Depth=4.4cm

4.5cm

4.5cm

PIPE DIAMETER=9cm

ELEVATION(cm)

LENGTH(cm)
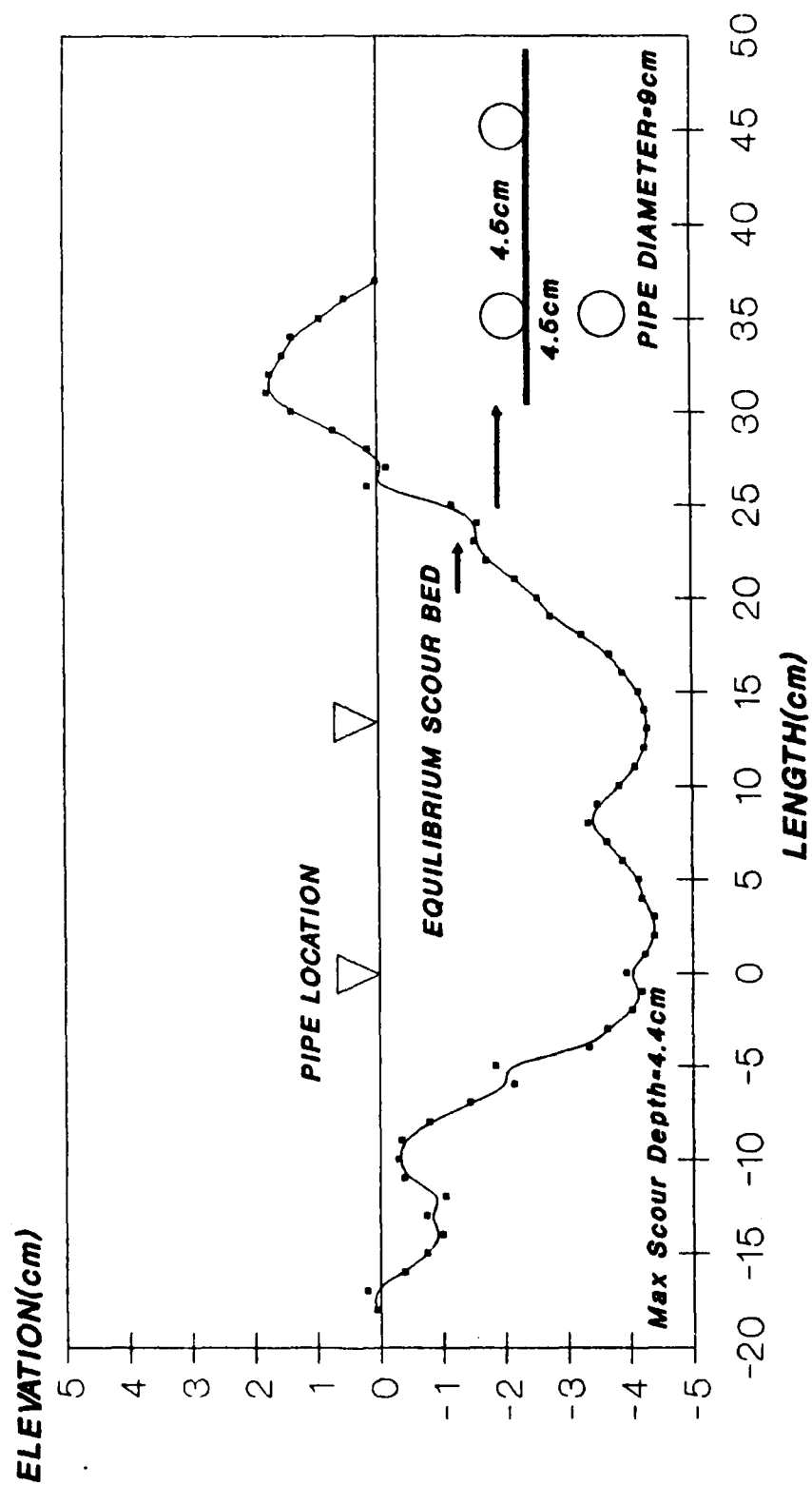
TEST No.40: CURRENT AND WAVE
U= 0.37m/sec, H= 6cm, T= 1.2sec, L= 1.0m
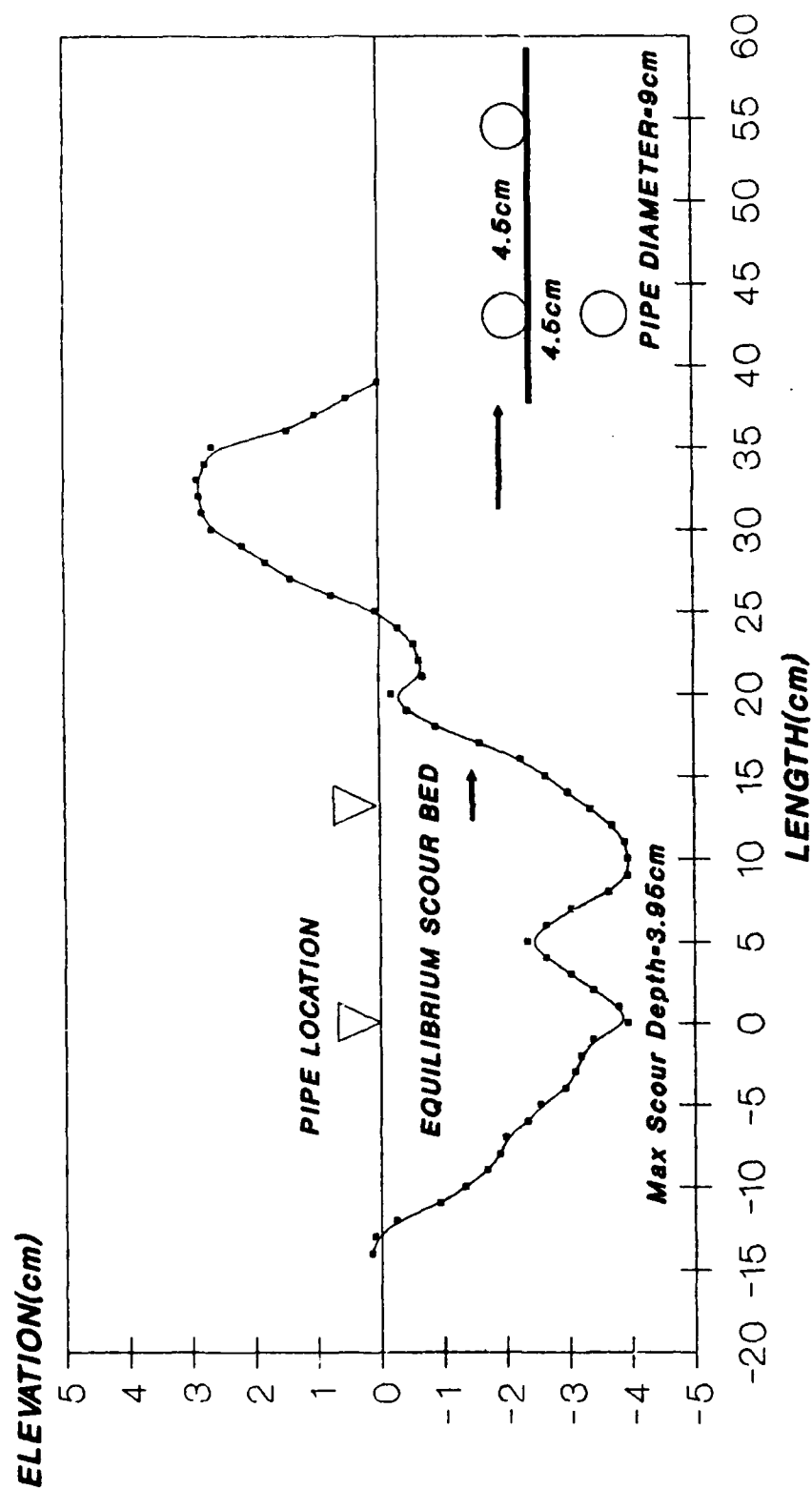
TEST No.41: CURRENT
U= 0.37m/sec
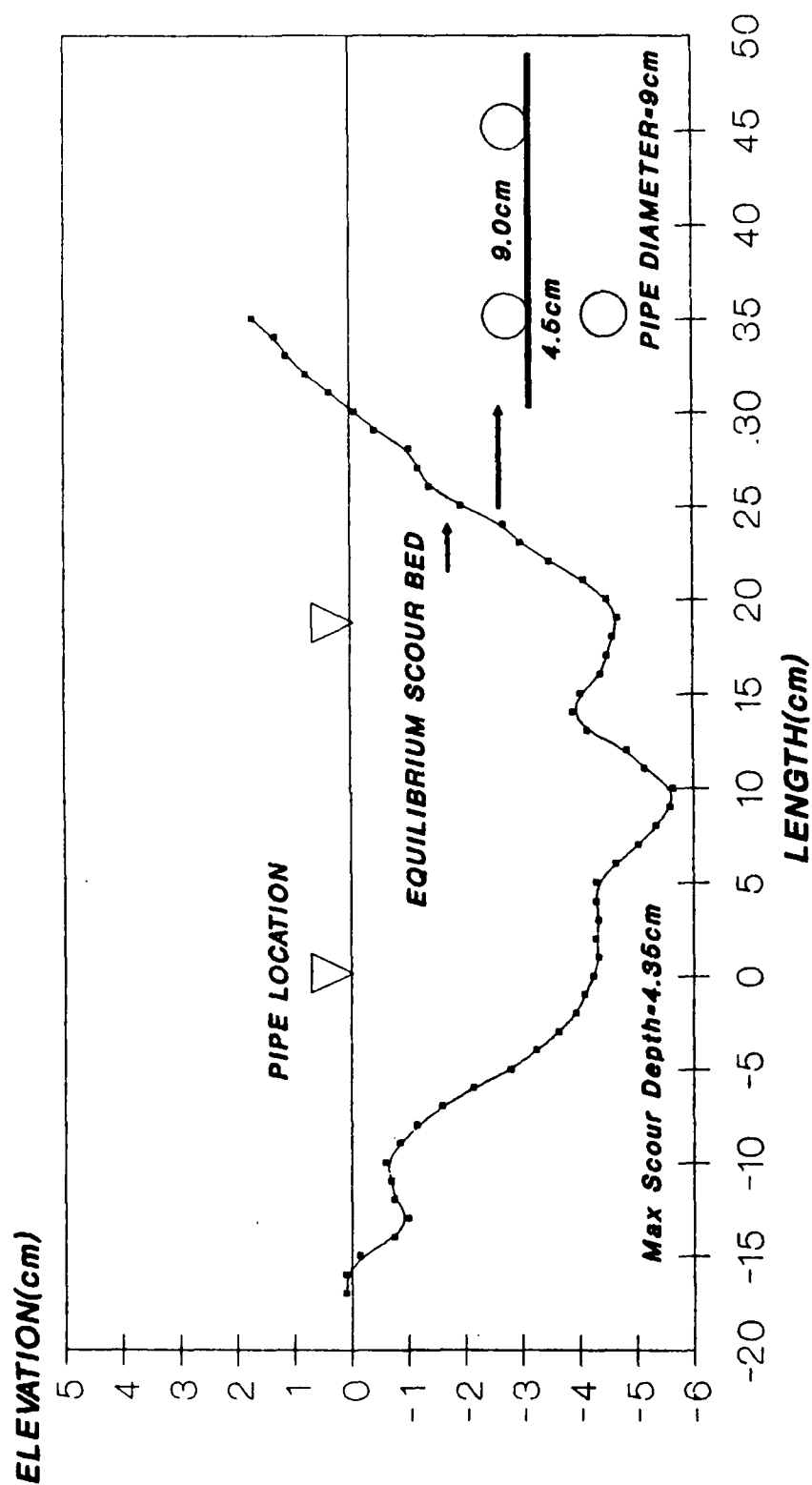
TEST No.42: CURRENT AND WAVE
U= 0.37m/sec, H= 6cm, T= 1.2sec, L= 1.0m

PIPE LOCATION

EQUILIBRIUM SCOUR BED

Max Scour Depth=4.05cm

9cm

4.5cm

PIPE DIAMETER=9cm

ELEVATION(cm)

LENGTH(cm)
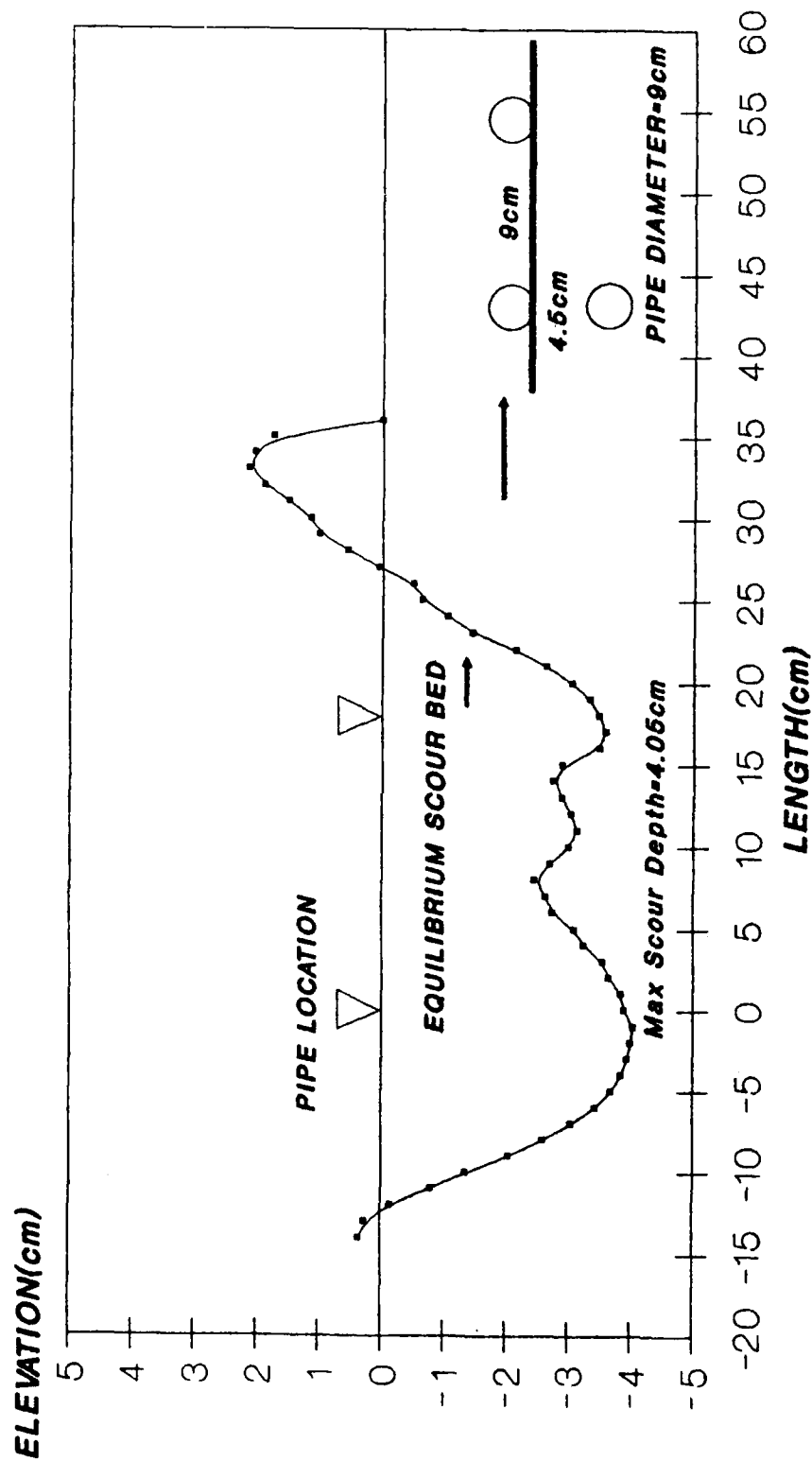
TEST No.43: CURRENT
U= 0.26m/sec

PIPE LOCATION

EQUILIBRIUM SCOUR BED

Max Scour Depth=1.55cm

PIPE DIAMETER=3cm

ELEVATION(cm)

LENGTH(cm)
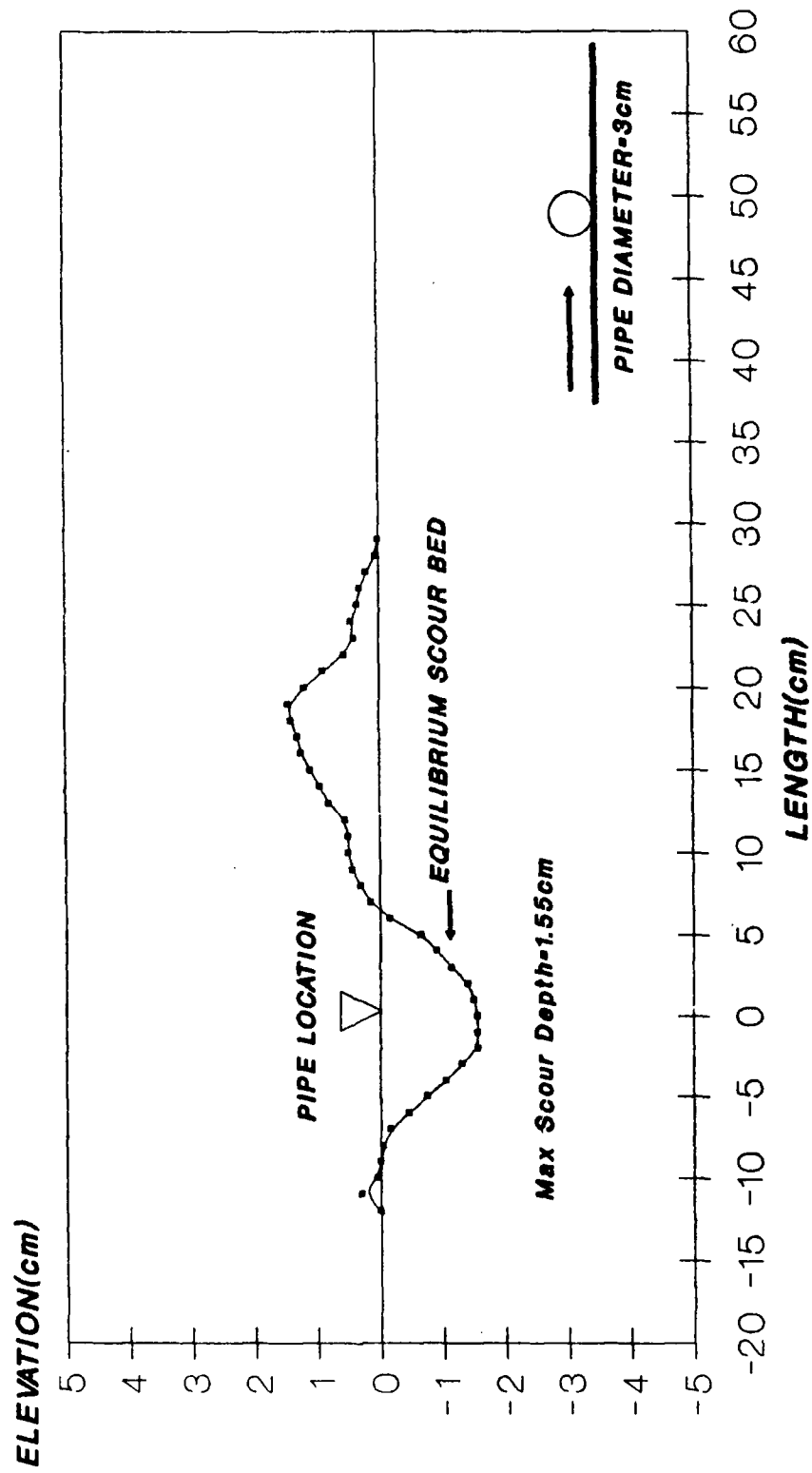
TEST No.44: CURRENT
U= 0.26m/sec

PIPE LOCATION

EQUILIBRIUM SCOUR BED

Max Scour Depth=1.20cm

PIPE DIAMETER=3cm

ELEVATION(cm)

LENGTH(cm)
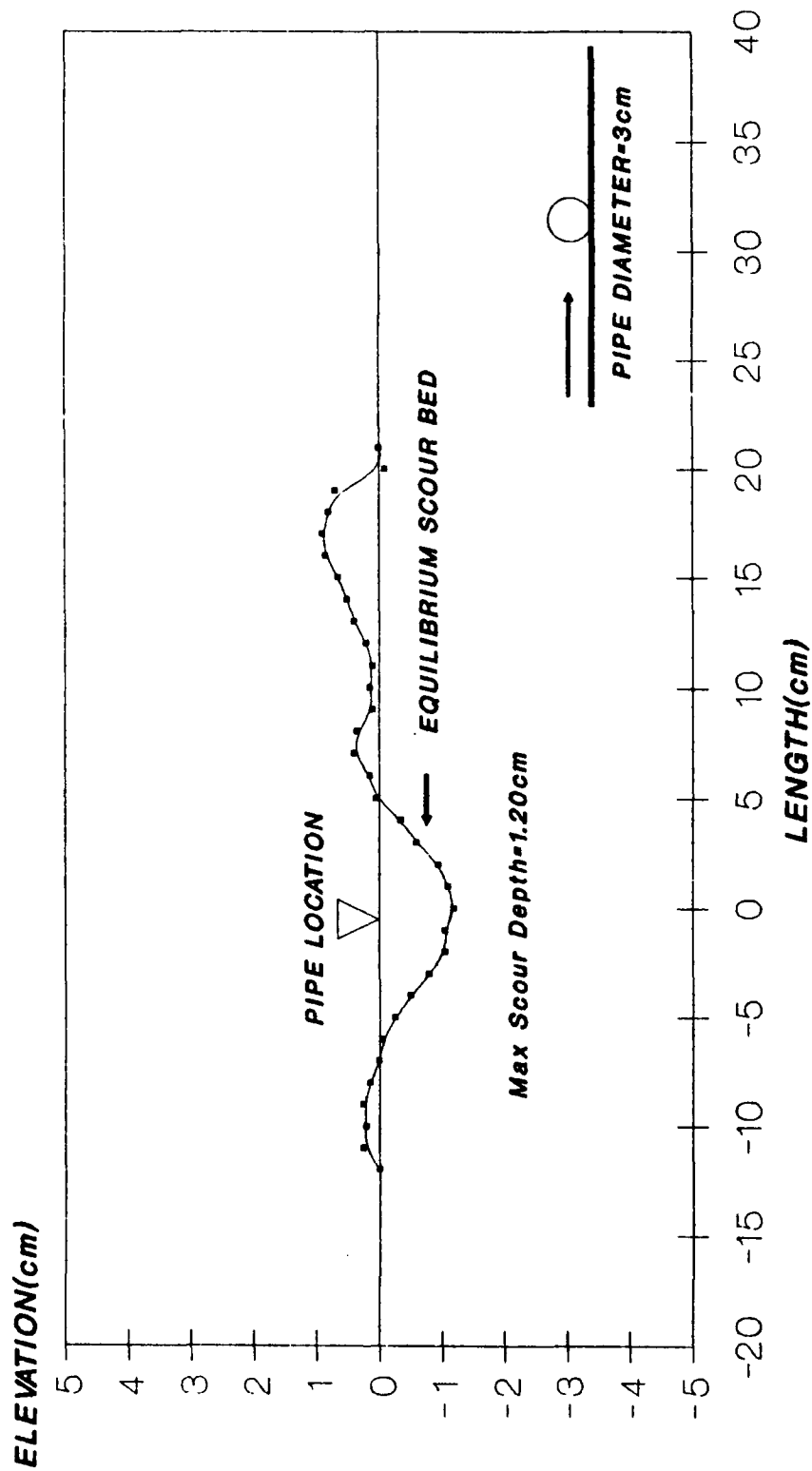
TEST No.45: CURRENT
U= 0.26m/sec
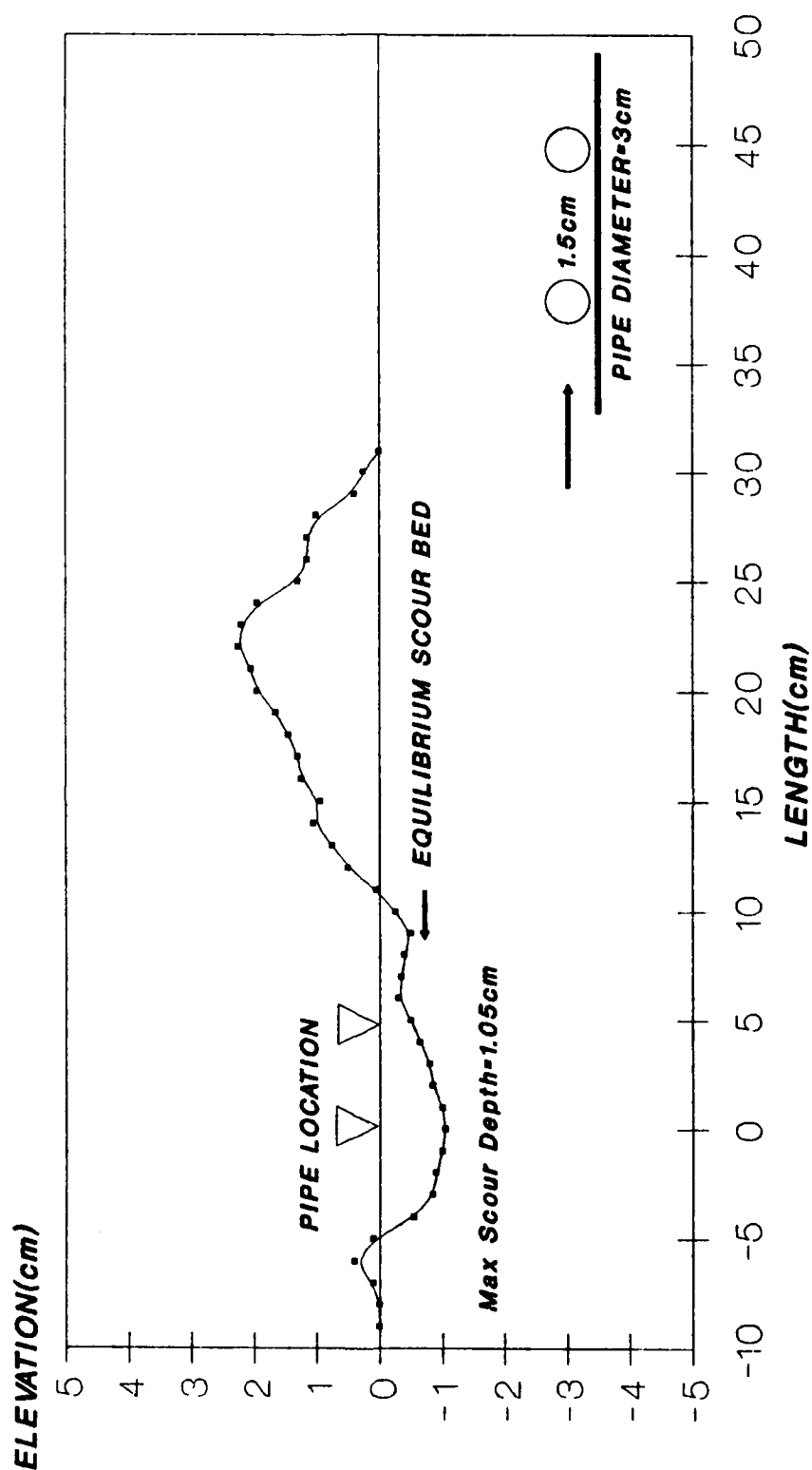
TEST No.46: CURRENT AND WAVE
U= 0.26m/sec, H= 6cm, T= 1.2sec, L= 1.0m
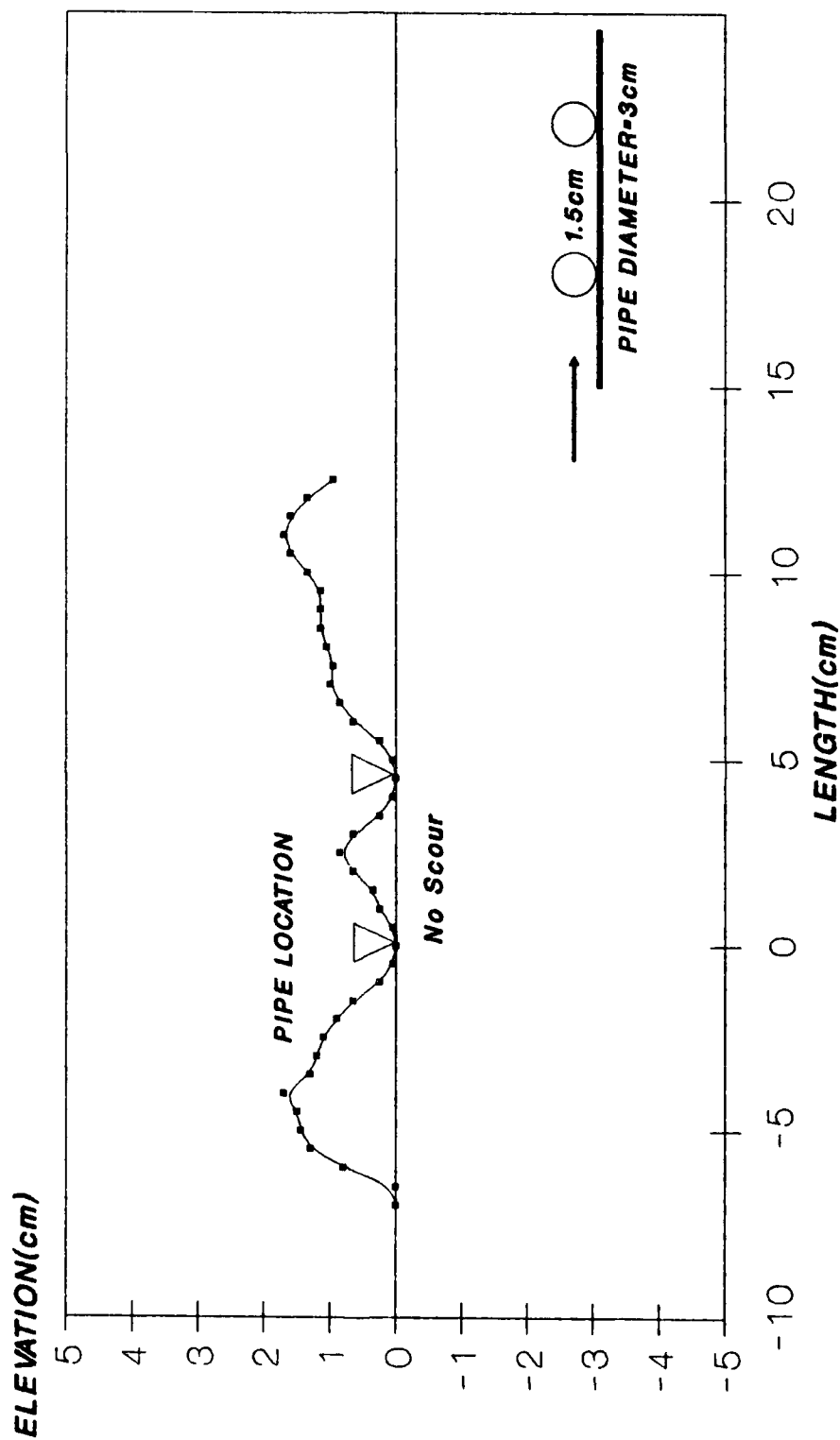
TEST No.47: CURRENT
U= 0.26m/sec

ELEVATION(cm)

PIPE LOCATION

EQUILIBRIUM SCOUR BED

Max Scour Depth=1.40cm

3cm

PIPE DIAMETER=3cm

LENGTH(cm)
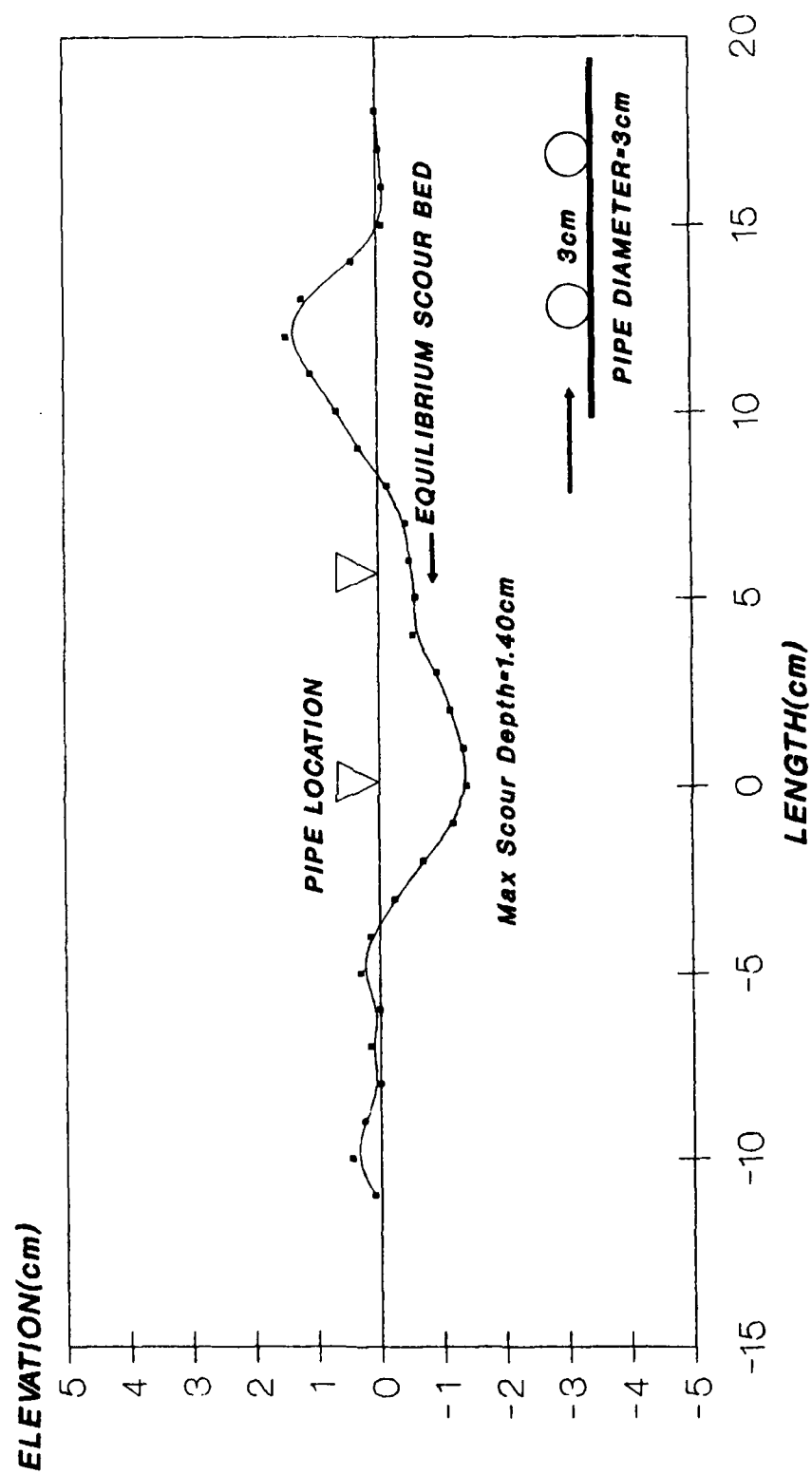
TEST No.48: CURRENT AND WAVE
U= 0.26m/sec, H= 6cm, T= 1.2sec, L= 1.0m

ELEVATION(cm)

PIPE LOCATION

No Scour, Pipes partially buried

3cm

PIPE DIAMETER=3cm

LENGTH(cm)
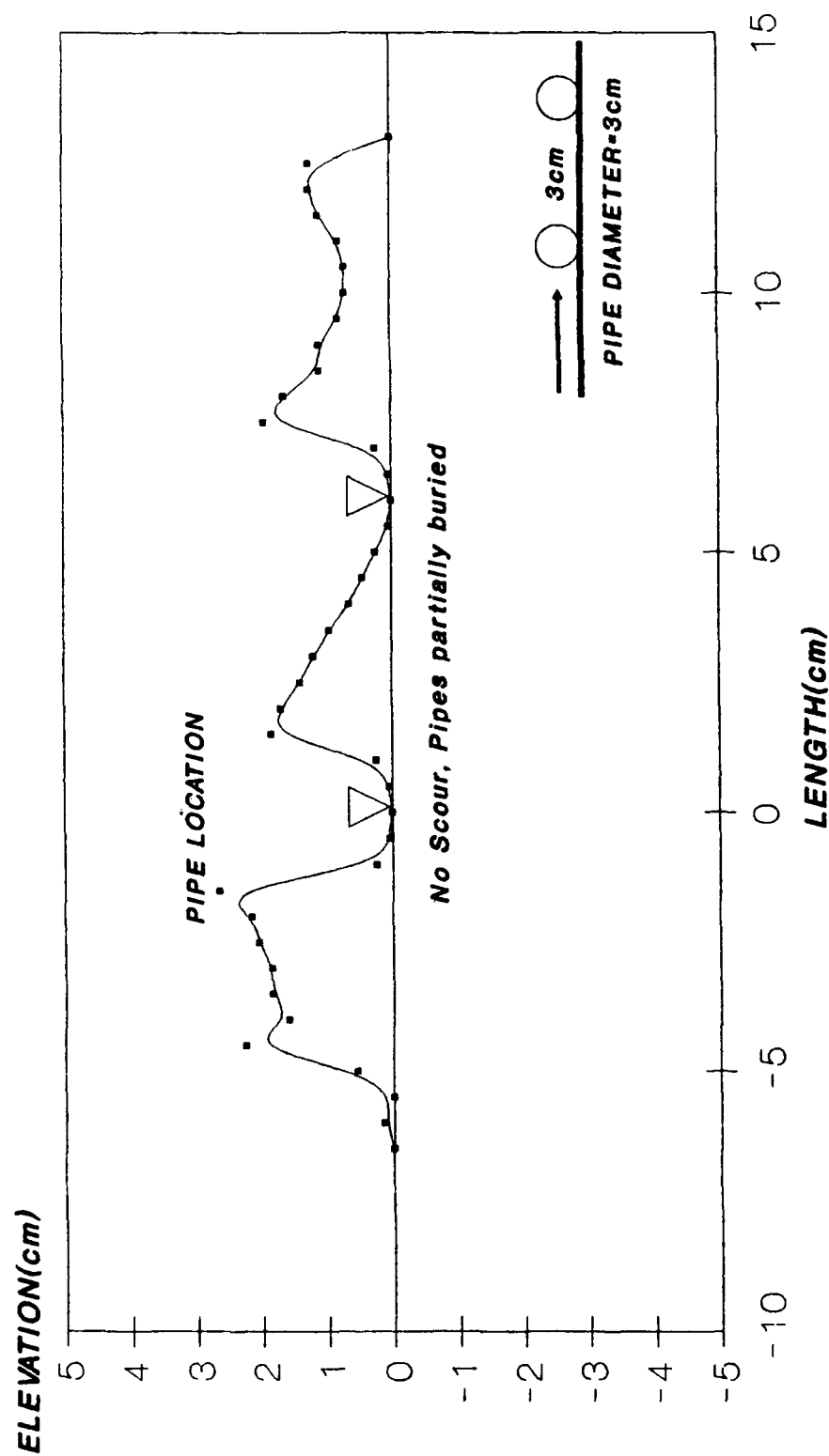
TEST No.49: CURRENT
U= 0.26m/sec

ELEVATION(cm)

PIPE LOCATION

EQUILIBRIUM SCOUR BED

Max Scour Depth=1.40cm

1.5cm 1.5cm 1.5cm

PIPE DIAMETER=3cm

LENGTH(cm)
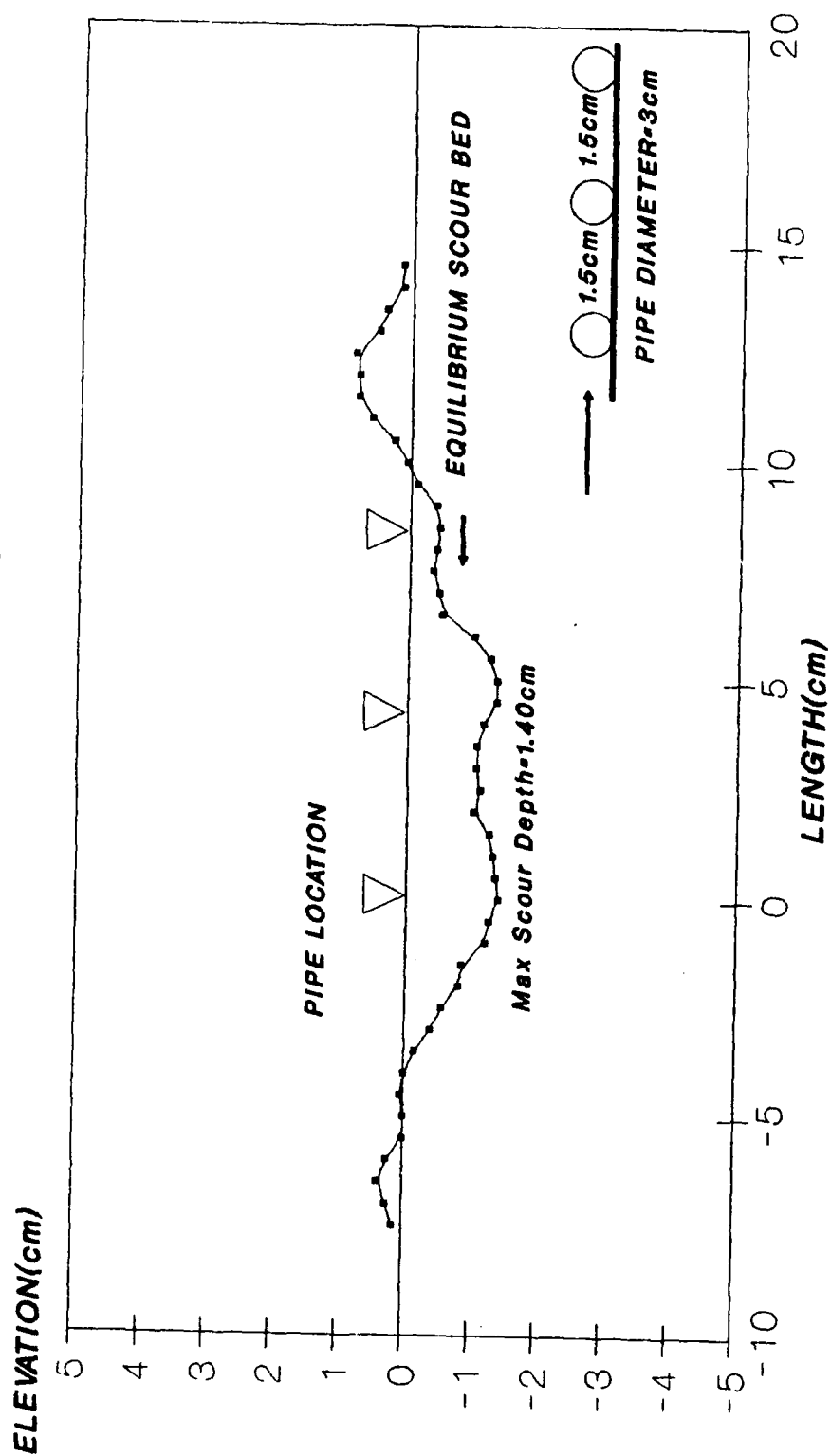
TEST No.50: CURRENT AND WAVE
U= 0.26m/sec, H= 6cm, T= 1.2sec, L= 1.0m
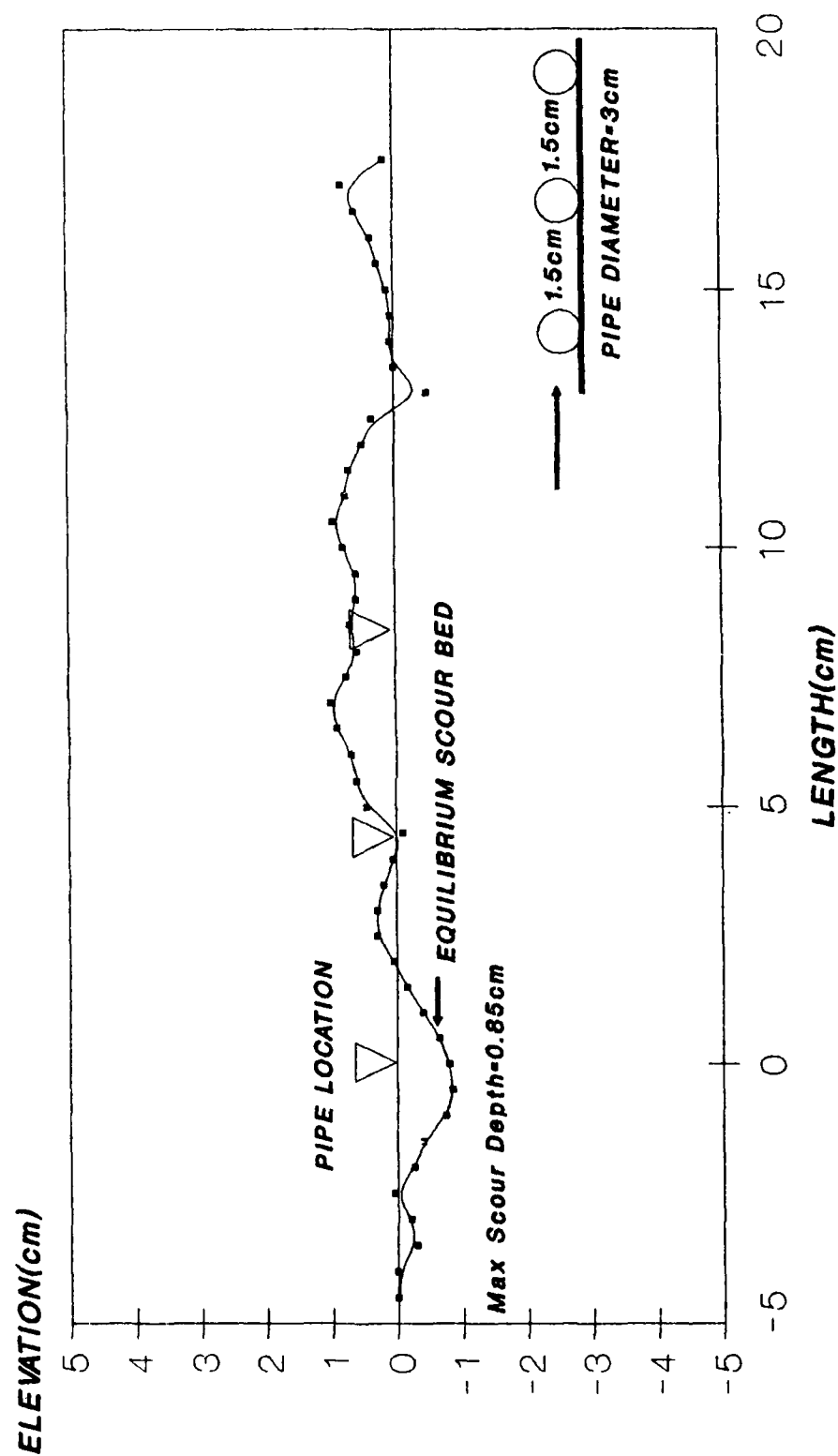
TEST No.51: CURRENT
U= 0.26m/sec
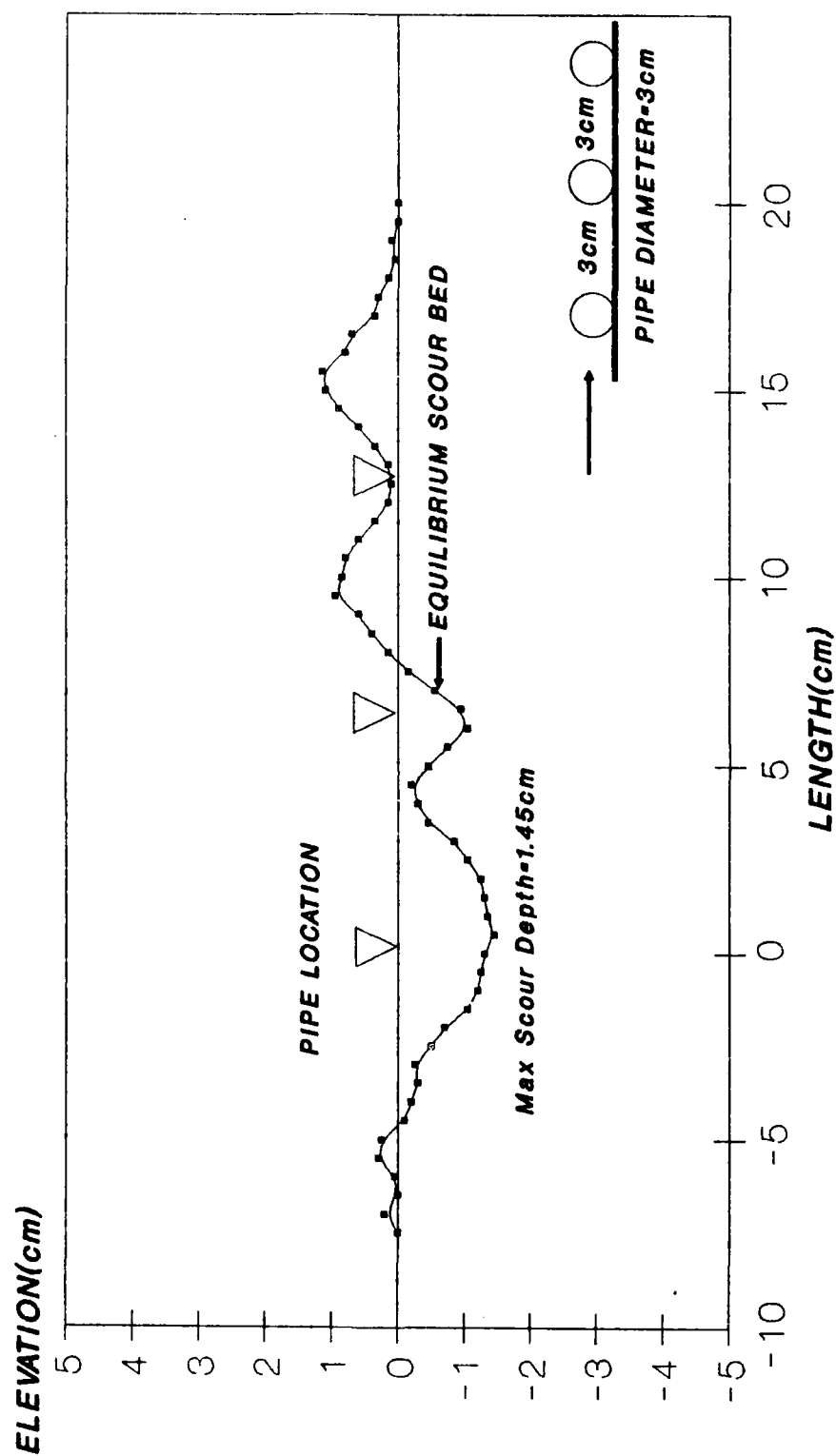
TEST No.52: CURRENT AND WAVE
U= 0.26m/sec, H= 6cm, T= 1.2sec, L= 1.0m
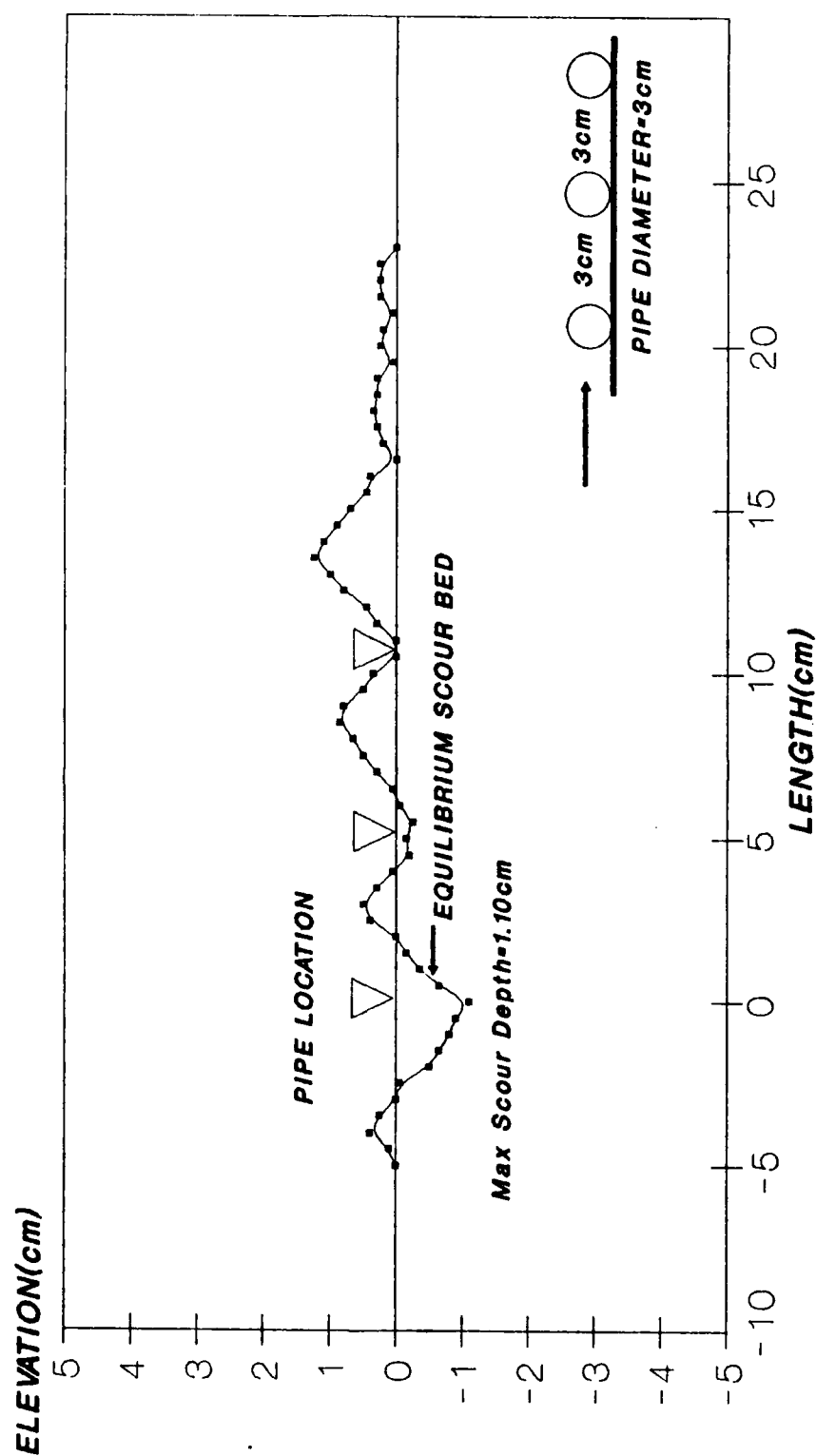
TEST No.53: CURRENT
U = 0.26m/sec

ELEVATION(cm)

PIPE LOCATION

EQUILIBRIUM SCOUR BED

Max Scour Depth=2.20cm

PIPE DIAMETER=6cm

LENGTH(cm)
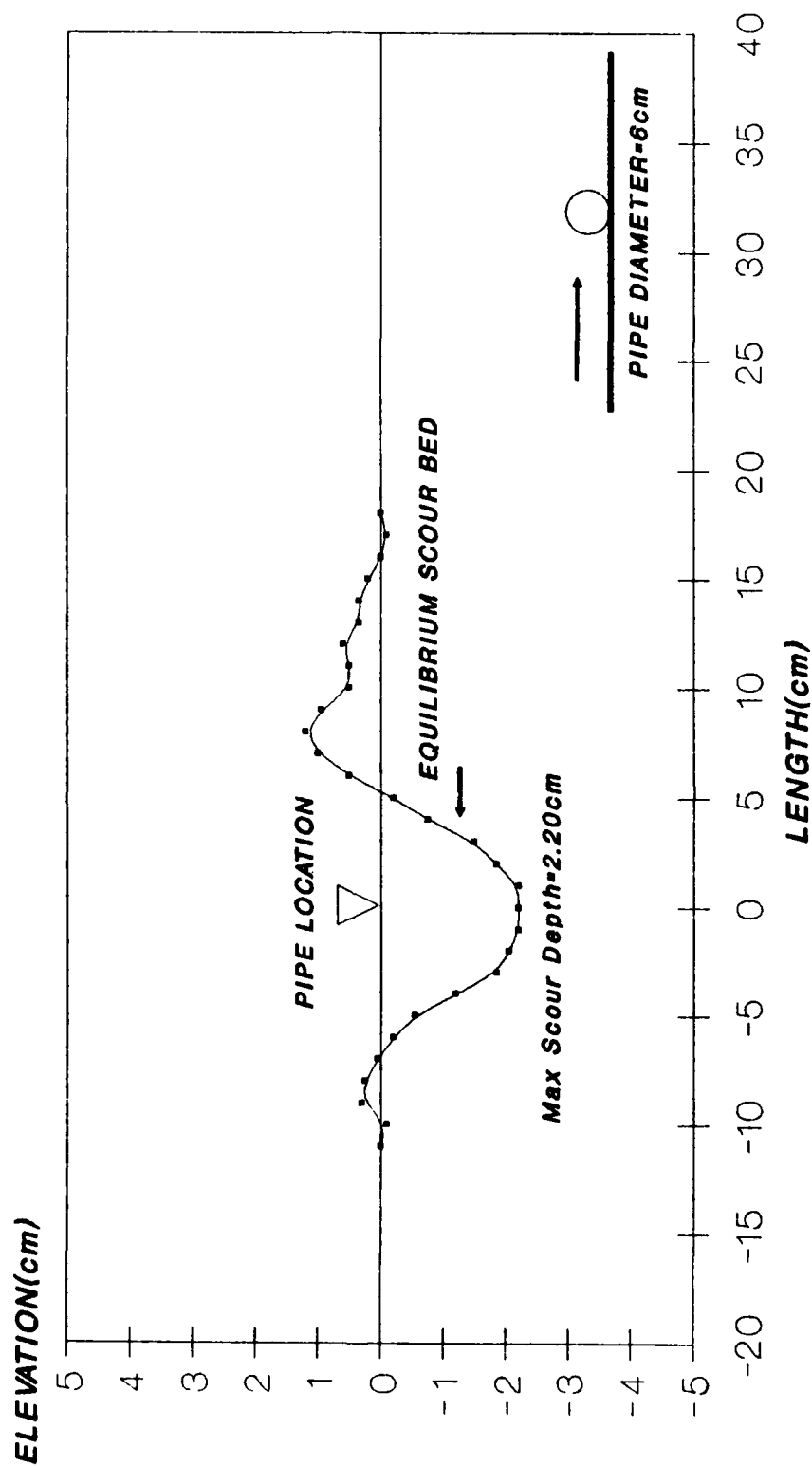
TEST No.54: CURRENT AND WAVE
U= 0.25m/sec, H= 6cm, T= 1.2sec, L= 1.0m

ELEVATION(cm)

PIPE LOCATION

EQUILIBRIUM SCOUR BED

Max Scour Depth=2.00cm

PIPE DIAMETER=6cm

LENGTH(cm)
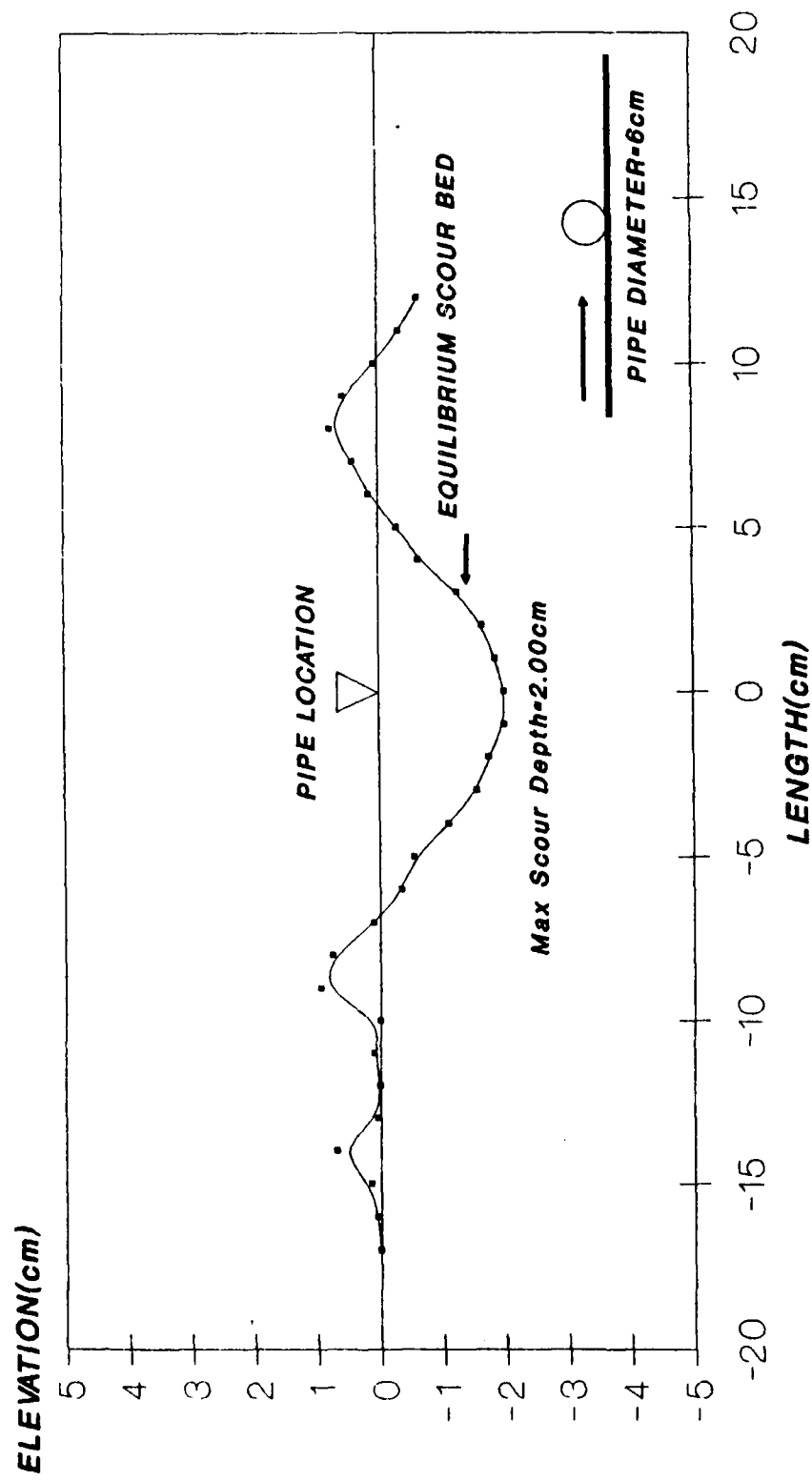
TEST No.55: CURRENT
U= 0.26m/sec
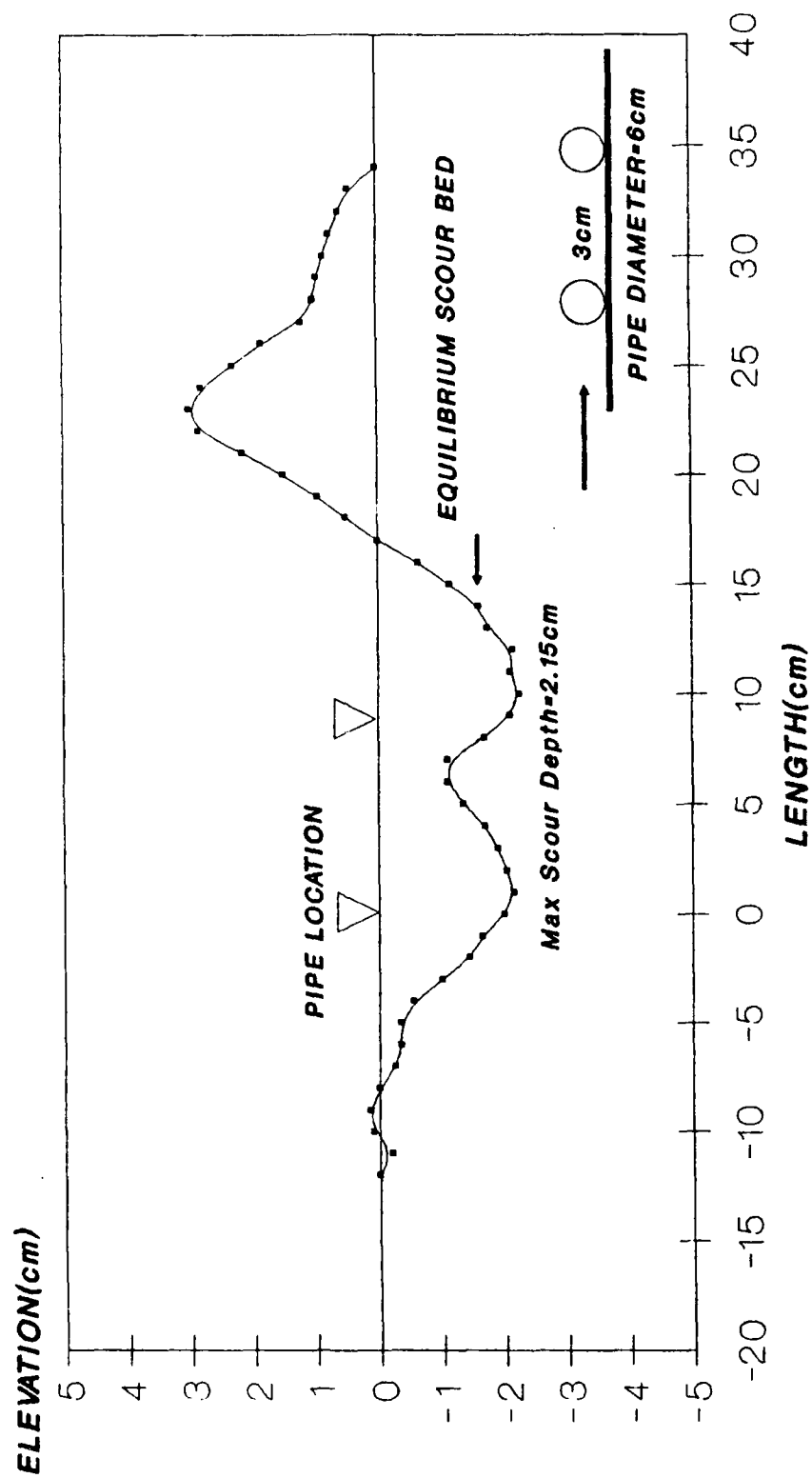
TEST No.56: CURRENT AND WAVE
U= 0.26m/sec, H= 6cm, T= 1.2sec, L= 1.0m
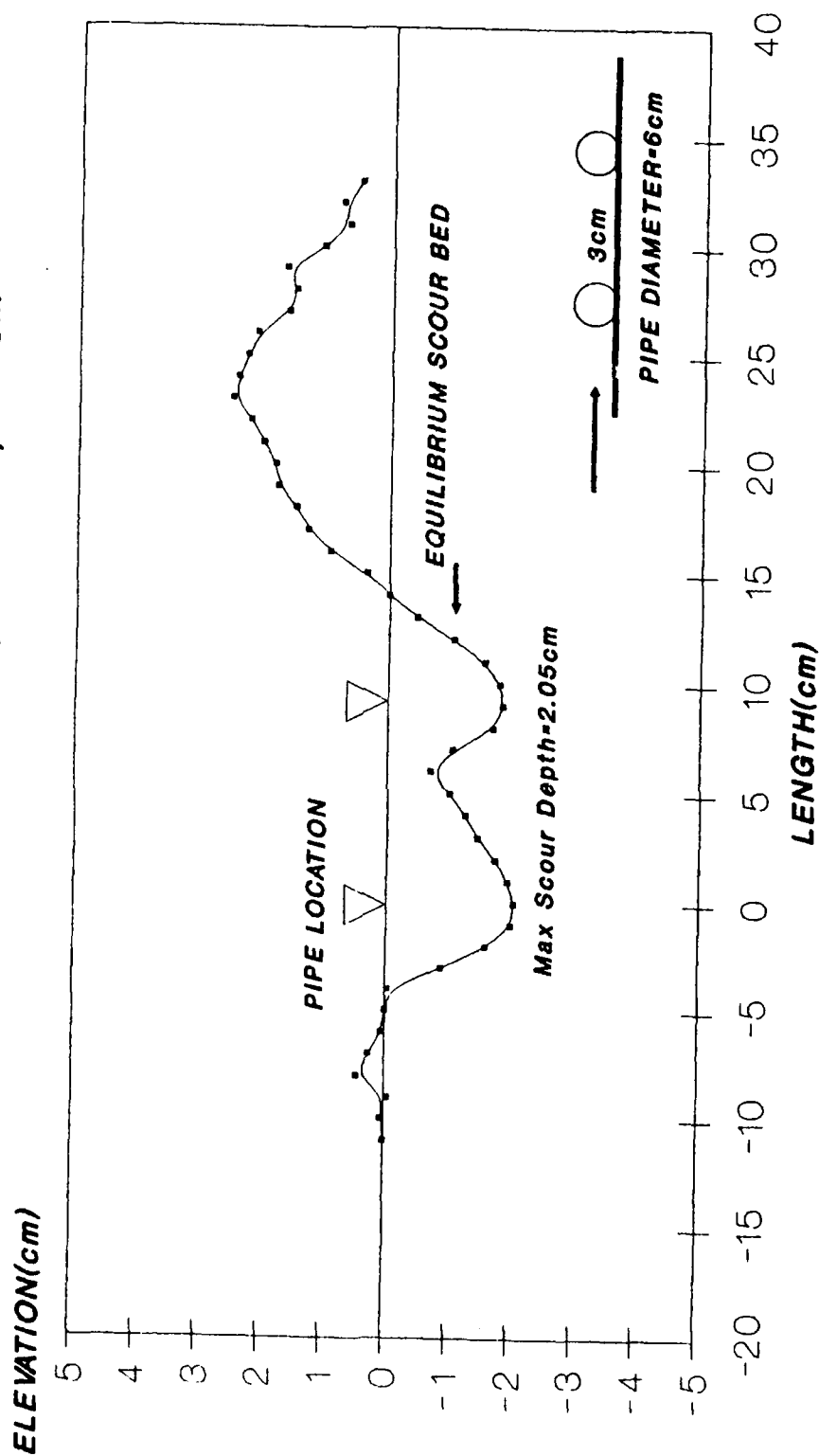
TEST No.57: CURRENT
U= 0.26m/sec

144
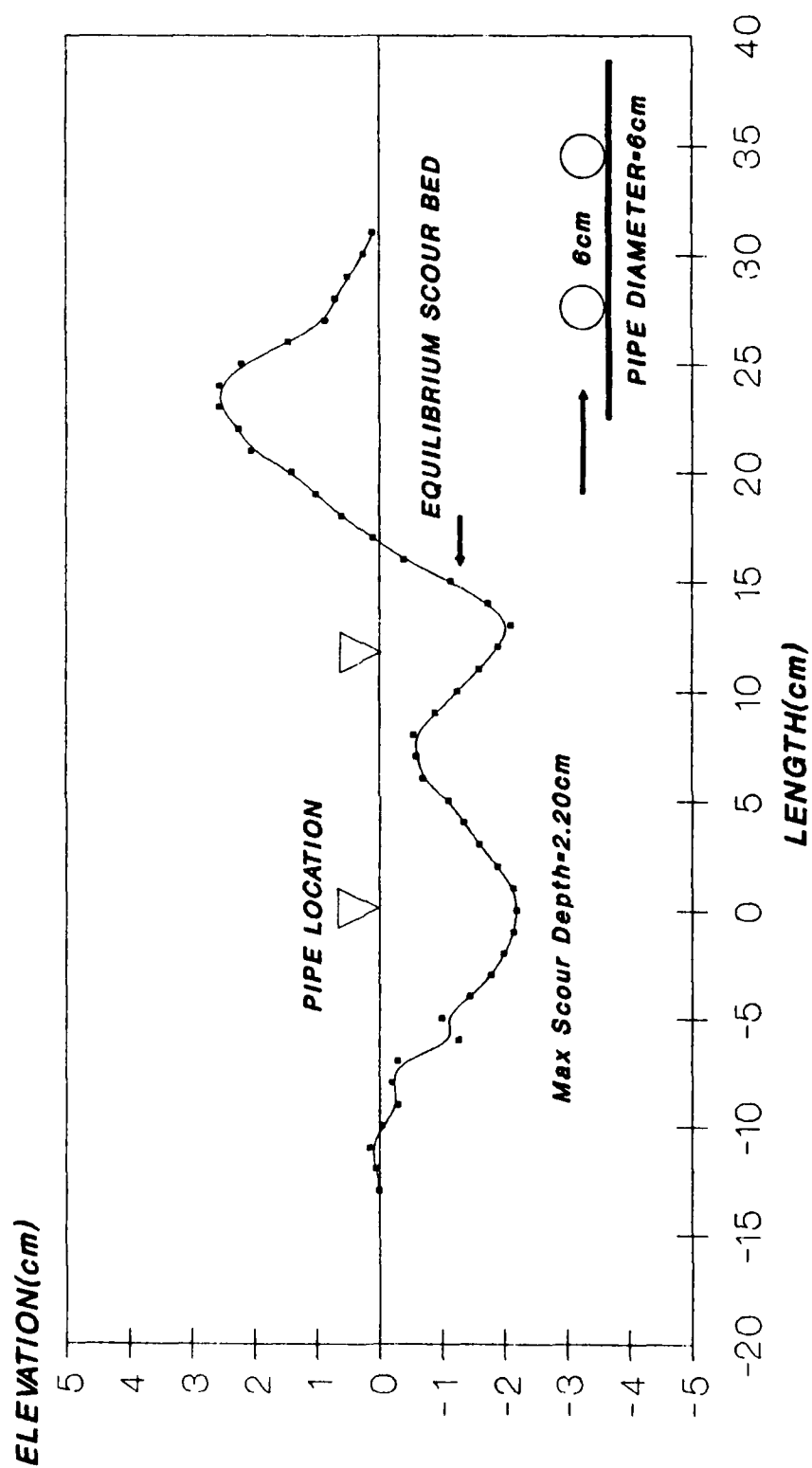
TEST No.58: CURRENT AND WAVE
U= 0.26m/sec, H= 6cm, T= 1.2sec, L= 1.0m

PIPE LOCATION

EQUILIBRIUM SCOUR BED

Max Scour Depth=2.30cm

6cm

PIPE DIAMETER=6cm

ELEVATION(cm)

LENGTH(cm)
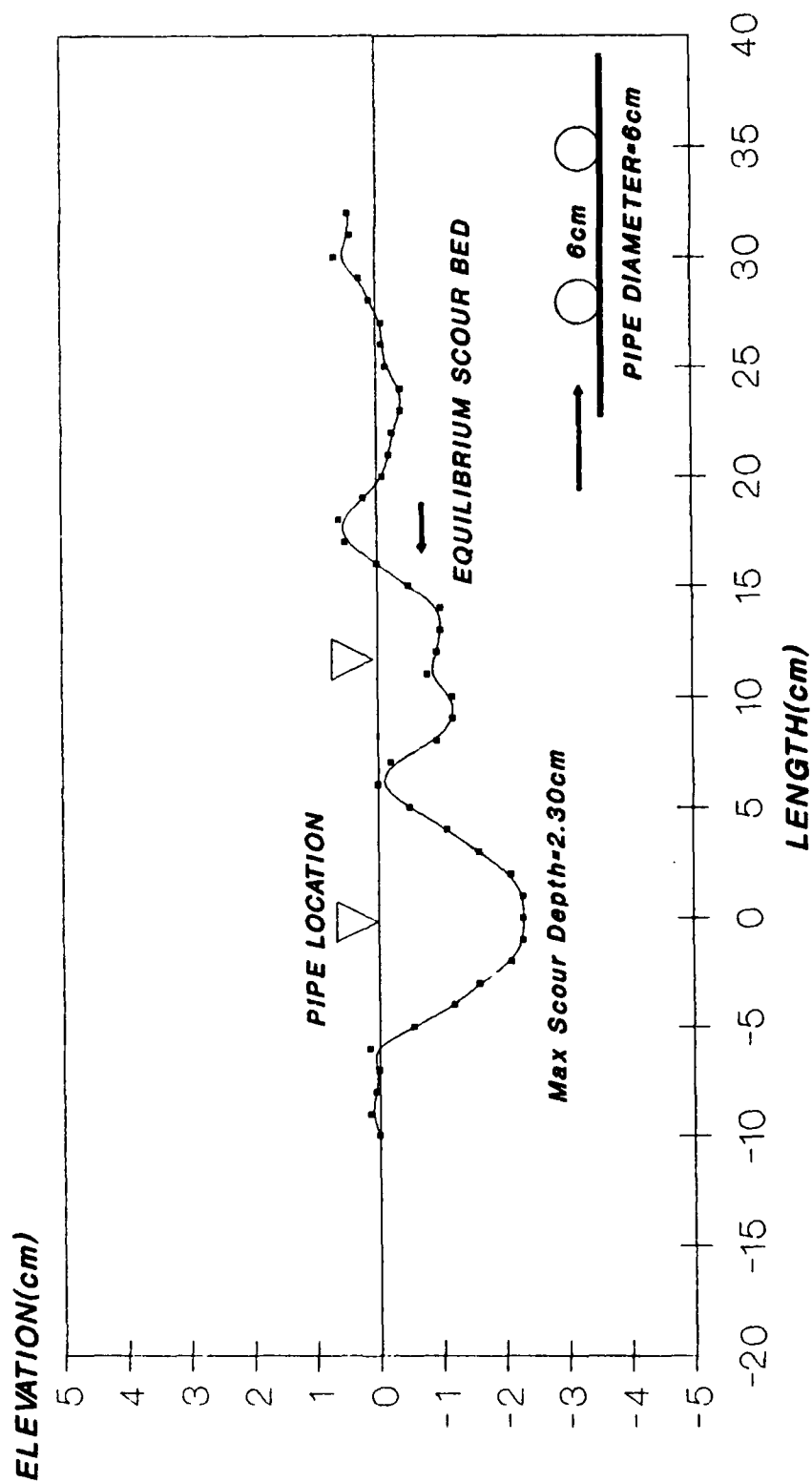
TEST No.59: CURRENT
U= 0.26m/sec
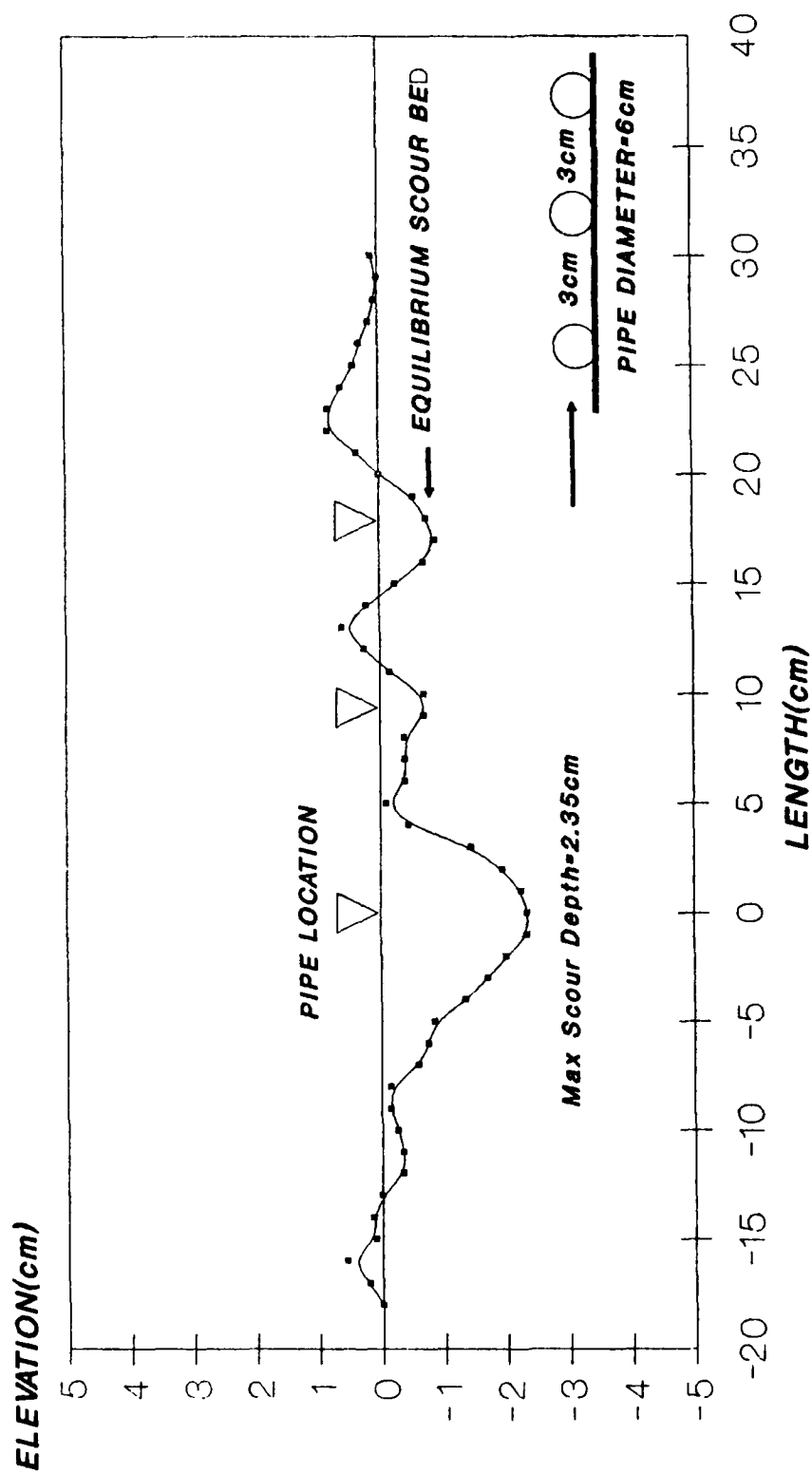
TEST No.60: CURRENT AND WAVE
U= 0.26m/sec, H= 6cm, T= 1.2sec, L= 1.0m
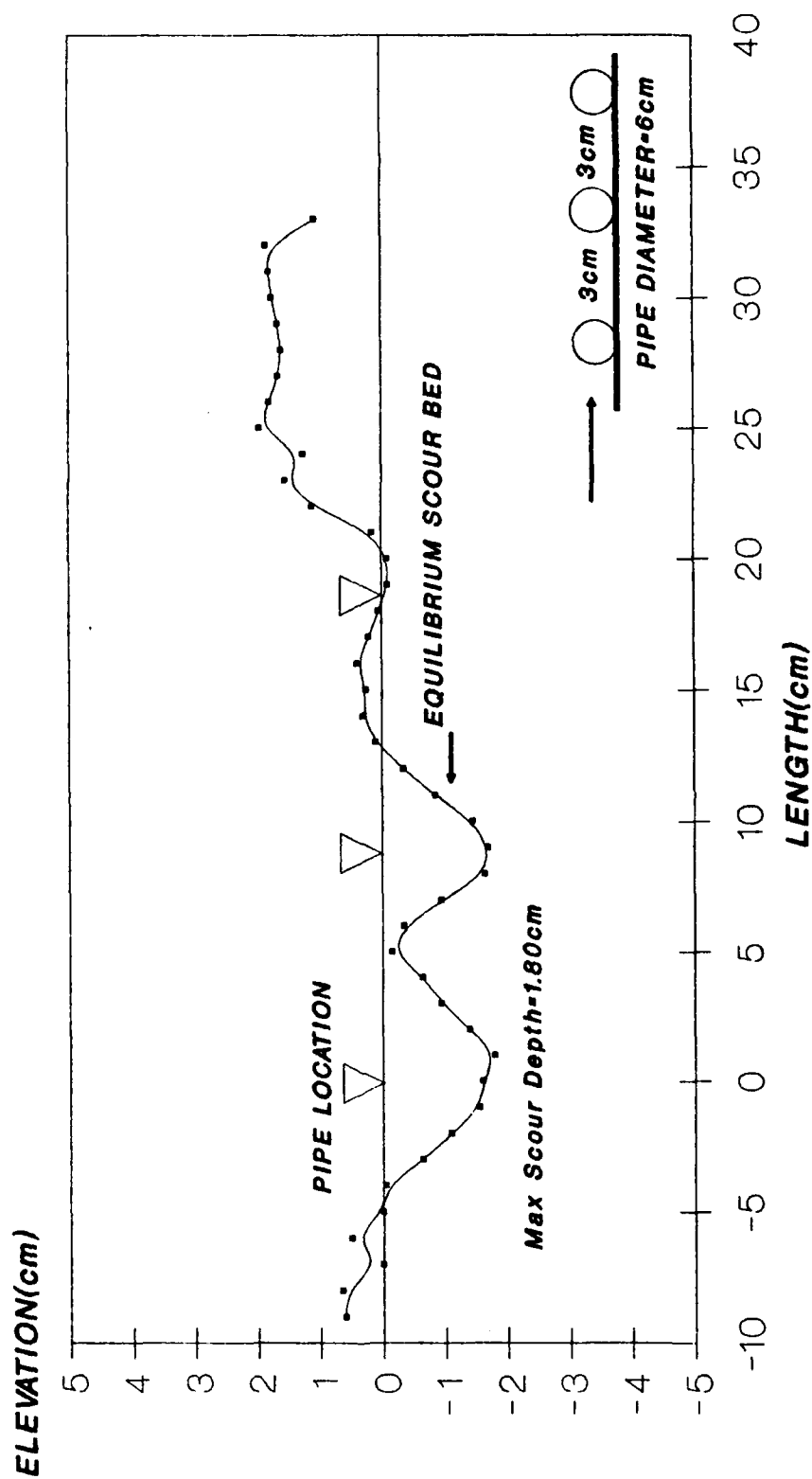
TEST No.61: CURRENT
U= 0.26m/sec
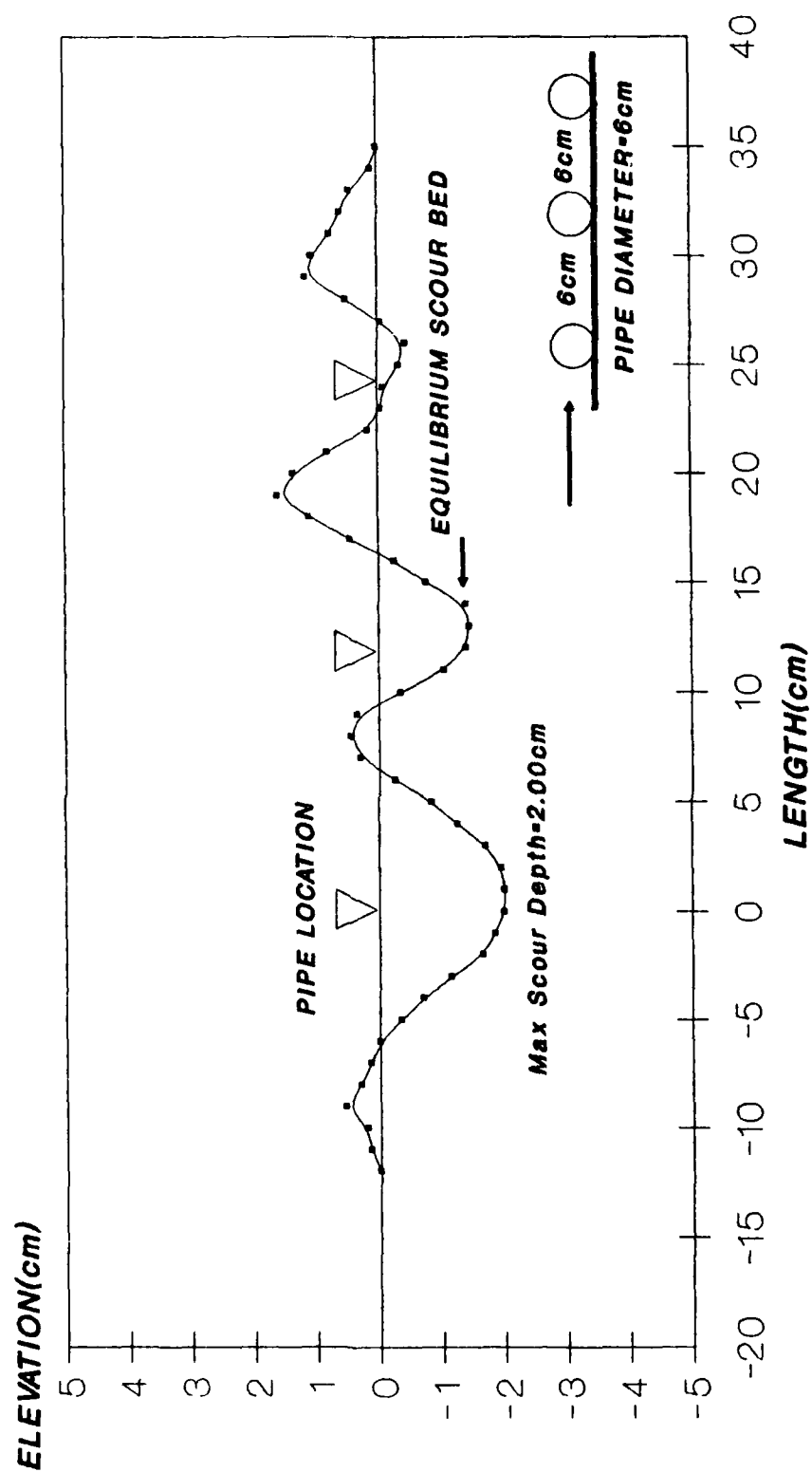
TEST No.62: CURRENT AND WAVE
U= 0.26m/sec, H= 6cm, T= 1.2sec, L= 1.0m
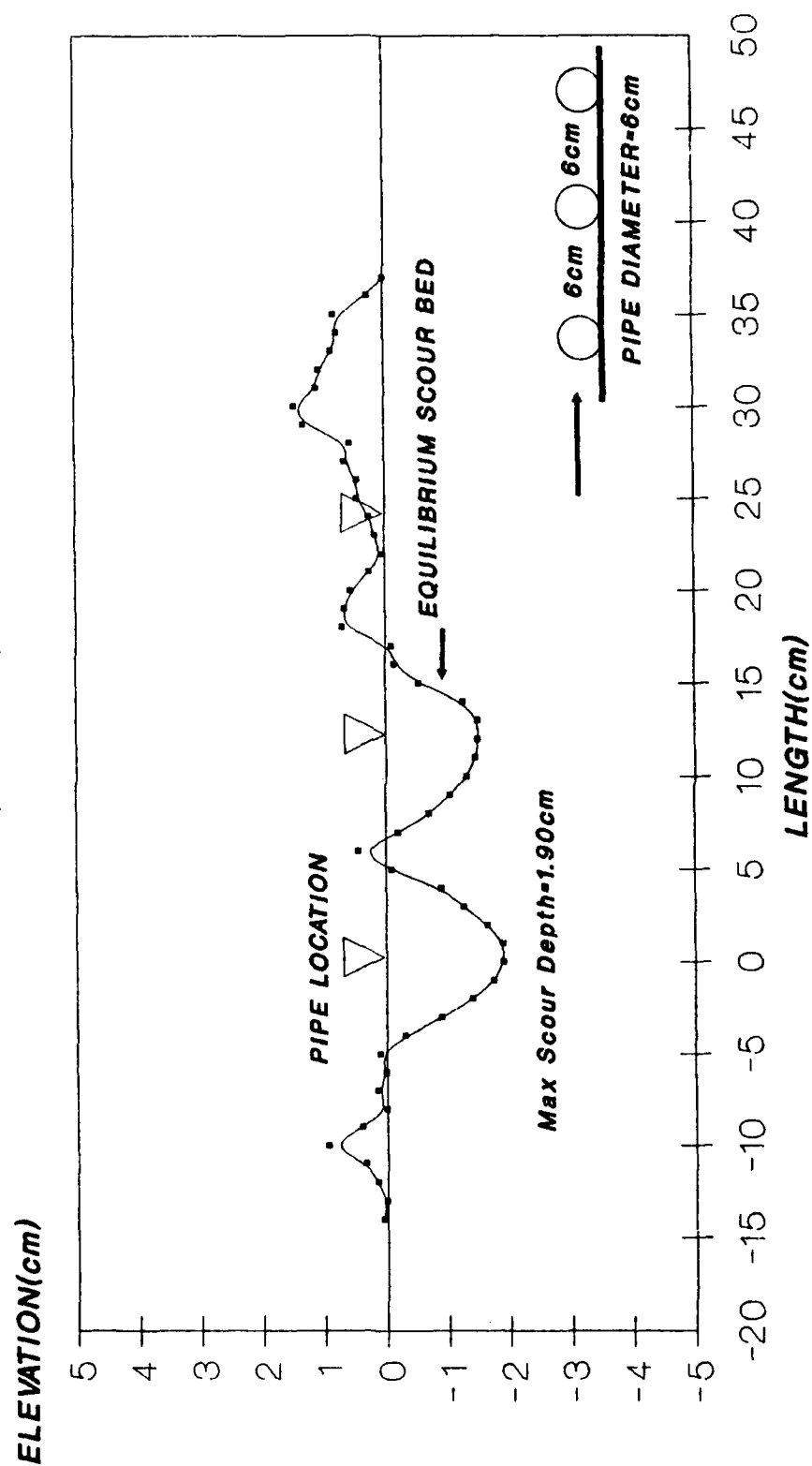
TEST No.63: CURRENT
U= 0.26m/sec
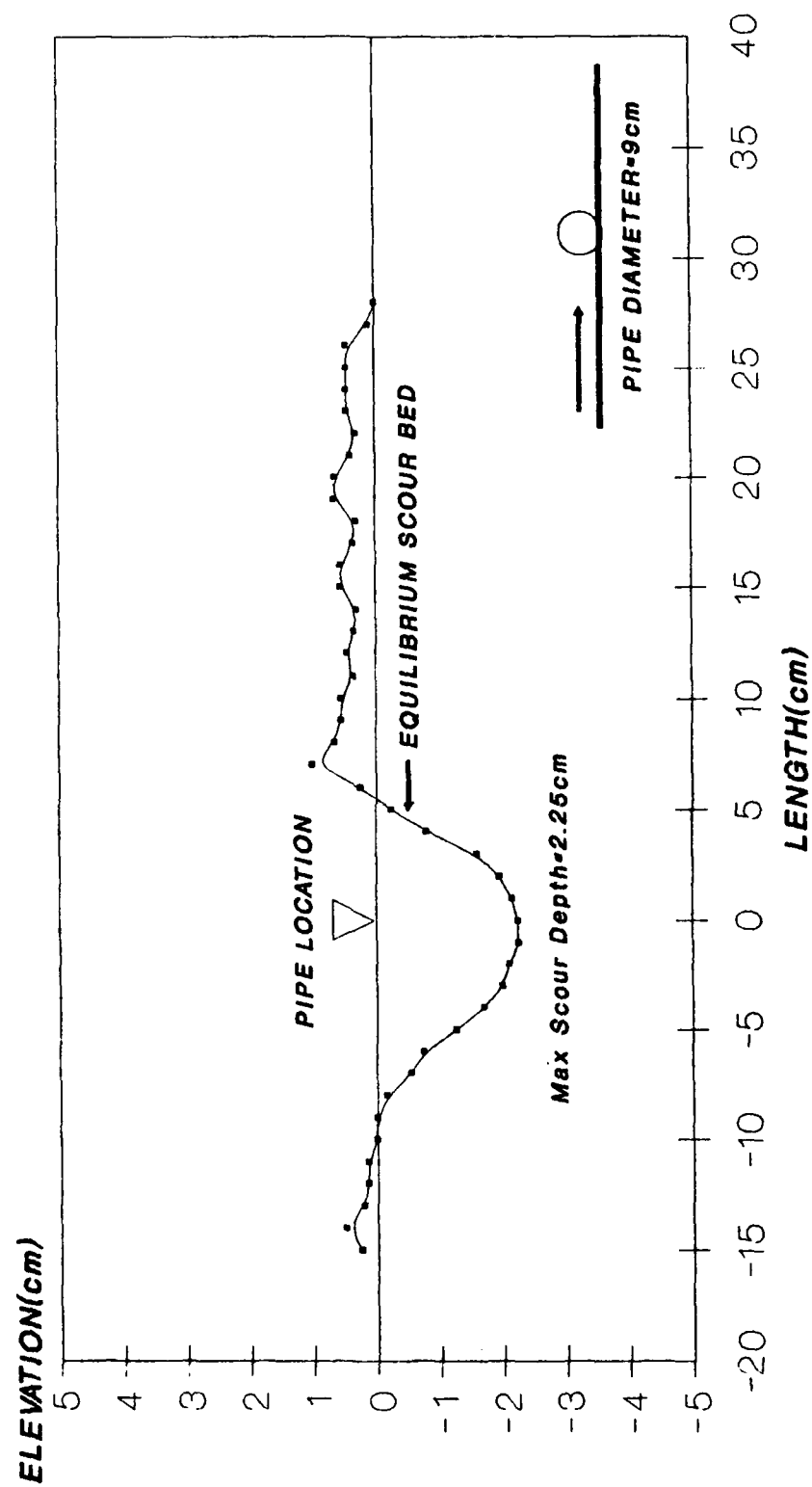
TEST No.64: CURRENT AND WAVE
U= 0.26m/sec, H= 6cm, T= 1.2sec, L= 1.0m

PIPE LOCATION

EQUILIBRIUM SCOUR BED

Max Scour Depth=2.00cm

PIPE DIAMETER=9cm

ELEVATION(cm)

LENGTH(cm)
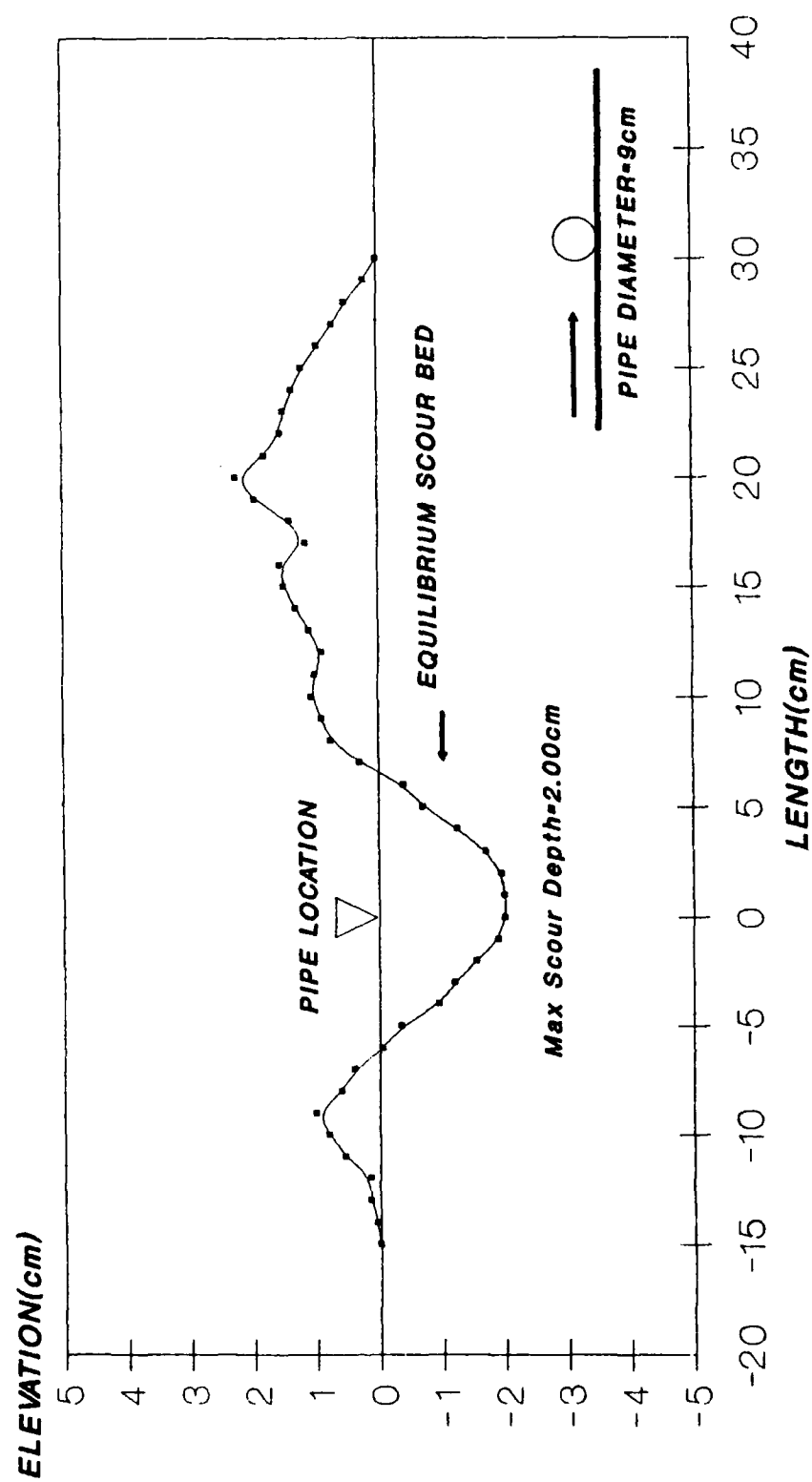
TEST No.65: CURRENT
U= 0.26m/sec
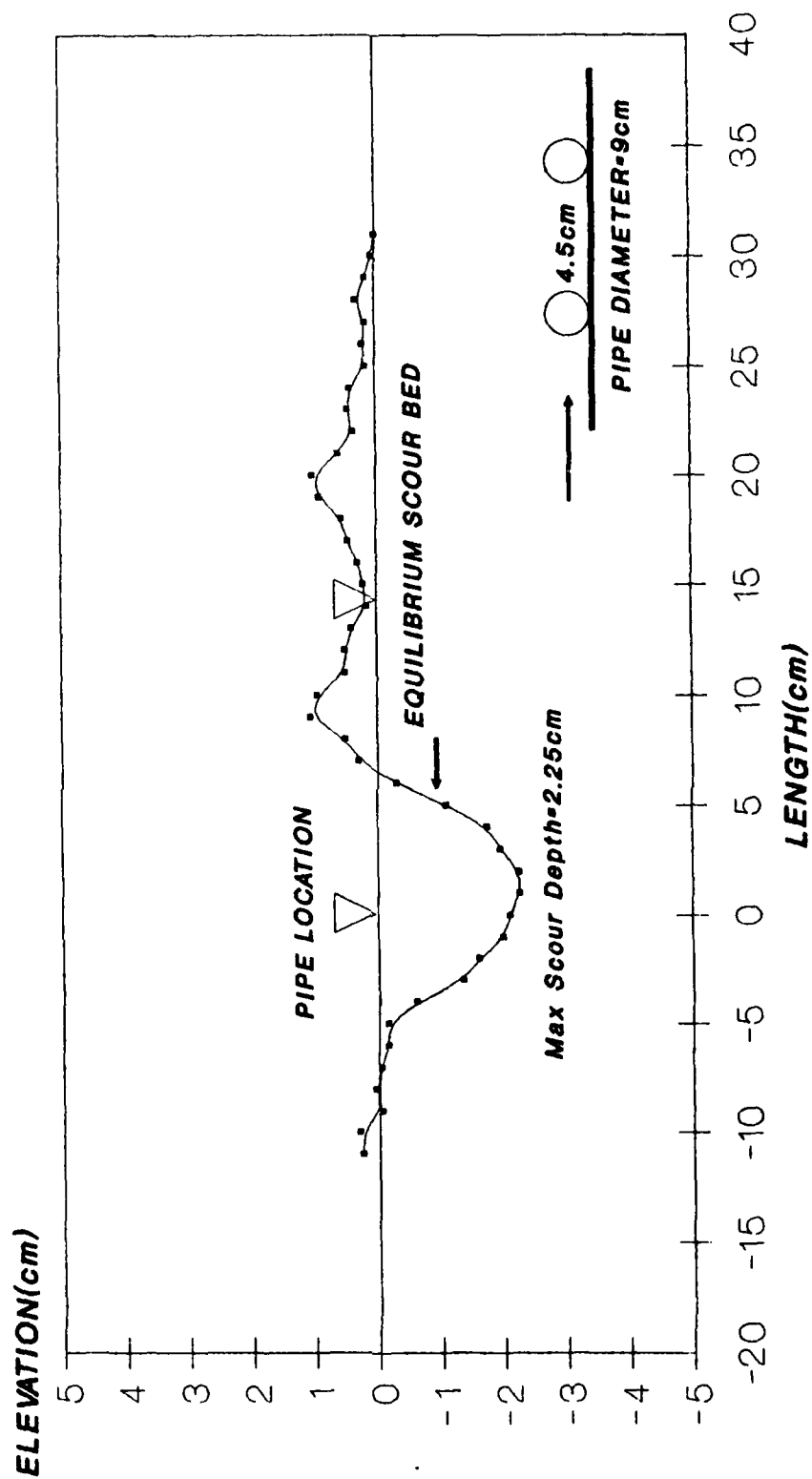
TEST No.66: CURRENT AND WAVE
U= 0.26m/sec, H= 6cm, T= 1.2sec, L= 1.0m
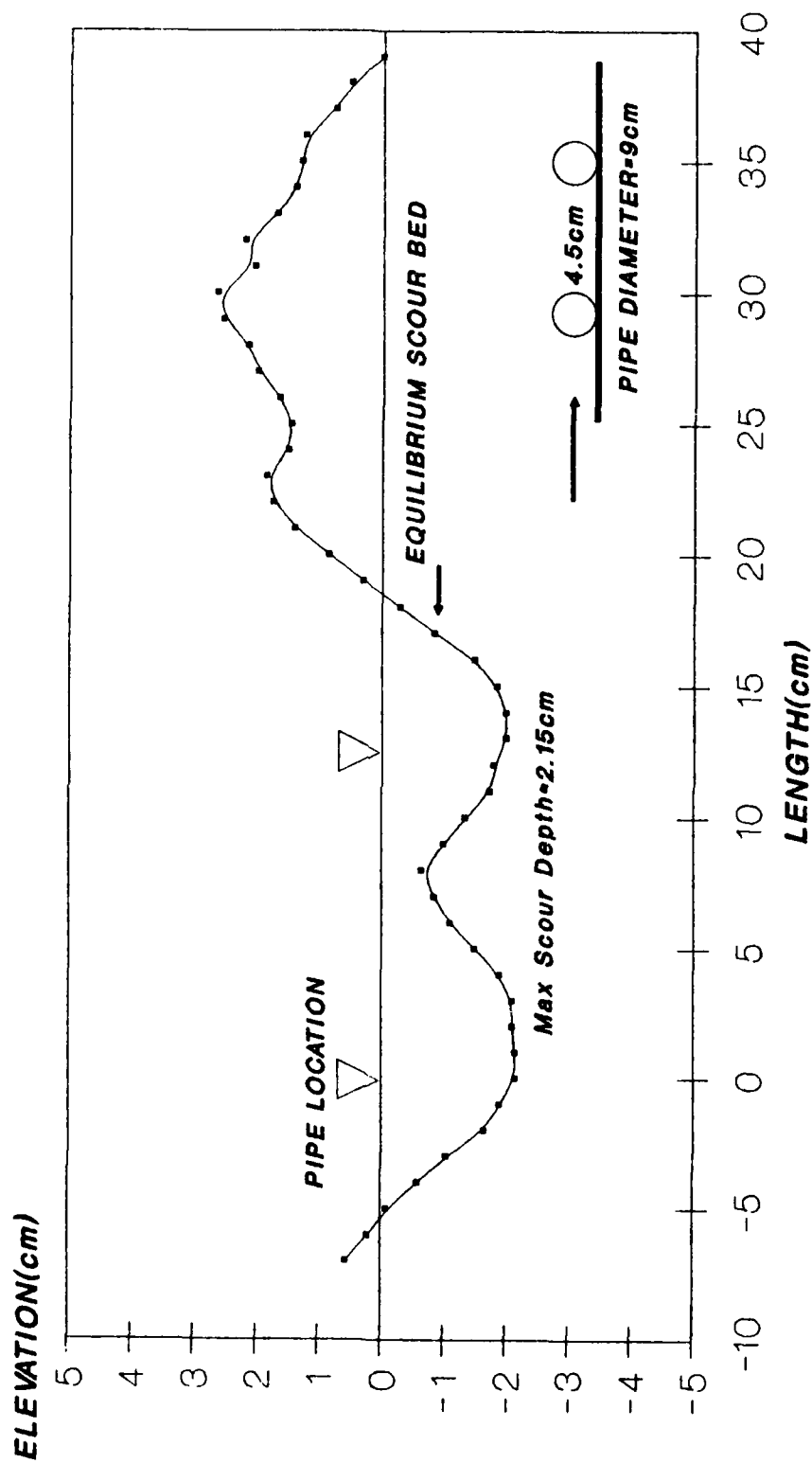
TEST No.67: CURRENT
U= 0.26m/sec
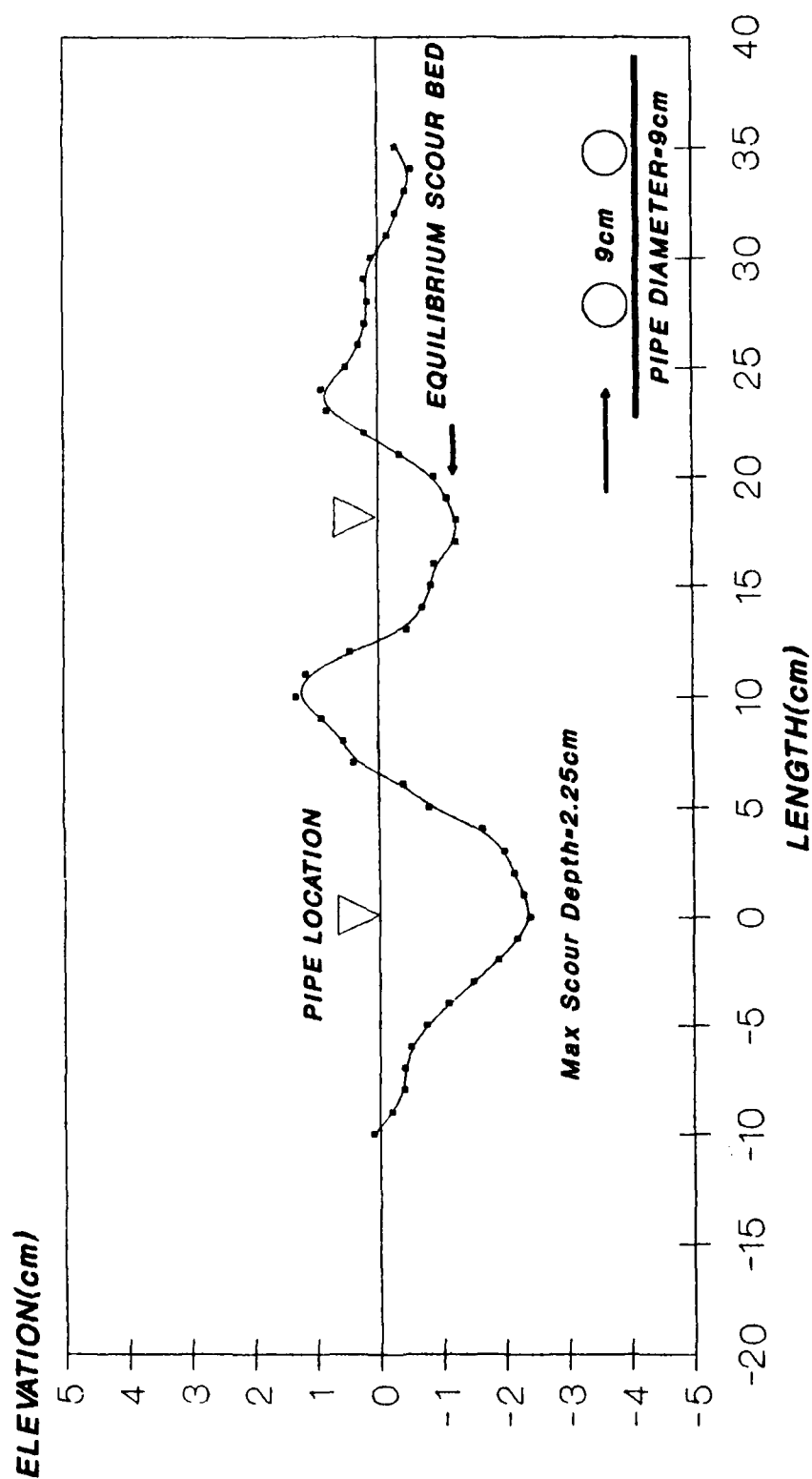
TEST No.68: CURRENT AND WAVE
U= 0.26m/sec, H= 6cm, T= 1.2sec, L= 1.0m

ELEVATION(cm)

PIPE LOCATION

EQUILIBRIUM SCOUR BED

Max Scour Depth=2.30cm

9cm

PIPE DIAMETER=9cm

LENGTH(cm)
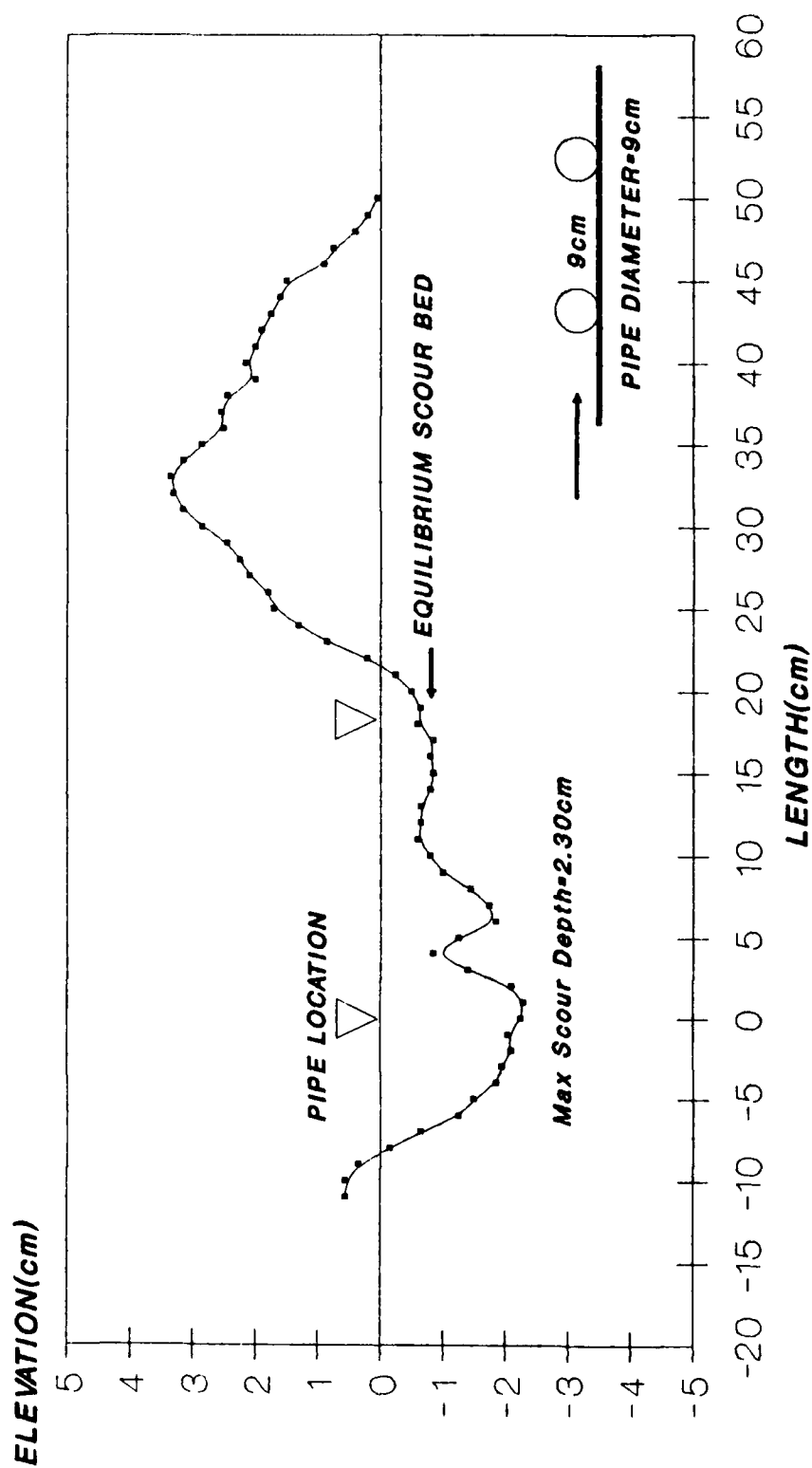
TEST No.69: CURRENT
U= 0.26m/sec
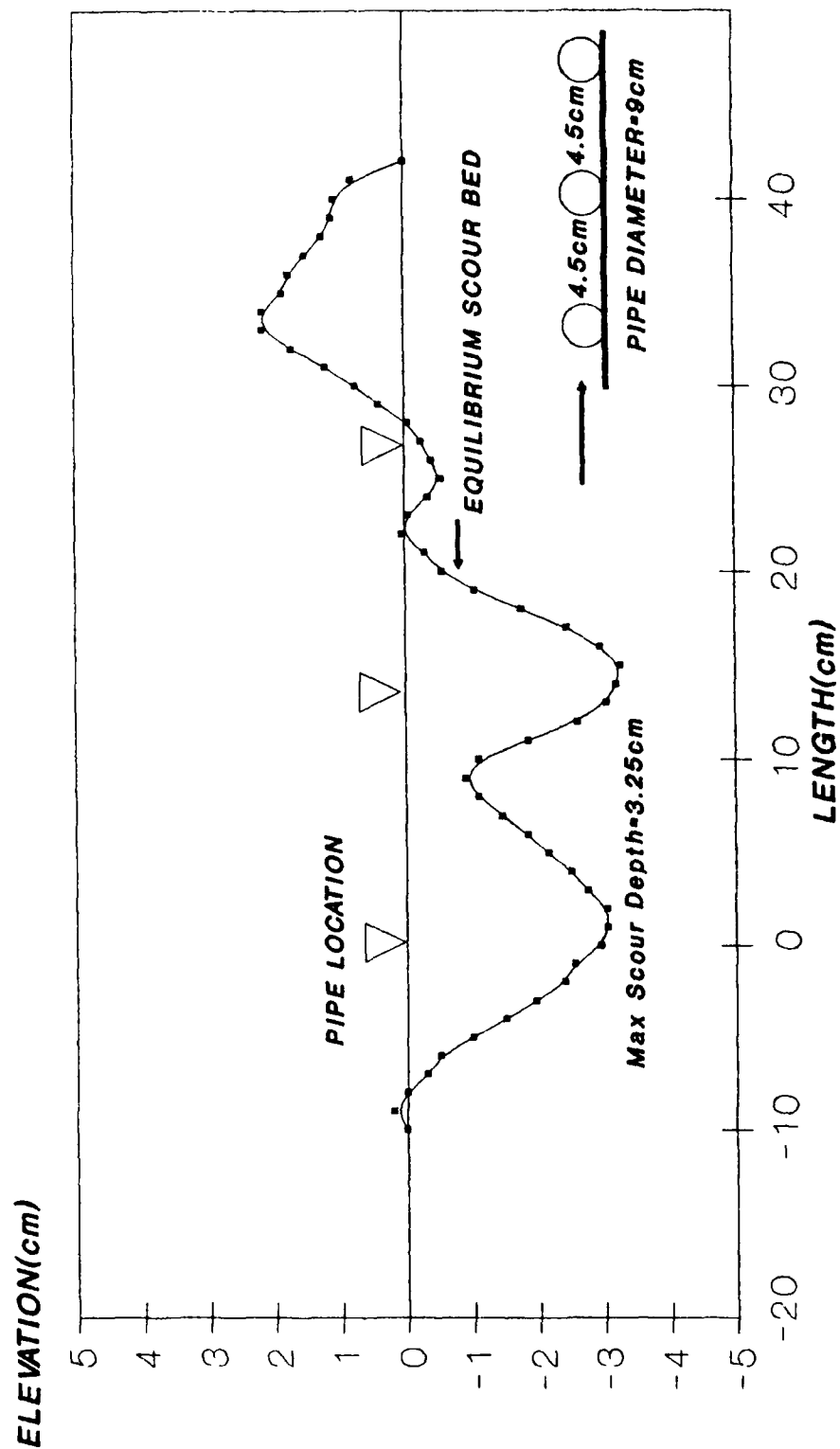
TEST No.70: CURRENT AND WAVE
U= 0.26m/sec, H= 6cm, T= 1.2sec, L= 1.0m
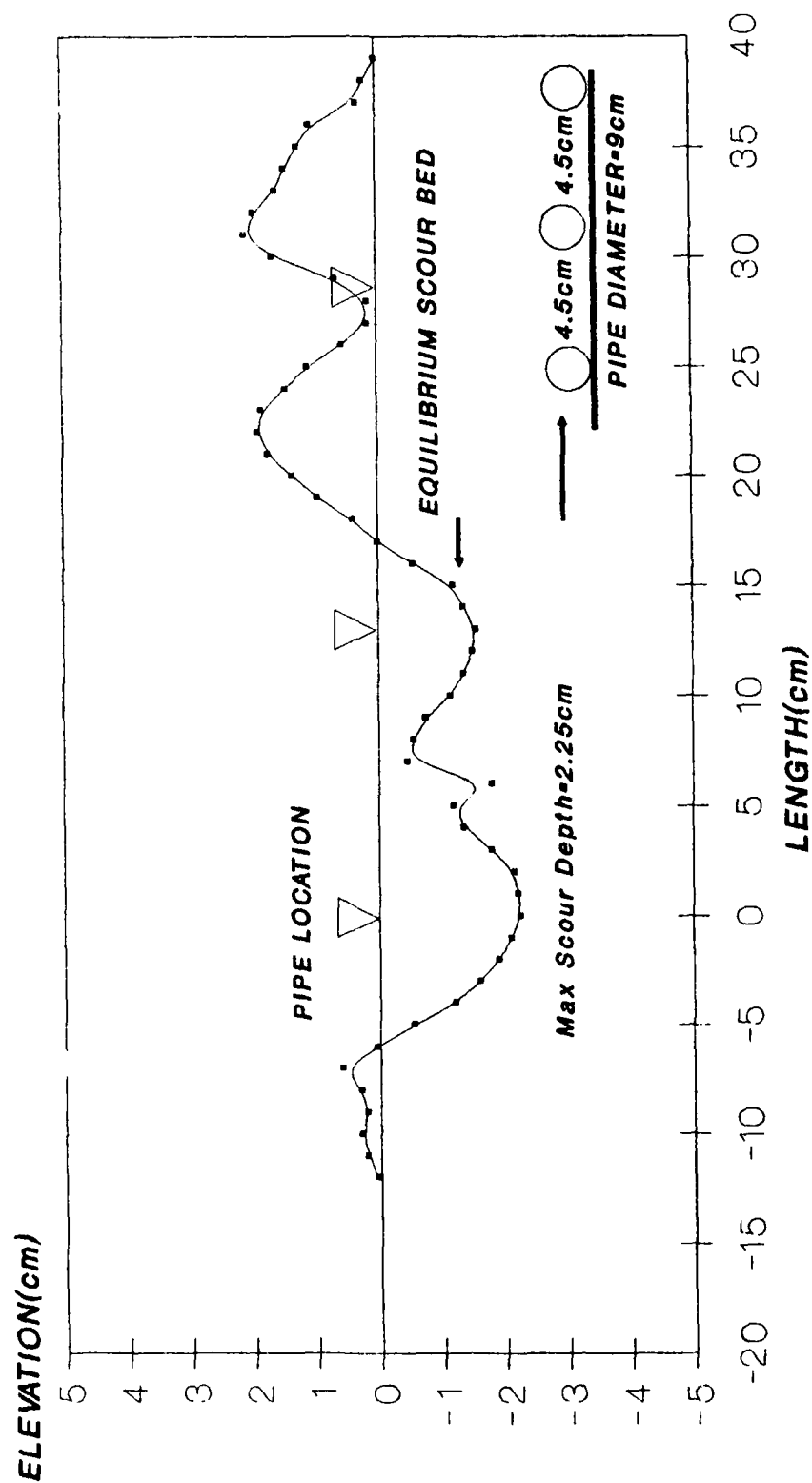
TEST No.71: CURRENT
U= 0.26m/sec
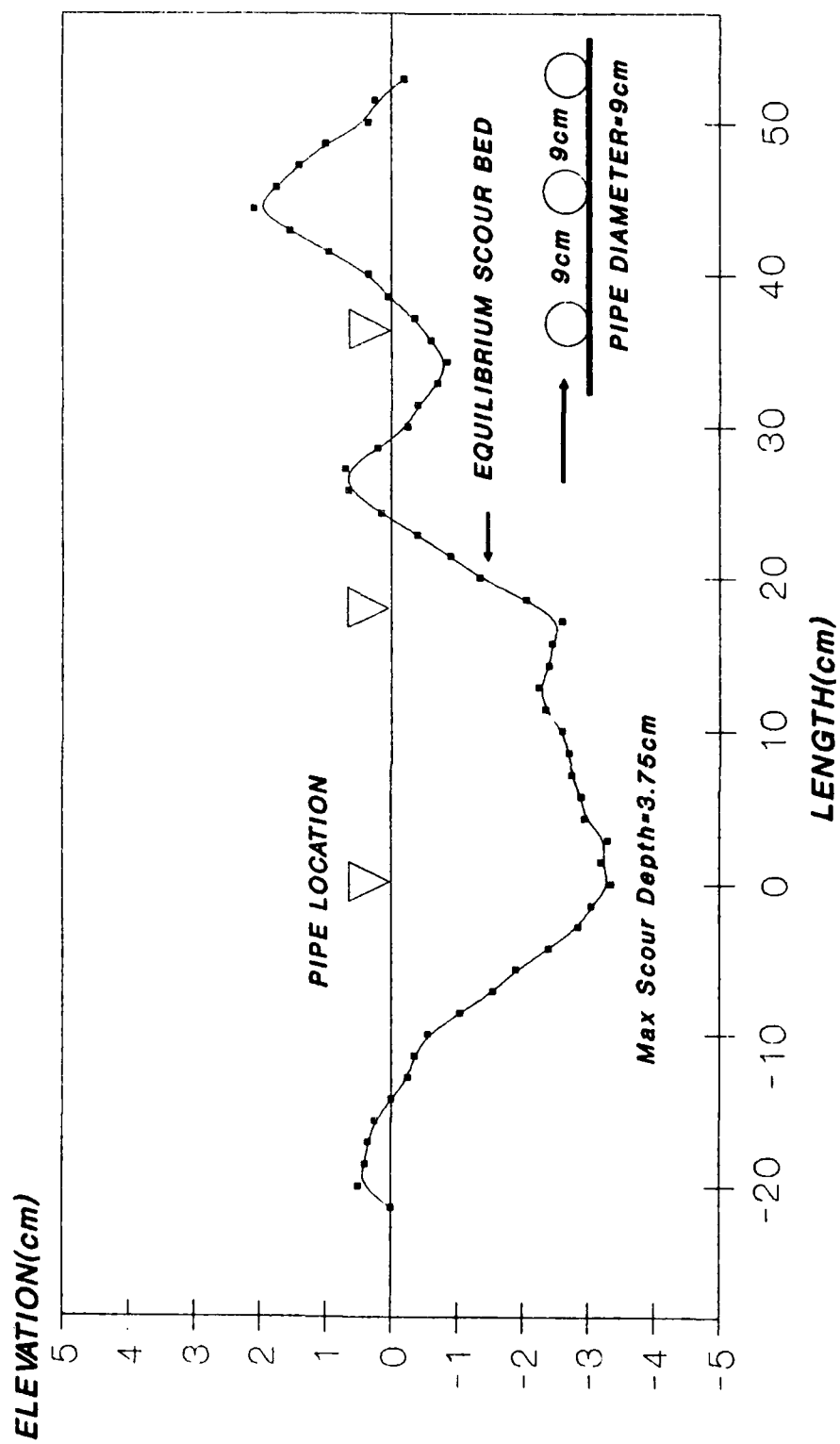
TEST No.72: CURRENT AND WAVE
U= 0.26m/sec, H= 6cm, T= 1.2sec, L= 1.0m

ELEVATION(cm)

PIPE LOCATION

EQUILIBRIUM SCOUR BED

Max Scour Depth=2.50cm

9cm 9cm

PIPE DIAMETER=9cm

LENGTH(cm)
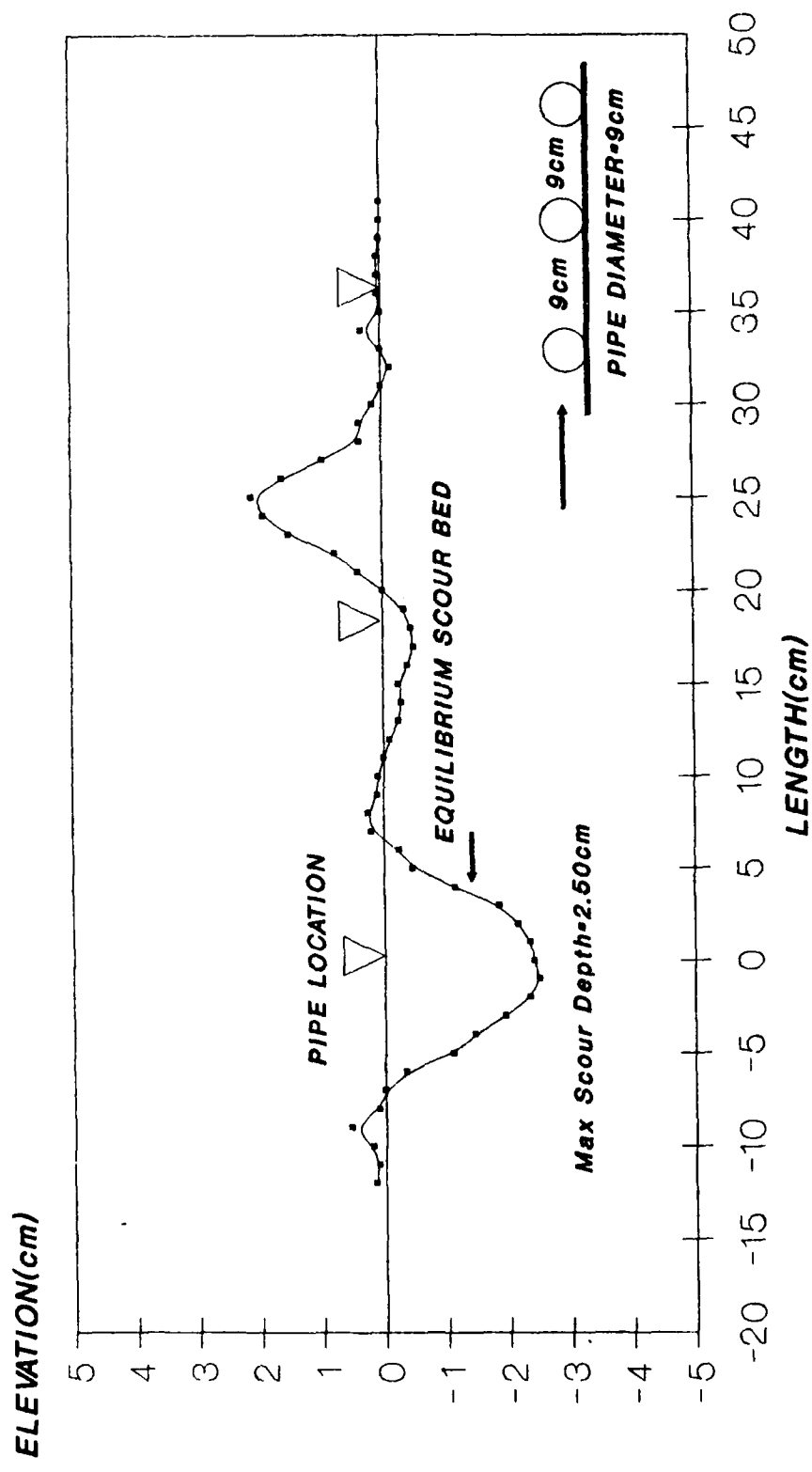
APPENDIX III

NOTATION

The following symbols are used in this paper:

A = projected area of particle on plane perpendicular to flow;

c = frictional drag coefficient of sand bed;

C_d = drag coefficient;

C_1 = form coefficient defining effective surface area of particle;

D = pipe diameter;

d_s = effective sediment diameter;

d_{50} = mean particle diameter;

F_d = drag force on particle;

g = gravitational acceleration;

H = wave height;

$h_{(x)}$ = vertical distance from pipe center to bottom of scour hole;

KC = Keulegan–Carpenter Number;

K_s = sediment factor;

L = wave length;

Nfp = pipe Froude Number;

Nrp = pipe Reynolds number;

Ns = sediment Froude Number;

R_e = Reynolds Number;

R_* = boundary Reynolds Number;

Sd = maximum equilibrium scour depth;

S_f = sand factor;

T = wave period;

NOTATION – CONTINUED

U = mean local fluid velocity near pipe;

U_c = current velocity;

U_d = local velocity at a distance d above the bed;

U_r = wave Ursell Number;

U_w = wave velocity;

U_{100} = fluid velocity at 100 cms above the bed;

$\bar{U}$ = mean fluid velocity;

U_* = turbulent shear velocity;

V_c = critical velocity of sediment motion;

w = width of trench;

y = water depth;

Z = depth of interest;

Δ = relative density of sediment in water;

ϵ = distance between pipe and bed;

μ = dynamic viscosity;

ν = kinematic viscosity;

ρ = fluid density;

ρ_s = sediment density;

θ = Shields parameter;

τ = shear stress;

τ_c = critical shear stress; and

τ_o = bed shear stress.

VITA

Joseph Henry Westerhorstmann was born in New York City on March 24, 1953. In 1980 he graduated from the University of Florida with a Bachelor of Science in Civil Engineering degree. Upon graduation he was commissioned an Ensign in the U.S. Navy Civil Engineer Corps, and has remained on active duty since that time. He was sent to Texas A&M University by the Navy to study Ocean Engineering, receiving the Master of Science in Ocean Engineering degree in December, 1988. He is a Registered Civil Engineer in California. His permanent address is Dolphin Point 201, Clear Water, Florida.